Advances in Islet Transplantation Including Development of a Novel Cell Encapsulation Platform for the Treatment of Diabetic Pets

By

Stephen Harrington

Submitted to the Bioengineering program and the Graduate Faculty of the University of Kansas in partial fulfillment of the requirements for the degree of Doctor of Philosophy

Committee Members:

Dr. Lisa Stehno-Bittel, *Co-Chair*

Dr. Lisa Friis, *Co-Chair*

Dr. Stevin Gehrke

Dr. Arghya Paul

Dr. Sara Wilson

Date Defended: February 22nd, 2017

The Dissertation Committee for Stephen Harrington certifies
that this is the approved version of the following dissertation:

Advances in Islet Transplantation Including Development of a Novel Cell Encapsulation Platform for the Treatment of Diabetic Pets

Committee Chair:

Dr. Lisa Stehno-Bittel, *Co-Chair*

Dr. Lisa Friis, *Co-Chair*

Date Approved: February 22nd, 2017

ABSTRACT

Islet transplantation as a treatment for type-1 diabetes in humans has reached a plateau, and major breakthroughs in stem-cell based therapies and immunoprotection strategies are now needed to advance the field. The primary goal within this dissertation was to approach innovation in islet transplantation from a new perspective: veterinary medicine and canine diabetes. Canine diabetes, while strikingly similar to type-1 diabetes in humans, has been entirely overlooked as a market for islet transplantation, and is in significant need of better treatment options. The obvious clinical need and regulatory advantage in veterinary medicine creates an attractive environment to cultivate much needed innovation in the field of islet transplantation. This overall goal was addressed with the following specific aims:

1] develop and optimize practical, ethical, and cost effective methods for obtaining transplant quality islets from canine donors

2] demonstrate and evaluate long-term efficacy of an alternative (non-alginate) hydrogel for immunoprotected islet transplantation in an allogeneic diabetic rat model

3] develop a non-toxic, simple, and readily translatable method for fabricating hydrogel (non-alginate) microspheres for cell encapsulation and delivery

In accomplishing these aims, significant groundwork for islet transplantation as a treatment option for diabetic canines has been laid. A major focus of this research was in the evaluation and development of an islet encapsulation system based on a hyaluronic

acid (HA) based hydrogel as an alternative to standard alginate microspheres. Islets transplanted within the HA gel reversed diabetes in immune competent allogeneic rats for a minimum of 10 months. In light of these results, I developed, characterized, and patented a novel method for producing islet-laden HA hydrogel microspheres designed for use with readily available materials and cGMP complaint equipment. Furthermore, this novel method has great potential as a platform technology for generating cell-laden hydrogel microspheres using a variety of biomaterials for broad application in regenerative medicine and three-dimensional tissue culture.

ACKNOWLEDGEMENTS

There are so many individuals I wish to thank for their support, guidance, and love in this endeavor. Though there were times I was convinced I never wanted to see another islet for the rest of my life, all of the wonderful people surrounding me these past five years have made this journey one I will always look back on with a smile.

- I'd first like to thank my tireless advisor, Dr. Lisa Stehno-Bittel, the most talented wearer of multiple hats I have known or will ever know. Your extraordinary work ethic, optimism, and humility despite tremendous accomplishment has been inspiring beyond words, and I am humbled and flat out lucky to have learned from your example in so many ways. Thank you so much for helping my scattered brain to focus and teaching me to listen to my data.
- To my co-chair Lisa Friis, thank you for making a chemist feel so welcome in the School of Engineering from day one. Your passion, expertise, and honest advice have had a huge impact on my development as a researcher interested in commercialization.
- I would like to thank all of my committee members past and present, Dr. Sara Wilson, Dr. Stevin Gehrke, Dr. Arghya Paul, Dr. Michael Detamore, and Dr. Omar Aljitawi, for your guidance, support, and time. Dr. Wilson, I would like to thank you specifically for your support of and willingness to oversee my work with Likarda during my dissertation studies, which has been a truly rewarding experience.
- To my lab manager and dear friend, Janette Williams, your seamless blend of mentorship, friendship, and timely humor is probably the reason I am still reasonably sane. Your infectious laugh is a true joy to witness, and your willingness to use it for my ridiculous jokes has not gone unnoticed. I am forever in your debt.

- To Dr. Karthik Ramachandran, KU Bioengineering alum and Vice President of Likarda, I am lucky to have a boss that is also my friend. Your optimism and eternally-open mind kept me going when research got frustrating. From innovation happy hour, endless streams of newfangled gadgets, to seven-day work weeks, you are a true entrepreneur, and I sincerely thank you for the opportunity to work with and learn from you.
- Thank you to all my friends and colleagues of the Diabetes Research Lab and Likarda, who are, in order of appearance, Dr. Sonia Rawal, Dr. Lesya Novikova, Dr. Annie Lee, Caitlin Cole, Donald Muathe, Dr. Lindsey Ott, and Dr. Francis Karanu. Not one of you has ever hesitated to drop what you were doing to help me, from lending an open ear or sharing your expertise, to feeding islets or prepping solutions. Dr. Karanu, I owe you a debt of gratitude for your continual support, advice, and selflessness, particularly in these recent months as I have been glued to my desk chair.
- This project would never have gotten off the ground were it not for the amazing veterinarians and staff at Stateline Animal Hospital, Wayside Waifs, the Cheri's Hope Foundation, and the University of Kansas Medical Center. I would like to thank Dr. Vern Otte, Dr. Sally Barchman, Dr. Luke Pickett, Geoff Hall, Dr. Travis Hagedorn, Jill Hess, and the late Dr. Cheryl Jones for graciously donating your time and energy to this cause over the years.
- Finally, I would like to thank my family, biological and otherwise, for their unconditional support of and love for me throughout my life. Dad (Mike Harrington), you are a beacon of integrity, hard work, and flawless nerdy jokes, and I have strived to live by your example in hopes that someday the same will be said of me, and yes, including the latter. Mom (Cyndi White), you were always the first to remind me not to get too big for my britches, but also the first to come to my rescue when misfortune struck, like that cold day when we fell through the ice as kids and you warmed us up with a fire and hot cocoa *before* telling us

how stupid we were. Thank you so much for your encouragement and standing offer of a home-cooked meal throughout my graduate work, and for listening to me ramble on about science. Big Sister (Kim Campos), thanks for always being there for me, and for balancing out my science with your creativity at family gatherings. Also, it turns out you were right, and I am *still* not older than you even though I have been taller for years now – maybe someday. Kathy, it has been a joy having you as a part of my family; your loving and calming presence is wonderful to be around, and I am so thankful you fell victim to my father's actuarial charm. Hunter, Evan, Seth, Eric, the Ryans, and Forrest: you guys keep me honest and well-stocked with laughs, and I love you all dearly. To my love and best friend Elizabeth Rush, you are the yin to my yang, my coin-toss girl. Thank you for your unyielding patience, sense of humor, and encouragement over the years, and for quietly tricking me into doing so many fun things I would never do on my own.

TABLE OF CONTENTS

LIST OF FIGURES

CHAPTER 1

No Figures

CHAPTER 2

CHAPTER 3

CHAPTER 4

CHAPTER 5

CHAPTER 6

No figures

APPENDIX A

APPENDIX B

LIST OF TABLES

CHAPTER 1: Introduction to Dissertation

The promise of islet transplantation as a cure for type-1 diabetes is as exciting as it is evasive. Despite decades of research, the procedure still resides in the experimental realm, used only as a last resort when standard treatments fail. This dissertation, through a unique industry collaboration, was shaped by a fresh approach to the commercial translation of islet transplantation: *bring it to pets, not people*. Through this approach came practical advancements applicable not only to canine islet transplantation specifically, but to the field in general, as commercial success in the veterinary space could serve as a blueprint for human translation. Further, in addressing this goal I developed a novel and versatile cell encapsulation platform based on hydrogel microspheres with broad potential value in tissue engineering and regenerative medicine, resulting in an issued United States Patent.

Islet transplantation in humans has been stifled for the following basic reason: the costs, both financial and punitive, far outweigh the benefits for the vast majority of patients. Recipients of islet transplants must take harmful anti-rejection drugs, and donor islets are scarce and expensive to procure. Alternatively, most type-1 diabetics can effectively manage their diabetes via insulin therapy, and therefore cannot justify an islet transplant. The same is not true for diabetic canines, which are of course unable to care for themselves. Instead, their human counterparts must administer twice daily insulin injections and closely regulate their diet. Despite these efforts, many diabetic dogs experience major medical complications and, sadly, are often euthanized. Thus, the

veterinary community is in dire need of a better way to address the growing problem of diabetes in pets.

An important advantage to the veterinary pathway is a more hospitable regulatory environment, enabling the much-needed innovation in this field to move more efficiently into the clinic. However, the cost and complexity of current methods for obtaining quality islets are too extreme to be viable in veterinary medicine; improvement in the area of canine islet isolation will be vital to achieving this overall goal. Beyond this, there is a major need for progress – for both human and veterinary application - in the prevention of transplant rejection through islet encapsulation. Current encapsulation strategies are dependent on sodium alginate hydrogel spheres, which have long suffered from poor biocompatibility and consistent failure outside of the laboratory. This dissertation sought to address these needs through the following specific aims:

1] develop and optimize practical, ethical, and cost effective methods for obtaining transplant quality islets from canine donors

2] demonstrate and evaluate long-term efficacy of an alternative (non-alginate) hydrogel for immunoprotected islet transplantation in an allogeneic diabetic rat model

3] develop a non-toxic, simple, and readily translatable method for fabricating hydrogel (non-alginate) microspheres for cell encapsulation and delivery

Chapter 2 of this dissertation contains supportive background material and describes the problems driving the three specific aims. I begin with a review of islet transplantation

under the purview of human diabetes, and the challenges facing the field today. Next, I discuss the historical role of canines in islet transplantation, and establish a basis for the veterinary application of this treatment. The chapter concludes by re-examining some of the challenges to islet transplantation in the context of canines and veterinary medicine, thus providing motivation for the research presented in the subsequent chapters.

Chapter 3 addresses my first aim by confronting the challenges to islet isolation that are unique to veterinary medicine and the canine anatomy. Specifically, it describes a simplified method for isolating canine islets, optimized to account for the marked size variability of canine pancreas and the deleterious conditions surrounding deceased donor-based organ procurement (i.e. as opposed to heart-beating pancreas retrieval standard in human practice).

Chapter 4 addresses the second aim to identify and evaluate an alternative material to the standard sodium alginate gels as an islet encapsulant. In these studies, we examined a hyaluronic acid (HA) based hydrogel system for potential use as an immunoprotective biomaterial for islet transplantation. The HA gel was characterized *in vitro* to elucidate material-derived effects on encapsulated islet viability, morphology, survival, and function over 28 days. These studies included a direct comparison to both alginate-encapsulated islets and un-encapsulated controls. The gel was then examined *in vivo* using an allogeneic diabetic rat model to monitor long-term efficacy and biocompatibility of islets transplanted in the HA gel. Islet-HA transplants reversed diabetes in four out of four

recipients for a minimum of 10 months and showed no signs of a negative host response to the biomaterial.

Chapter 5 addresses the third and final aim to develop a method for fabricating islet-microspheres from alternative hydrogel materials (i.e. not alginate). Microspheres are highly preferred for simple delivery and improved diffusion characteristics compared to macroscopic hydrogel constructs. However, current techniques for fabricating islet-hydrogel microspheres are highly limited, with sodium alginate by far the most common material due to its unique, near instantaneous gelation kinetics. Here, I introduce a novel method for producing islet/cell-laden microspheres compatible with a variety of hydrogel systems, including photo-initiated and chemically cross-linked hydrogels. The method was developed with standard, fully sterile, cGMP-compliant droplet generation instrumentation and readily available materials to facilitate smooth commercial translation, regulatory compliance, and scale, and was awarded a United States Patent.

Chapter 6 concludes with a concise summary of the experimental chapters and a discussion of potential applications and opportunities for future development. Supplemental data and commentary related to the primary dissertation work, including studies performed toward the development of the novel microencapsulation method, are provided in two appendices.

CHAPTER 2: Background

Introduction to Human Islet Transplantation

Nearly two decades ago, seven type-1 diabetic patients were effectively cured by a simple intravenous injection of pancreatic islets. [1] This landmark study, now known as the Edmonton Protocol [1], gave hope of a normal lifestyle to type-1 diabetics, which total about 1.25 million in the United States alone. [2,3] Transplant success rates and duration have continued to improve since these initial reports [3–5], yet the number of patients treated annually has essentially not changed in ten years according to the most recently available data from the Collaborative Islet Transplant Registry (CITR) [2], shown in **figure 2.1**. This is even more disheartening considering the rising prevalence of type-1 diabetes, which is increasing by 3% per year, globally. [6] The following sections explore the two fundamental challenges responsible for the unfortunate obstruction of an otherwise promising treatment: donor islet supply and graft rejection.

Human Donor Islet Supply and Islet Isolation

Islet transplants, like a heart or lung transplant, require organs from deceased donors. However, unlike heart or lung transplants, islets from multiple donors are typically required to restore insulin independence in a single recipient. For example, 2,146 donated pancreas were used to treat a total of 864 patients in North America from 1999-2012, an average of 2.48 donors per recipient. [7] In theory, one donor pancreas does contain a sufficient quantity of islets to properly regulate blood glucose in a typical recipient. However, isolation of islets from the pancreas is markedly inefficient in practice, and has

thus been a major focus of type-1 diabetes research for decades.

Essentially all current islet isolation protocols used for clinical islet transplantation are based on a method described by Ricordi et al. in 1988. [8] Donor pancreas are first preserved during procurement by vascular flushing with an organ preservation solution and transported on ice to a processing facility. The pancreas is then perfused with a solution of digestive enzymes through the pancreatic ductal system, warmed, and then digested with the aid of an automated mechanical agitation device. During digestion, islets are liberated from their collagenous matrix in the pancreatic tissue. The pancreatic digest is then further processed to separate the islets, which account for only 1-2% of the pancreas, from the other pancreatic tissue, called exocrine or acinar tissue. [9] This is achieved by density gradient centrifugation, exploiting the lower native density of islets relative to the exocrine tissue. Briefly, the pancreatic digest is deposited into a vessel containing layers of fluid of variable density, typically Ficoll, and then centrifuged. Islets travel to lower density regions and can be collected separately from the heavier exocrine tissue. In practice, islets are rarely obtained at 100% purity, as exocrine tissue is highly susceptible to environmental stress and often swells with water, reducing its density to within the range of islets. Numerous strategies have been developed to help alleviate this issue, and are covered in greater detail in later in this dissertation. [10–15]

The method reported by Ricordi in 1988 yielded 164,600 islets per pancreas (an average of 2279 islets/gram of pancreas) with an islet purity of 78.5%. [8] By comparison, a multi-center analysis of 204 isolations performed between 2002 to 2010 returned an average

of 353,900 islets per pancreas, demonstrating the clear progress made in the field. [16] However, this number is still well short of the roughly 1 million islets generally estimated to reside in the average human pancreas. Furthermore, because islets, which are aggregates of hundreds to thousands of cells, range in size from approximately 50-400 microns in diameter, simply counting the number of islets quickly proved to be a poor measure of actual islet cells present. [17–22] Thus, the method for conversion to "islet equivalents", or IEQ, was developed and published, again by Ricordi et al., which defined an islet equivalent as the number of islet cells contained in one islet of 150 microns in diameter. [23] Islet preparations are converted to IEQ through a process of binning islets by size range and then multiplying by a standard conversion factor. As an example, the islet number of 353,900 mentioned above converted to 244,400 IEQ, indicating that a majority of the islets were below 150 microns in diameter. [16]

Islet isolation protocols have continued to improve, particularly in the wake of the inspiring clinical results of the Edmonton Protocol in 2000. Barbaro et al. reported an even higher average yield of 368,419 IEQ/pancreas from 132 isolations performed between 2004 and 2006 using a custom density gradient. Experimental islet isolation protocols (i.e. not implemented for clinical transplantation) report islet yields that are better still. Noguchi et al. described an isolation method utilizing yet another custom density gradient that returned 594,136 IEQ per human pancreas (N=11) in a 2009 publication.

While advancements in islet isolation have been of great value toward the ongoing pursuit to expand the reach of islet transplantation, the availability of islets for transplant is

ultimately governed by the number of qualified donor pancreas. That number, unfortunately, is only a small fraction of what is needed. The United States Organ Procurement and Transplantation Network reported a national average of 1,475 pancreas donations per year from 1988 through 2016, the majority of which were transplanted as whole organs. [24–26] Meanwhile, an estimated 40,000 new cases of type-1 diabetes are diagnosed every year to add to the 1.25 million patients currently diagnosed in the United States. [2,3,6] With an average of 2.48 donor pancreas required per recipient, it is abundantly clear that the current donor-based approach can never reach the overwhelming majority of diabetic patients. This reality, however, was understood and accepted long ago by the islet transplantation community. Consequently, extensive research has been underway for decades in search of an alternative and scalable replacement for donor-derived islets, namely, through stem cell-based approaches.

Islet Graft Rejection and Immunoprotection in Humans

While donor supply is clearly a current challenge for clinical islet transplants, the second area of need is in the prevention graft rejection. Islet transplants, though far less invasive than a traditional organ transplant, are just as vulnerable to rejection by the host's immune system. In fact, a major factor in the success of the Edmonton Protocol was the immunosuppressive regime administered in conjunction with the islet infusions. Patients were given a cocktail of sirolimus, tracrolimus, and daclizumab, notably free of the traditional glucocorticoid based immunosuppressants that were known to cause islet cell damage and peripheral insulin resistance. [1,27,28] This approach led to vastly improved outcomes and transplant duration over then current protocols. For example, out of 267

islet allografts performed between 1990 and 1999, only 12.4 percent resulted in insulin independence for more than a week. [28] By comparison, all seven of the original Edmonton patients were insulin independent for a minimum of four months, with an average duration of one year. [28]

Further improvements in immunosuppression and transplantation protocols have led to reduced initial failure rates and prolonging graft lifetime. In the early phases after the Edmonton study, insulin independence rates were 10% after five years. As such, the significantly more invasive but more efficacious whole pancreas transplant was still the preferred option for patients able to withstand the surgical trauma. [29] Recent five-year insulin independence rates were 50% at high quality islet transplant centers and 40% for single donor transplants, [5,30–34] approaching outcomes of whole pancreas transplantation, which are between 60-80% graft survival at 5 years. [35,36] Thus, islet transplantation has gained significant ground as a less invasive alternative to pancreas transplant even in patients healthy enough to undergo an open abdominal surgery.

Immunosuppressive therapy after islet transplantation must be continued for the lifetime of the graft to prevent rejection, though rejection eventually occurs regardless in many cases. Along with these medications come side effects including nephrotoxicity, mouth ulcers, peripheral edema, hypertension, and increased infection risk. [37,38] Meanwhile exogenous insulin therapy continues to improve, and most type-1 diabetics can effectively self-manage their blood glucose levels to a point that immunosuppression would result in a much poorer quality of life. Thus, islet transplantation is relegated to patients with severe

and uncontrollable glycemic dysfunction, or to those that are already on immunosuppressive therapy for another transplant, most often a kidney. [3,5,39,40]

The glaring limitations of immunosuppression gave rise to another approach to islet transplantation called immunoprotection, otherwise known as cell encapsulation. The concept of immunoprotection is not to suppress the host immune system, but rather to hide from it. To accomplish this, cells are encapsulated within a semi-permeable, micro-porous polymer network, for example a hydrogel, that allows free exchange of nutrients and signaling molecules (e.g. insulin) while preventing host immune cells from contacting transplanted cells. [41–45] A graphical representation of this concept is provided in **figure 2.2** for additional clarity. This clever strategy is enabled by the tremendous size difference between cells and biomolecules. A typical T-cell is about 8 microns in diameter, while the hydrodynamic radius of albumin, a common biological protein, is only 3.5 nanometers, more than 1000 times smaller. [46] Through this approach, transplanted islets can be shielded from rejection without the use of harmful immunosuppressive drugs.

By far the most common material used for immunoprotection is calcium alginate, with the first successful allogeneic transplants reported by Lim and Sun in 1980 (in rodents). [47] Alginate is a seaweed derived polymer that, when combined with a free divalent cation, usually calcium, instantaneously cross-links into a rigid hydrogel network. Calcium-alginate gelation occurs so rapidly that droplets of liquid alginate solution dispensed into a bath containing calcium harden immediately into small, spherical, hydrogel microbeads that can be injected through a syringe. This remarkably simple fabrication process and

minimal cytotoxicity are the basis for the widespread popularity of this material for islet transplantation. Notably, the transplants performed by Lim and Sun lasted for only a few weeks, and many issues with encapsulated transplantation still remain, but more than sufficient progress has been made in this area to justify continued research.

Though significant progress has been achieved through sophisticated alginate purification techniques and improved microsphere geometry [48–53], long-term results have disappointed due to biocompatibility issues with this material. [54–59] In response, researchers have begun to explore new, advanced biomaterials and devices for islet transplantation and cell encapsulation in general. Much of the alginate-free technology has come in the form of macroscopic implantable devices. A recent macro-device, called the Beta-Air, consists of a small chamber containing islets surrounded by a semi-permeable synthetic mesh that allows for nutrient exchange. The device is surgically implanted beneath the skin and injected daily with oxygen through a transdermal port to improve islet survival. [60] Showing promise in rodents and pigs, a company was formed around the technology and began a phase I/II clinical trial (ID: NCT02064309) in humans in 2014 that is currently active. Another approach, known as conformal coating, utilizes advanced techniques to coat individual islets in an ultrathin polymer membrane in an effort to reduce transplant volume compared to traditional hydrogel microspheres. A company by the name Novocell showed promising results in baboons with a polyethylene glycol (PEG) based conformal coating, but could not replicate their results in a phase I clinical trial in humans (ID: NCT00260234). [39]

Immunoprotection has the potential to truly transform the field of islet transplantation. Eliminating the need for immunosuppression, and thereby numerous side effects, would dramatically expand the population of patients for which an islet transplant would be justifiable. Furthermore, viable immunoprotective technologies will be an integral component in the safe delivery of other cell-based therapies, including stem cells, as they become available.

Canines Diabetes and Islet Transplantation

Canines are known to spontaneously contract a form of diabetes that closely resembles type-1 diabetes in humans. It is perhaps for this reason that canines and islet transplantation have a very long history together. After the first reported attempt at a human islet transplant, published in 1977 [61], failed to reverse diabetes, the use of canine research models became increasingly common as investigators strived to better understand the procedure. [23,62–68] In fact, much of the progress in pancreas preservation, islet isolation, immunosuppression, and transplant surgery can be attributed to canine research throughout the evolution of islet transplantation. Multiple studies reported achieving insulin independence in dogs for several months and up to 600 days in some cases. [67,69–71] Of note, these studies were done using research animals with induced, not spontaneous, diabetes. However, Alejandro et al. reported insulin independence in 3 of 8 spontaneously diabetic dogs for 253-716 days. Interestingly, this study was published in 1988, long before the era of advanced immunosuppression agents that arrived with the Edmonton protocol, demonstrating the excellent potential of islet transplantation in dogs. [72]

Considering the historical success in canine islet transplantation research, the absence of this treatment from veterinary medicine seems like an obvious oversight. Approximately 1 in 400 dogs in the United States is diagnosed with diabetes and incidence rates are steadily climbing, yet treatment options for diabetic pets have stagnated while human diabetes care is improving rapidly. [73,74] The standard treatment for canine diabetes is twice daily insulin injections administered, of course, by a human counterpart. Glycemic control with this method is often very poor despite the best efforts by the pet's owner to control diet and monitor symptoms. As a result, these animals commonly experience diabetic complications including infection, loss of vision, and ketoacidosis. [75] Sadly, when faced with the reality of caring for a diabetic pet, euthanasia is an all too frequent alternative. These factors combined build a compelling case to re-examine islet transplantation in canines, but now as patients, not subjects.

The idea of islet transplantation in veterinary medicine presents an intriguing and potentially synergistic opportunity. The high prevalence of canine diabetes in conjunction with a poor standard of care has created extraordinary need in the veterinary community for improvement. Further, veterinary medicine is a more receptive environment for innovation both from a regulatory and financial risk perspective. To this point, a review by Scharp et al. describes 22 separate corporate attempts to translate human islet transplantation technologies that started and failed between 1980 and 2010. [76] Ironically, many of these companies showed initial promise in large animals, including canines, but were ultimately unsuccessful in humans. Alternatively, technologies developed for veterinary application would benefit from reduced regulatory scrutiny and, perhaps more

importantly, be exempt from the tremendous capital risk associated with moving from animal studies to human clinical trials. Moreover, successes achieved in canines could serve as a blueprint, even as preclinical data, for human applications in the future.

Canine Islet Isolation for Veterinary Medicine

A necessary element for bringing islet transplantation to canines is, of course, canine islet tissue, and there are several important points to consider in this regard. First and foremost is the fact that the vast majority of canine islet transplantation research utilized islets obtained from purpose-bred laboratory animals. While justifiable in experimental research, this would be profoundly unethical in clinical practice. Rather, tissues for canine islet transplants must be obtained, as with human transplants, through organ donation. This introduces another point of consideration: pancreas procurement conditions. Human pancreas are procured by a team of specially trained medical personnel, typically from a beating-heart donor, and preserved through a complex vascular flushing process. [16,77,78] In contrast, canine pancreas will most likely be obtained from deceased donors that were euthanized for other reasons at local veterinary clinics or animal shelters. Further, these canine organs will be exposed to increased periods of warm and cold ischemia relative to human organs, and complex vascular flushing procedures are not feasible in veterinary settings. Unfortunately, these harsh conditions can lead to extensive tissue damage and significantly diminish islet yield and quality. [79–82] Thus, new islet isolation strategies designed specifically for canine pancreas procured in sub-optimal conditions are needed.

A fundamental difference between human and canine islet isolation is the size of the

pancreas itself. The mass of a typical human pancreas is about 100 grams, with relatively small deviation amongst individuals.[16] The mass of a canine pancreas, which is strongly correlated to the mass of the animal, varies tremendously. In just our own laboratory, we have processed canine pancreas from as small as ten grams and to as large as 120 grams. Human islet isolation protocols are not designed to account for this level of variability, employing large, expensive equipment such as the COBE 2991 cell processor and the Ricordi automated digestion system, which require high volumes of costly materials for each individual pancreas.[8,83–86] Processing a 10-gram pancreas using these protocols would be a wildly inefficient endeavor in the already cost-conscious veterinary world. Rather, canine isolation protocols must be designed to accommodate the size variability of the canine pancreas, and with minimal use of costly, specialized materials and equipment.

Future Development in Immunoprotection

Immunoprotection strategies will be just as critical to the success of islet transplantation in pets as they are for human applications, and for essentially the same reasons. Freedom from insulin injections is often not worth the costs associated with a lifetime of immunosuppression, particularly when those costs are the direct responsibility of the pet's owner. Thus, an economically feasible veterinary islet transplantation protocol must also include an effective immunoprotection strategy. To this point, innovation in this area could be expedited in the less rigorous veterinary space, as entry into the target species can be achieved much faster than in humans, mitigating substantial risk in progressing to clinical trials.

Recently, advanced hydrogel materials derived from native and bioinspired materials have gained attention in cell encapsulation research due to excellent biocompatibility and bioactive characteristics. Examples of these materials include chitosan, a polymer derived from the shells of insects and crustaceans, synthetic self-assembling peptide gels, and gels conjugated to signaling proteins such as VEG-F. [87–89] Of particular note are hydrogels based on hyaluronic acid (HA), which is a primary component of native extracellular matrix. Hyaluronic acid gels have become increasingly popular due to their excellent mechanical properties and outstanding biocompatibility. [90–95] However, a key drawback to these advanced hydrogels is how they are fabricated. Unlike alginate, which forms a gel instantaneously, most hydrogels typically require several minutes to solidify. Therefore, the simple process for producing small, conveniently injectable microspheres that works with alginate does not apply to HA gels. Some methods for producing non-alginate-based hydrogels do exist, but are based on oil-emulsion techniques and are therefore not an attractive option for encapsulating living cells for transplant, where sterility, cytotoxicity, and process control are primary concerns. [96,97]

Summary

The penetration of islet transplantation in humans has plateaued, awaiting major breakthroughs in renewable stem-cell-derived islet tissues and immunoprotective delivery systems. Meanwhile, treatment options for diabetic pets are outdated and only marginally effective despite a high prevalence of the disease, and euthanasia is an unfortunate and common alternative to insulin therapy.

There is ample precedent of efficacy for canine islet transplantation throughout decades of research, yet it remains wholly unavailable diabetic dogs and their owners. While this is an obvious clinical need in a sizeable market, translating islet transplantation to canines is not without challenges. New protocols for islet isolation must be developed that account for the specific physiological and economic variables associated with canines and veterinary practice. Finally, while the demand on efficacy is far lower in canines than humans due to the substantial treatment gap, improvements in immunoprotection and non-donor-based tissue sources are still needed to achieve broad clinical relevance. However, the veterinary space is an ideal place to foster innovation in this area, with reduced regulatory burden and the benefit of a faster and less costly entry into the target species.

Chapter 2 Figures

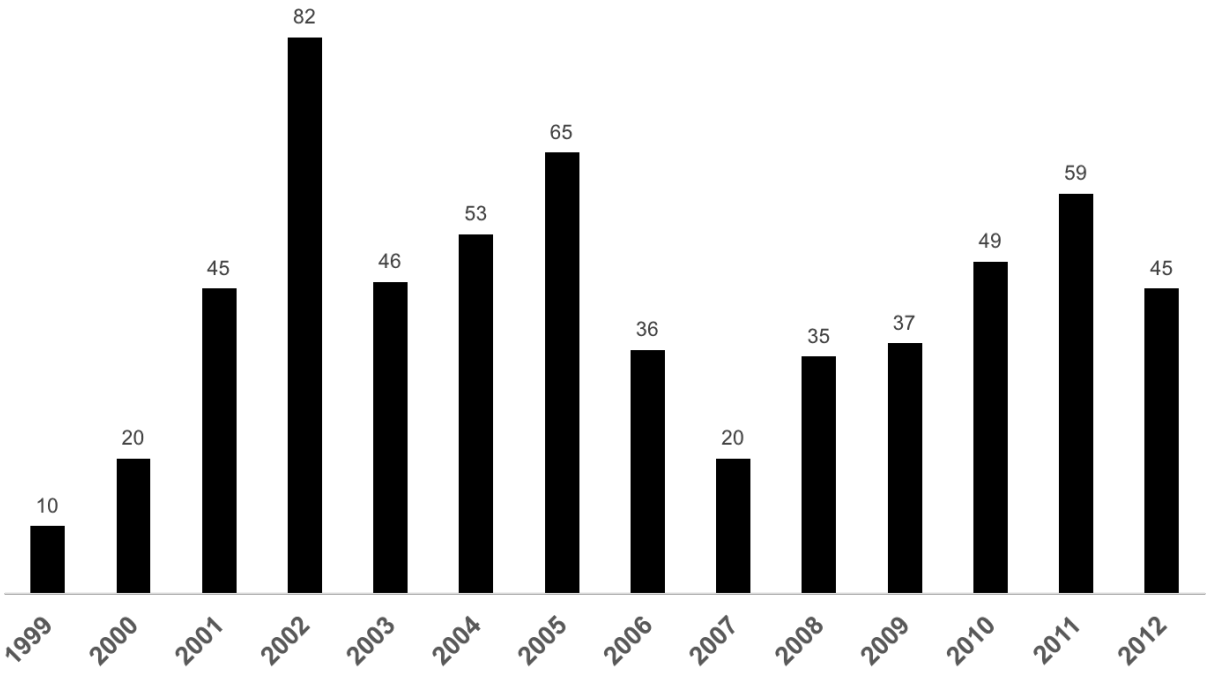

Figure 2.1. Number of patients that received islet transplants in the United States from 1999 to 2012.

Data shown are adapted from the Collaborative Islet Transplant Registry Eighth Annual Report, published December 31st, 2014. [2] After the initial publication of the Edmonton protocol, the numbers of islet transplantations sharply increase year over year, reaching its peak in 2002. However, as improvements slowed and exogenous insulin therapy began to progress rapidly, the use of islet transplantation stalled.

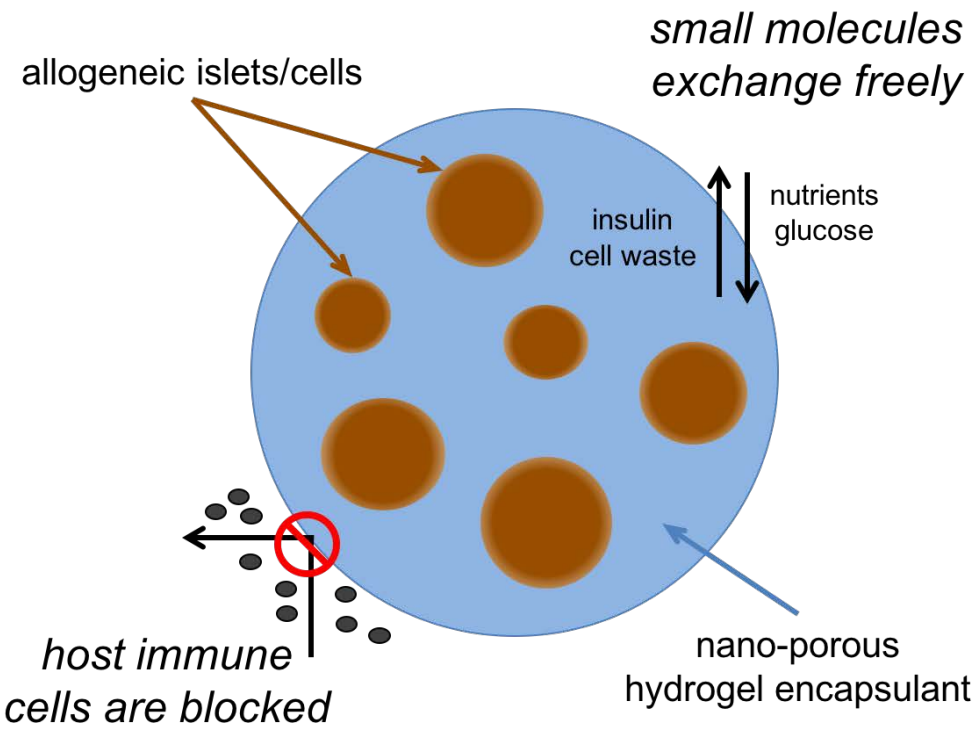

Figure 2.2. Cartoon depiction of immunoprotection (cell encapsulation) using a hydrogel.
Immunoprotection is enabled by the vast size disparity of cells vs. biomolecules through the use of a nano-porous polymer network or membrane, a hydrogel in this example. Pores are large enough for nutrients (amino acids, oxygen), signaling molecules (glucose, insulin), and cell waste to freely diffuse into and out of the gel, yet comparatively large immune cells are prevented from contacting the encapsulated cells, thus mitigating immune rejection.

CHAPTER 3: Increased Efficiency of Canine Islet Isolation from Deceased Donors[†]

Abstract

Canine diabetes is a strikingly prevalent and growing disease, and yet the standard treatment of a twice-daily insulin injection is both cumbersome to pet owners and only moderately effective. Islet transplantation has been performed with repeated success in canine research models, but has unfortunately not been made available to companion animals. A major barrier to the veterinary application of this treatment is the availability of high quality, ethically-obtained islet tissue. Standard protocols for islet isolation, developed primarily for human islet transplantation, include beating-heart organ donation, vascular perfusion of preservation solutions, specialized equipment. Unfortunately, these processes are prohibitively complex and expensive for veterinary use. Here, we describe simplified strategies for isolating quality islets from deceased canine donors without vascular preservation and with up to 90 minutes of cold ischemia time. An average of 1500 islet equivalents per kg of donor bodyweight was obtained with a purity of 70%. Islets were 95% viable and responsive to glucose stimulation for a week. Histological examination of the canine pancreas further confirmed marked regional disparities in islet distribution, with the vast majority of islet cells located in the tail and main body of the pancreas. We found that processing only the body and tail of the pancreas dramatically increased isolation efficiency without sacrificing islet total yield. Islet yield per gram of

[†] Submitted as **Harrington, S.**, Williams, S., Otte, V., Barchman, S., Jones, C., Ramachandran, K., Stehno-Bittel, L. "Increased Efficiency of Canine Islet Isolation from Deceased Donors," for *BMC Veterinary Research*, **2017**.

tissue increased from 773 to 1868 islet equivalents when the head of the pancreas was discarded. In summary, this study resulted in the development of a repeatable, cost efficient, and readily accessible method for obtaining viable and functional canine islets from deceased donors. These strategies provide a reliable and ethical means for obtaining donor islets, and thus represent an important step toward the potential application of islet transplantation as a treatment for canine diabetes.

Introduction

One in every 333 dogs in the United States is currently diagnosed with diabetes mellitus, and incidence rates are steadily increasing. [98] Indeed, rates of canine diabetes have more than doubled since 2007. [73,98] Apart from an obvious financial sacrifice, caring for a diabetic pet requires twice daily insulin injections, frequent veterinary assessments, and strict dietary constraints. Despite these extreme measures, glycemic control in diabetic canines often remains poor, which leads to major complications such as infections, diabetic ketoacidosis, and loss of vision. [75] As such, access to islet transplantation, which restores natural glucose regulation and eliminates the need for insulin injections, would be an extraordinary step forward in veterinary diabetes care. In humans with brittle diabetes, islet transplants have successfully provided normoglycemia since 2000, when the Edmonton protocol was introduced. [1] By 2005 approximately 70% of patients were insulin independent at 1 year after transplantation [29], and 37% were still insulin independent at 3 years. [5] More recent statistics indicate that 44% of diabetics are still insulin independent 3 years after their transplant. [4] Canines were used extensively as research and preclinical models for human islet transplantation with promising outcomes, and yet the veterinary application of this research has never been earnestly pursued. [64,67,69,70,99–102] Vrabelova et al. recently published an excellent review to this very point, demonstrating a promising opportunity to meet an obvious veterinary need. [68]

Perhaps the most critical factor for successful application of islet transplantation in companion animals will be reducing the cost of, and expanding access to, quality donor islets. Canine islet isolation protocols have been developed almost entirely with laboratory

animals under optimal, controlled conditions, i.e. beating-heart donors, minimal periods of ischemia, specialized equipment, and little regard to cost. However, these ideal conditions for islet isolation are simply not feasible in veterinary practice. Furthermore, the use of purpose-bred dogs for on-site, beating-heart pancreas procurement is both costly and regarded as highly unethical. Rather, donor pancreata will likely be obtained off-site from already euthanized donors at veterinary clinics through organ donation programs, and then transported to a separate facility for processing. Consequently, there is a clear need for a simple and cost effective strategy to obtain transplant quality islets from euthanized donors where ischemic injury is inevitable. Recently, some promising results were reported using euthanized canine donors, but islet yields were relatively low and inconsistent. [103] Further, the method utilized a costly Ricordi chamber and complex temperature controlled perfusion system. Thus, continued improvements in this space will be necessary to make veterinary islet transplantation a reality.

In the present study, we sought to develop a simple, scalable, and cost-effective method that could be used to consistently procure large quantities of transplant-quality canine islets from euthanized donors using standard laboratory equipment and materials. To accomplish this, we first developed a custom cold preservation solution and an advanced density gradient medium using readily available components. We also administered heparin prior to euthanasia and incorporated a simple ductal purging step to eliminate residual blood in lieu of more complex vascular preservation and flushing. Finally, because the canine pancreas is known to have a higher concentration of islet tissue in

the tail region [21,104], we evaluated the implications of omitting the head of the pancreas from the isolation process on overall islet yield, purity, viability and function.

Methods

Organ Preservation Solution

A modified Histidine-Tryptophan-Ketoglutarate (HTK) organ preservation solution was prepared in house with 5% (w/v) polyethylene glycol (PEG), average M.W. 8000, added as an oncotic agent to minimize cellular edema. [105–108] The modified HTK-PEG solution was sterilized by filtration through a 0.22 µm filter unit, and the pH and density was measured. The density of the HTK-PEG preservation solution was measured using a Densito 30PX densitometer (Mettler Toledo) approximately 1.022 g/mL at 20 °C. The solution pH was 7.2-7.4 at 4 °C with a theoretical osmolality of approximately 315 mOsm/kg.

Digestion Buffer

Pancreas digestion was carried out in a custom buffer of Hank's Balanced Salt Solution (HBSS) containing 10 mM HEPES and 3.2 mM calcium chloride, adjusted to pH 7.6-7.8 at room temperature. [77,109,110] This digestion buffer was also used to prepare collagenase solutions.

Collagenase Solution

A highly purified collagenase/thermolysin blend, Liberase T-Flex, (Roche Custom Biotech, Indianapolis, IN) was dissolved in the above-described HBSS digestion buffer.

Enzyme solutions were prepared immediately prior to use at 3 Wunsch Units (WU) of collagenase and 0.018 mg thermolysin per mL of buffer. Sufficient volume of enzyme solution was prepared for each individual pancreas to achieve approximately 10 WU per gram of digested tissue.

High Osmolality Iodixanol/HTK Density Gradient Medium

A custom density gradient medium was prepared by first adding 5 M sodium chloride to a concentrated solution of iodixanol (OptiPrep, CosmoBio USA) to a final calculated osmolality of 700 mOsm/kg and a density of 1.315 g/mL at 20 °C, as measured with a Densito 30PX densitometer (Mettler Toledo). This high osmolality iodixanol stock was then mixed with the modified HTK-PEG preservation solution to create solutions of various desired densities. [111] The calculated osmolality of the final gradient media was approximately 450 mOsm/kg.[11,12,14,112]

Pancreas Donors

Pancreata were obtained from canine donors at local veterinary clinics with consent of the owners for organ donation. Animals were already scheduled for euthanasia for other reasons and had no known endocrine disorders. Euthanasia was performed by the licensed veterinarian overseeing the care of each animal, and the clinical veterinarian confirmed death with loss of heart function. Collection of the donor pancreata after death, and from animals euthanized for reasons other than tissue procurement, was determined to be exempt from IACUC review by the University of Kansas Medical Center. Canine donor and procurement information for organs is provided in **Table 3.1.**

Donor pancreata were categorized into four experimental groups: whole pancreas (W), tail and body (TB), no heparin/ductal flush (NH), and histological study (IHC). The IHC group was not used for pancreas digestion or islet isolation.

Pancreas Procurement and Preservation

Prior to euthanasia, donors were given heparin sulfate intravenously at 300 units/kg with the exception of the NH study group. After cardiac death, the abdominal fur was shaved, and the surface sanitized with Povidone-Iodine sponges (Medline Industries, Inc.) and rinsed with 70% ethanol. Then, the abdominal cavity was accessed via gross midline incision and a small lateral incision near the stomach. The major splenic and pancreaticoduodenal vessels leading into the pancreas were ligated and the duodenum was double clamped with large hemostats on either side of the pancreas. The major vessels were severed above the ligatures to minimize blood contamination as the pancreas was removed with the attached duodenal section. The isolated pancreas was then immersed in cold HTK-PEG preservation solution and transported to the laboratory for processing.

Tissue Processing for Histological Studies

For histological analysis (donor ICH1, **Table 3.1**), the pancreas was manually dissected into three parts (head, middle and tail). The tissues were fixed using the general methods we have previously described.[113] Samples were placed in 10% normal buffered formalin in phosphate buffered saline (PBS), pH 7.2, for three days at +4°C. Tissues were

embedded in paraffin using an automated vacuum tissue processor Leica ASP300S (Leica Microsystems Inc. Bannockburn, IL) and stored at +4°C. The samples were sectioned in 7 µm thicknesses using a microtome RM2255 (Leica Microsystems) and mounted directly on Superfrost/Plus microscope slides (Fisher, Pittsburgh, PA). After cutting, the slides were dried overnight at +40°C in an oven and stored at +4°C until processed.

Paraffin embedded sections were deparaffinized and subsequently dehydrated in xylene followed by ethanol and PBS serial rehydration. Antigen retrieval was completed in a steamer using 0.01M citrate buffer, pH 6.2, with 0.002M EDTA, for 30 min. After cooling for 20 min, slides were washed in PBS 2 times and permeabilized in1% Triton X-100 in PBS for 30 min, and subsequently rinsed in PBS. After washing, sections were encircled with a PAP pen. Sections were incubated in 10% normal donkey serum, 1% BSA, 0.03% Triton X-100, all diluted in PBS, for 30 min to block nonspecific binding sites and rinsed by dipping in PBS once. Blocked sections were used for immunofluorescence and immunohistochemistry staining.

Immunofluorescence

The immunofluorescence procedures have been described by our group previously. [113] Blocked sections were incubated with a primary antibody mix at +4°C, overnight, in a wet chamber. The following primary antibodies were used to stain the pancreas: anti-insulin (1:400, Abcam, Cambridge, MA, #ab7842), anti-glucagon (1:400, Abcam, #ab10988),

anti-somatostatin (1:400, Abcam, #ab53165). Sections were rinsed in PBS 3 times, 10 minutes each, and incubated for 2 hr at room temperature in a mix of fluorophore-conjugated secondary antibodies in wet chamber protected from light. Appropriate secondary antibodies were used that were conjugated with DyLight 488 (1:400, Jackson ImmunoResearch Laboratories Inc., West Grove, PA), Alexa 555 (1:400, Molecular Probes, Eugene, OR), or Alexa 647 (1:400, Molecular Probes). The same solution was used to dilute primary and secondary antibodies: 1% NDS, 1% BSA, 0.03% Triton X-100. After incubation with secondary antibody, slides were washed in PBS 3 times, 10 minutes each, and mounted with anti-fading agent Gel/Mount (Biomeda, Foster City, CA). Stained slides were viewed using a Nikon C1Si microscope. Images were captured on a Nikon C1Si or C1 Plus confocal microscope, and were analyzed using Nikon software EZ-C1 3.90 Free viewer.

Immunohistochemistry

Immunohistochemistry procedures have been described previously. [113] Anti-insulin (1:200, **Santa Cruz Biotechnology, Inc.,** Santa Cruz, CA, #sc9168), anti-glucagon (1:200, Santa Cruz Biotechnology, #sc13091), or anti-somatostatin (1:200, Abcam, #ab15365) primary antibodies were used for pancreas immunostaining. Staining was developed using Histostain-*Plus* Broad Spectrum (AEC) Kit (Invitrogen, Frederick, MD). Slides were counterstained with hematoxylin to identify cell nuclei.

After staining, slides were rinsed in deionized water and placed on coverslips in Clear Mount mounting medium (Electron Microscopy Sciences, Hatfield, PA). The specificity of

immunoreactivity was confirmed by omitting the primary antibody from some sections. The staining was observed using a light microscope Nikon Eclipse 80i (Nikon Instruments, Melville, NY). Images were analyzed using Adobe Photoshop CZ4 extended software.

Pancreas Digestion

For organs used to isolate islets, the pancreas was placed on a cooled sterile surgical tray for processing. The attached duodenal section was resected from the pancreas and discarded, and the mass of the pancreas was recorded. The accessory pancreatic duct was located and cannulated using a sterile 18 G, 20 G, or 22 G catheter, depending on the size of the ductal lumen.[103] Six pancreata (groups W and TB, **Table 3.1**) underwent a preliminary saline ductal flush and rinse. These pancreata were completely distended with saline via the accessory duct and immersed in cold sterile saline solution to purge the organ of excess blood. In order to examine the effectiveness of the ductal purging technique, four pancreata did not undergo a preliminary ductal saline flush and rinse (group NH, **Table 3.1**). Heparin was not administered in these donors. All pancreata were next perfused with freshly prepared collagenase solution (described above) using a 30 mL syringe and flexible Luer extension set. Phenol red dye was included in the enzyme buffer to visually confirm the complete perfusion of enzyme throughout the gland. Heparinized and flushed pancreata were further divided into two groups. In the first group (group W, **Table 3.1**), the whole pancreas was filled with collagenase and processed. In the second group (group TB, **Table 3.1**), the head of the pancreas was not perfused by ensuring the catheter was only in the main tail/body branch, and subsequently ligating the head of the pancreas with a large hemostat. The unfilled pancreas head was then

removed, weighed and discarded. The digested tissue mass was recorded for each isolation.

Following enzyme perfusion, pancreata were cut into 2-3 cm pieces and divided into 250 mL polycarbonate flasks containing 10 silicon nitride beads for mechanical disruption. Each 250 mL flask contained a maximum of 25 g of tissue. Flasks were then filled with additional cold digestion buffer to a total volume of ~250 mL. Finally, the flasks were placed in a 38°C shaking water bath at 120 rpm with occasional manual shaking. During the digestion process, small samples of the tissue were stained with dithizone to evaluate the extent of islet liberation from exocrine tissue. When at least 50% of islets were free of exocrine, or no improvement in islet liberation was observed in subsequent samples, digestion was stopped by transferring the tissue into a 500 mL centrifuge bottle containing 250 mL cold RPMI 1640 media with 10% bovine calf serum (BCS). Bottles were placed on ice and the tissue was allowed to settle by gravity for 15 minutes. The supernatant was discarded and the tissue was transferred to 225 mL centrifuge tubes, rinsed with additional RPMI with 10% BCS, and centrifuged at 400 rcf (relative centrifugal force) for 5 minutes at 4°C. [103]

Digestion times were evaluated using a one-tailed student's t-test to determine if the heparin and saline flush treatment resulted in significantly reduced digestion times compared to the untreated group. Pairwise comparisons of donor bodyweight, warm ischemia time and cold ischemia time were made using a two-tailed student's t-test to

detect significant differences between the heparin treated and non-treated donor groups. Significance was defined as $p < 0.05$.

Islet Purification

Tissue pellets were re-suspended in cold HTK-PEG solution and triturated several times with a 25 mL serological pipette and then a 30 mL syringe. The tissue was passed through a 500 µm steel mesh to remove large, undigested debris. [17] The tissue digest was collected in clean 225 mL centrifuge tubes and pelleted at 400 rcf for 5 min at 4°C and the supernatant discarded. Pellets were dried by inverting the tubes on sterile gauze for 60 s and then weighed. The tissue was re-suspended in HTK-PEG solution at an approximate concentration of 0.1 g per mL and stored at 4°C for a minimum of 45 min. [114,115]

After the cold incubation period, an initial test gradient purification was performed to verify the appropriate density for islet purification. Fifteen mL of tissue/HTK-PEG suspension was combined with 6.5 mL of the high osmolality iodixanol stock to bring the density of the medium to 1.110 g/mL and incubated on ice for 5 minutes. The tissue digest was deposited beneath 25 mL of RPMI with 10% BCS in a 50 mL centrifuge tube to generate a two-layer discontinuous gradient. The gradient was centrifuged at 400 rcf for 5 minutes at 4°C. The entire supernatant (containing purified islets) was poured in a clean tube and centrifuged again while the pellet (containing exocrine tissue) was discarded. The second pellet, which contained the purified islets, was evaluated by dithizone staining for exocrine

contamination before processing the remaining tissue. If necessary, the density of the gradient medium was modified in order to achieve a minimum target islet purity of 60%.

Islet purity was evaluated by visual inspection at 24 h after isolation under a light microscope using dithizone stain to distinguish islets from non-islet tissues. [116] Dithizone stain (Sigma Aldrich) was prepared by dissolving dithizone in dimethyl sulfoxide (DMSO) at 10 mg/mL, and then diluting with PBS to a concentration of 0.2 mg/mL, and was added to islet suspensions at 10% v/v. To obtain purity, five representative samples from each donor were stained and examined via bright field microscopy. Islet purity was estimated to the nearest 5% for each sample and the values were averaged to obtain the final purity. Pairwise comparisons between the tail/body and whole pancreas groups were made using a two-tailed student's t-test. Significance was defined as $p < 0.05$. Isolations with islet purity below 60% were considered unacceptable, and were not used for further studies.

Islet Culture

Isolated canine islets were cultured in 150 mm petri dishes in 25 mL of CMRL 1066 media (with a glucose concentration of 5.6 mM) supplemented with 10% fetal bovine serum, 2 mM glutamine (GIBCO® GlutaMAX, ThermoFisher Scientific), and an antibiotic-antimycotic (GIBCO® Anti-Anti 100X, ThermoFisher Scientific) at 37 °C and 5% CO_2 at a maximum density of 5000 islet equivalents per dish. [19,117] Media was exchanged the morning after isolation followed by every other day at a minimum of 50% by volume.

Islet Yield Assessment

Islet yields of each isolation were calculated according to the standard method of conversion to islets equivalents, or "IEQ", which accounts for the size variation of native islets. [23] Due to the size disparity of canine donors, islet yield was also calculated per gram of digested tissue and per kilogram of donor bodyweight.

Pairwise comparisons between tail/body and whole pancreas groups of islet yield was done using a one-tailed student's t-test to determine whether yield per gram of digested pancreas was significantly higher in the tail/body group. Pairwise comparisons of donor bodyweight, warm ischemia time and cold ischemia time were made using a two-tailed student's t-test to detect significant differences between the groups. Significance was defined as $p < 0.05$.

Viability Assessment

Islet viability was evaluated using a live/dead fluorescence assay. Islets in PBS were stained with calcein AM and PI at 4 µM and 1 µg /mL, respectively and imaged by fluorescence microscopy. [19,118] Dithizone stain (described above) was added at 10% v/v to distinguish islets from exocrine and ductal tissue, which were not included in the viability calculations. Fluorescence images were analyzed using Adobe Photoshop CC. The percentage of dead cells was obtained by dividing the number of red pixels (propidium iodide) per islet by the total islet pixels. Data are reported as percent viability. Viability was assessed between 24 and 72 h after isolation. Twenty-five individual islets per isolation were analyzed to determine the percent viability. Pairwise comparisons

between the tail/body and whole pancreas groups were made using a two-tailed student's t-test. Significance was defined as $p < 0.05$.

Glucose Stimulated Insulin Secretion via Static Incubation

Glucose stimulated insulin secretion (GSIS) of the isolated canine islets was evaluated by static incubation of islets in buffers containing varying levels of glucose. All glucose solutions were made in an EBSS (Earl's Balanced Salt Solution) buffer with 0.1% BSA and sodium bicarbonate added, pH 7.4 at 37°C. [117] All incubation steps were completed at 37 °C at 5% CO_2. First, islets were equilibrated to the basal medium of 2.8 mM glucose for 1 h. Using Transwell inserts (8.0 um pore size) in a 24-well plate, approximately 50 islets were transferred to a low glucose condition of 2.8 mM glucose, followed by 22.4 mM (high) glucose, and finally 30 mM KCl, a standard insulin secretagogue [119] for 90 min each. Supernatant media was collected after low, high, and KCl incubations and stored at -80 °C until insulin quantification was performed. GSIS was assessed after 3 and 7 days of culture.

Insulin concentration was determined with alphaLISA insulin assays (Perkin Elmer, Waltham, MA) and a EnSpire® plate reader (Perkin Elmer) equipped with the corresponding alpha technology. Assays were carried out according to the manufacturer's instructions with insulin standards fit to a 12-point curve fit to a 5-parameter logistic curve. Insulin concentration data were then used to calculate stimulation indices, which is the ratio of insulin secretion in high glucose to low glucose. Stimulation indices of islets from the tail/body and whole pancreas isolation groups were compared using a two-tailed

student's t-test to identify significant differences in insulin secretion between the two groups. Significance was defined as $p < 0.05$.

Results

Effect of Pre-mortem Heparin and Ductal Saline Flush

The method reported herein incorporated two additional steps to enhance enzymatic digestion of the pancreas compared to previously reported procedures. [103,120,121] First, heparin sulfate was administered pre-mortem to prevent blood coagulation within the pancreatic tissue after euthanasia. Second, the pancreas was distended with cold saline solution and then rinsed by immersion in cold saline followed by enzymatic perfusion. We detected no significant difference in donor bodyweight, warm ischemia time, or cold ischemia time between the heparinized and non-heparinized donors (**Table 3.1**). Digestion time was significantly reduced when heparin and saline treatments were included compared to the untreated group (**Figure 3.1**). Pancreatic tissues digested quickly and uniformly after heparin and ductal saline flush treatments. Without treatment, the pancreatic digest contained larger and more granular particles that were unable to pass through a 500 μm screen, indicating incomplete and non-uniform digestion. Furthermore, isolation results obtained from the untreated pancreata were considered unacceptable for further evaluation because they did not meet our minimum criteria of 60% islet purity.

Regional Distribution of Endocrine Cells in Canine Pancreas

The distribution of islets within the pancreas is not uniform in the dog, as reported previously.[104,122] Specifically, the body and tail of the canine pancreas has been reported to contain more glucagon and insulin-positive cells, indicating more islet tissue compared to the head of the pancreas.[21,123] We examined portions of the canine pancreas using immunohistochemistry and immunofluorescence. **Figure 3.2** illustrates typical images from canine pancreatic sections from the head, body and tail of the pancreas. Insulin staining was less frequently noted in the head compared to other sections of the pancreas, and was most abundant in the tail region. The same was true of glucagon and somatostatin. However, glucagon-positive cells were rare in both the head and body sections, and were often found surrounded by the appearance of acinar cells rather than other islet cells as shown in **Figure 3.2**.

To further identify whether glucagon cells were located independently of the islet structures in the canine pancreatic head, body and tail, triple-labeled immunofluorescence was employed. Typical images are shown in **Figure 3.3** from each region. In the head, there was no co-localization of the insulin- or somatostatin-positive cells corresponded with glucagon staining. In fact, there were almost no glucagon-positive cells noted in the head of the pancreas, corresponding to the results noted using immunohistochemistry (**Figure 3.2**). The body and tail both displayed larger islets with a mixture of insulin-, glucagon-, and somatostatin-positive cells. In the body and tail, all three cell types were found both in islet structures and as independent cells scattered through the exocrine tissue.

Effect of Pancreas Region on Yield of Islets

Due to the uneven distribution of islets within the pancreas, we conducted studies to determine whether exclusion of the head of the pancreas would improve the efficiency of the islet isolation process. Pancreata were divided into two groups for the regional islet isolation studies (W and TB), as shown in **Table 3.1**. In group W, the whole pancreas was digested, while only the tail and body of the pancreas were digested in group TB. There were no significant differences in the warm or cold ischemia times or donor bodyweights between the two groups (W vs TB, **Table 3.1**). **Table 3.2** summarizes the isolation outcomes for the two groups, and illustrates that the total tissue mass digested in the whole pancreas group was nearly double that in the tail and body group. When the average islet yield (IEQ) was normalized to donor bodyweight, there was no significant difference in the total islet yield between the two groups (**Figure 3.4A**). However, when the islet yield was normalized to the actual mass of pancreas digested, isolation from the tail/body region was far more efficient (**Figure 3.4B**).

Islet Purity, Morphology, and Viability

While yield was greater per gram of tissue when only processing the body and tail of the pancreas, the final purity of each preparation was not different between the two approaches. Dithizone staining was used to distinguish between islet and non-islet tissues. Representative bright field images are shown in **Figure 3.5** *(top row)***.** Islets from both groups displayed typical morphology, indicated by smooth, round edges and strong red dithizone staining. **Table 3.2** shows that the percentage of islet cells in each preparation was approximately 70%, regardless of the starting tissue.

Islet viability was evaluated after isolation via a fluorescent live/dead assay with a representative image shown in **Figure 3.5** *(bottom row)***.** Green fluorescence staining within the islet clusters indicated live cells, and red fluorescence identified necrotic cells. The average islet viability for the whole pancreas isolations was 95.5 +/- 0.60 % and for the body and tail was 95.4 +/- 0.2 %. The results demonstrate very good viability of isolated islets from both groups and no significant difference between them.

Glucose Stimulated Insulin Secretion

Islet function was evaluated via glucose stimulated insulin secretion. Islets were incubated in low (2.8 mM) and then high glucose (22.4 mM) and the secreted insulin in each condition was quantified and normalized to the IEQ. Secretion indices (SI), or the ratio of secreted insulin in high glucose to that in low glucose, were measured at 3, and 7 days post isolation. **Figure 3.6** displays SI values for the whole pancreas and tail and body groups. Analysis detected no statistical differences in secretion index between the groups at either time point. Secretion indices were greater than or equal to 2 for all measurements, demonstrating good secretory function of the islets.

Discussion

In this series of studies, we describe a combination of techniques for optimizing and simplifying canine islet isolation from sub-optimal donor sources. Pancreatic tissues for veterinary islet transplantation will likely be from off-site cadaveric donors, and will inevitably be exposed to prolonged warm and cold ischemia. Unfortunately, all of these factors are known to markedly diminish islet yield and quality. [79–82]

Islets are purified via density gradient centrifugation, exploiting their lighter native density compared to pancreatic exocrine cells. Periods of warm or cold ischemia cause significant edema (swelling) of the pancreatic tissue, which alters the cellular density and thus diminishes isolation quality. [81,124] The extended ischemia times inherent to off-site, post-euthanasia pancreas procurement exacerbate this cellular swelling, often to a point when successful isolation of islets is impossible. Fortunately, numerous strategies have already been employed in human islet isolation research to prevent and even reverse ischemic damage, generally through the use of colloid-containing organ preservation solutions and hyperosmotic density gradient media. [16,78,125–128] However, these strategies have been applied primarily to beating-heart human donor pancreata processed with specialized islet isolation equipment, and are not well known to be effective with canine tissue and under the sub-optimal conditions described above.

For these studies, we utilized a modified HTK preservation solution containing polyethylene glycol (PEG) as a colloid, because PEG is known to have many protective effects against cellular swelling and ischemic injury in general. [129–131] Further, there is emerging evidence of the benefits of PEG for islet isolation and transplantation specifically. [106,132] Then, we added a hyperosmotic iodixanol stock to this modified HTK solution to create a custom, easily adjustable density gradient solution at approximately 450 mOsm/kg. Mildly hypertonic environments between 400-500 mOsm/kg have been shown to selectively increase exocrine tissue density over islets, thus enhancing purification efficiency. [11,12,14,112,133] With the benefits of these readily accessible materials,

we were able to achieve consistent, high quality islet isolations without the use of the Ricordi chamber and other complex, specialized equipment.

Vascular flushing has become standard practice for human pancreas preservation for islet isolation, but requires extensive training, and increases the time and cost of pancreas procurement substantially. [16,78,108] As such, this technique is not well suited for veterinary applications. In lieu of traditional vascular flushing, we incorporated a pre-mortem heparin injection followed by a ductal purging step directly prior to enzyme perfusion. Further, the treatment reduced average digestion times by 18 min per pancreas, and drastically improved isolation outcomes. These results are well in line with previous reports that shorter digestion times strongly correlate to both higher numbers of islets recovered per pancreas as well as IEQs per gram. [134]

In contrast to humans, islet cell distribution and islet morphology are highly disproportionate throughout the canine pancreas. Wieczorek et al. showed that the majority of islet cells were located in the left lobe (i.e. tail and body) and were large and compact. [104] Conversely, the right lobe (i.e. head) contained mostly single cells and small islets, along with pancreatic polypeptide cells. The histological evaluations described here further corroborate these findings. Thus, we evaluated the effect of completely omitting the head of the pancreas in islet isolation as a means of increasing processing efficiency and reducing material costs. Islet yield per gram essentially doubled when only the tail and body were used while viabilty, purity, and function of the islets were not affected.

To our knowledge, this is only the second report of successful islet isolation from deceased canine donors [103], and the first to do so without the use of the Ricordi system and with up to 90 minutes of cold ischemia time. Islets isolated by our method were 95% viable, had good purity and were responsive to glucose stimulation. We obtained an average of 1868 IEQ/g of digested pancreas (tail/body), which compares favorably to the median of 608 IEQ/g reported by Vrabelova et al. [103] Woolcott et al. reported yields of approximately 3600 IEQ/g, but pancreata in these studies were obtained from heart-beating donors with no reported cold ischemia. [121] Similarly, Lakey et al. reported a range of 3800 – 4490 IEQ/g using a comparable enzyme blend, but again used heart-beating donors and did not report any periods of cold ischemia. [135] Unfortunately, these ideal experimental conditions are likely unattainable for veterinary applications, and would raise considerable ethical concerns. In contrast, our method, which utilized deceased donors with extended periods of warm and cold ischemia, acheived yields of greater than 1500 IEQ/kg of donor bodyweight. Generally, between 5,000-10,000 IEQ per kg are needed to reverse diabetes in canines. [67,70,99,136,137] Thus, our method could obtain, from a single 35 kg canine donor, enough islets to reverse diabetes in a 10 kg recipient.

The implications of these results move the field one step closer to a clinical canine islet isolation procedure. There are indubitably other barriers that must be addressed such as immunoprotection and quality assurance of grafts. We, and others, continue to work on these challenges. Currently we are testing a variety of micro-encapsulation methods to block immune rejection without systemic immunocompromising drugs.

In conclusion, we have demonstrated a simple and repeatable method for isolating quality canine islets from deceased donors. Furthermore, our findings, in corroboration with previous histological studies [21], suggest that the head of the canine pancreas contains almost no recoverable islet tissue, and may be safely omitted from the isolation process. While efforts to improve upon these processes should certainly continue, these results represent a promising step forward in overcoming one of the most critical barriers to veterinary islet transplantation.

Chapter 3 Figures and Tables

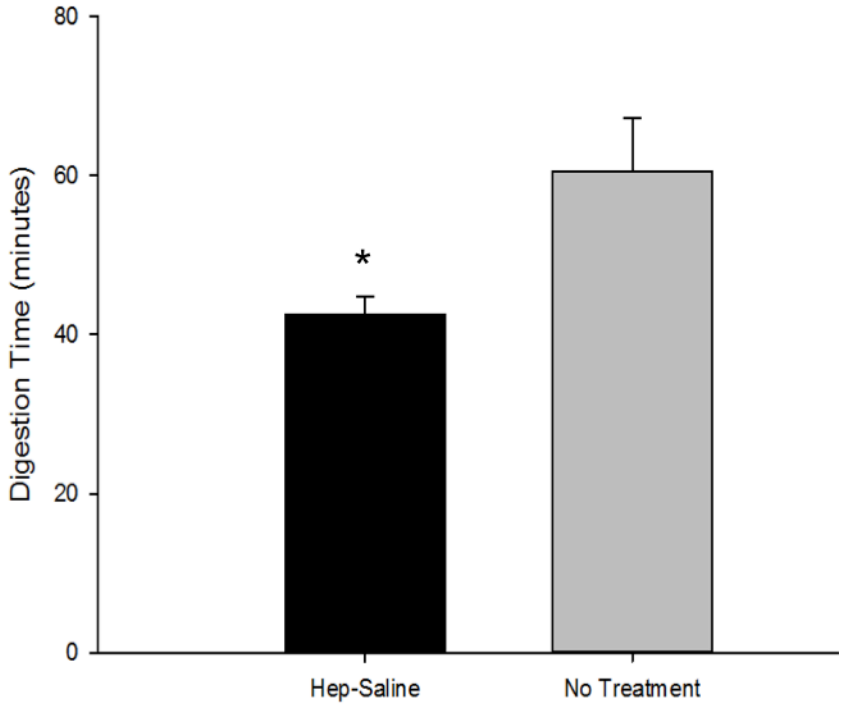

Figure 3.1. Effect of heparin and ductal flush.
The effects of pre-mortem heparin and post-mortem ductal saline flushing steps on enzymatic digestion were evaluated. Digestion times were reduced significantly when these steps were incorporated (* denotes significance, p= 0.01; N=6 for the Hep-Saline group and N = 4 for the no treatment group).

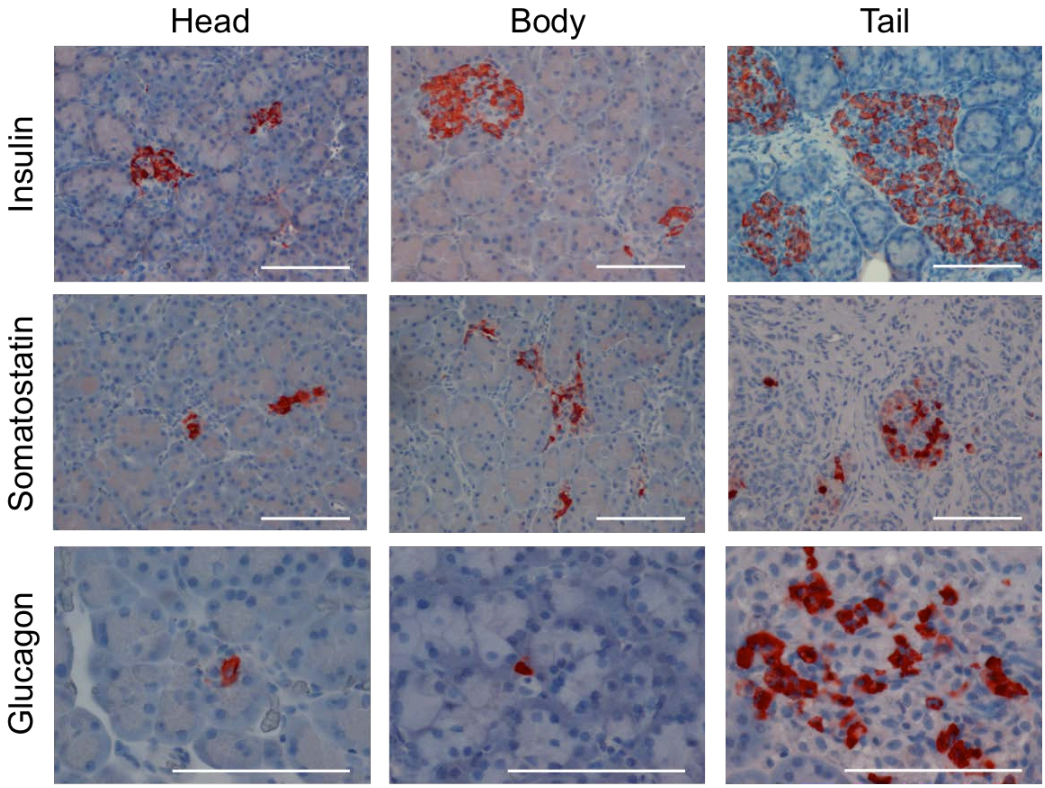

Figure 3.2. Immunohistochemistry of canine pancreas by region.
Tissue sections of the three major regions of the pancreas were stained with antibodies for insulin (*top row*), somatostatin (*center row*), and glucagon (*bottom row*) to identify the three major islet cell types (beta, delta, and alpha cells, respectively). Insulin positive cells were primarily located in the body (center column) and tail (*right column*), with the highest concentration and largest sized clusters in the tail. Insulin positive cells in the head of the pancreas (*left column*) were far less prevalent and occurred primarily in very small clusters or single cells. Similar patterns were observed for somatostatin, while glucagon positive cells were present in extremely low numbers in the head and body and often appeared as isolated single cells. Glucagon images are displayed at higher magnification to better illustrate single cells. Scale bars = 200 μm.

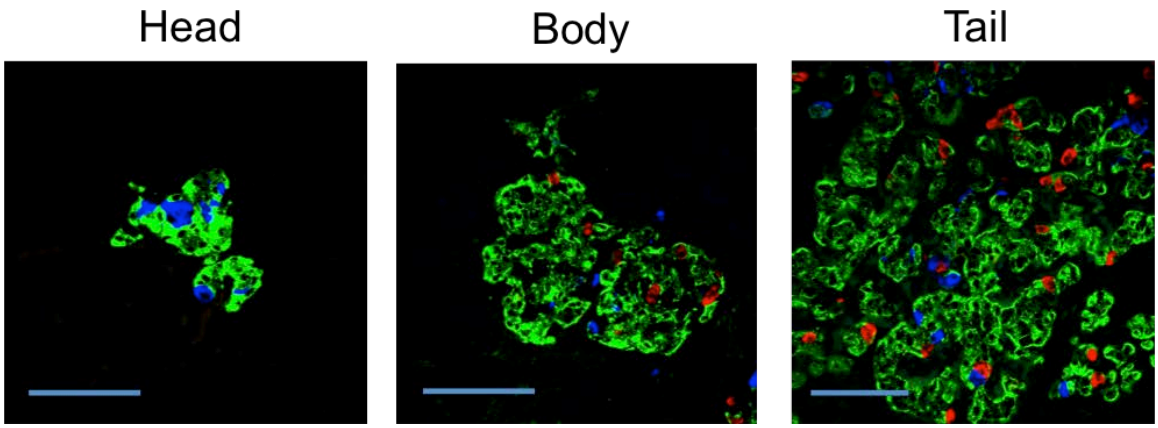

Figure 3.3. Immunofluorescence of canine pancreas by region.
Pancreatic sections were triple-stained with fluorescent antibodies for insulin (*green*), glucagon (*red*), and somatostatin (*blue*) to identify variations in the co-localization of pancreatic cell types within different regions of the pancreas. Interestingly, glucagon-positive cells were rarely observed in the head of the pancreas, and were typically not co-localized with insulin- and somatostatin-positive cells. Insulin- and somatostatin-positive cells were co-localized in the head region, and were typically in clusters of only a few cells. In contrast, the tail and body region contained structures consisting of large numbers of cells that predominantly contained all three endocrine cell types, with the highest concentration and largest clusters of cells located in the tail region. Scale bars = 100 μm.

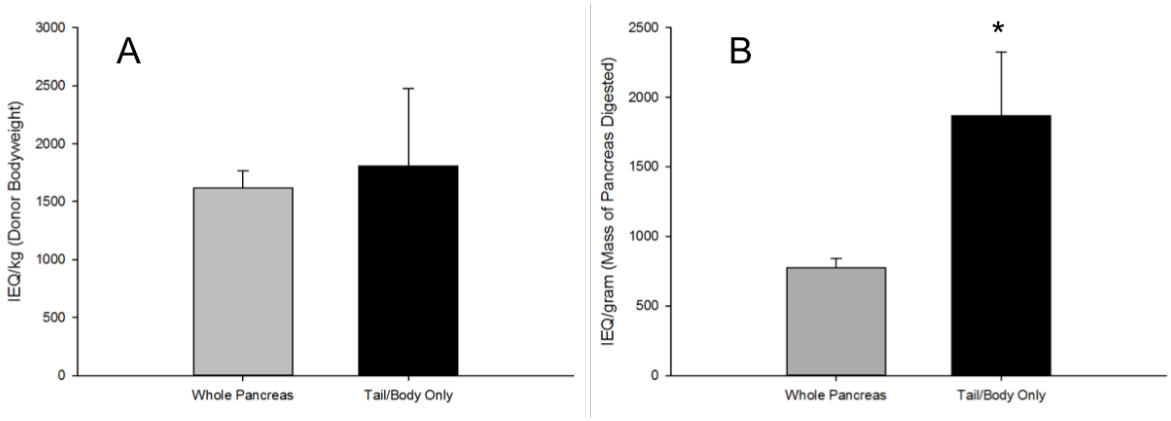

Figure 3.4. Effect of pancreas region on islet yield.
The effect of processing only the tail and body of the pancreas were evaluated. No significant difference in islet yield was observed when the whole pancreas was processed versus only the tail and body **(A)**. IEQ values were normalized to donor bodyweight (per kg) to account for the high variability of canine donor size. Islet yield per gram of tissue digested was significantly improved by omitting the head of the pancreas from processing **(B)** (* denotes significance, p = 0.04; N=3 per animals/group).

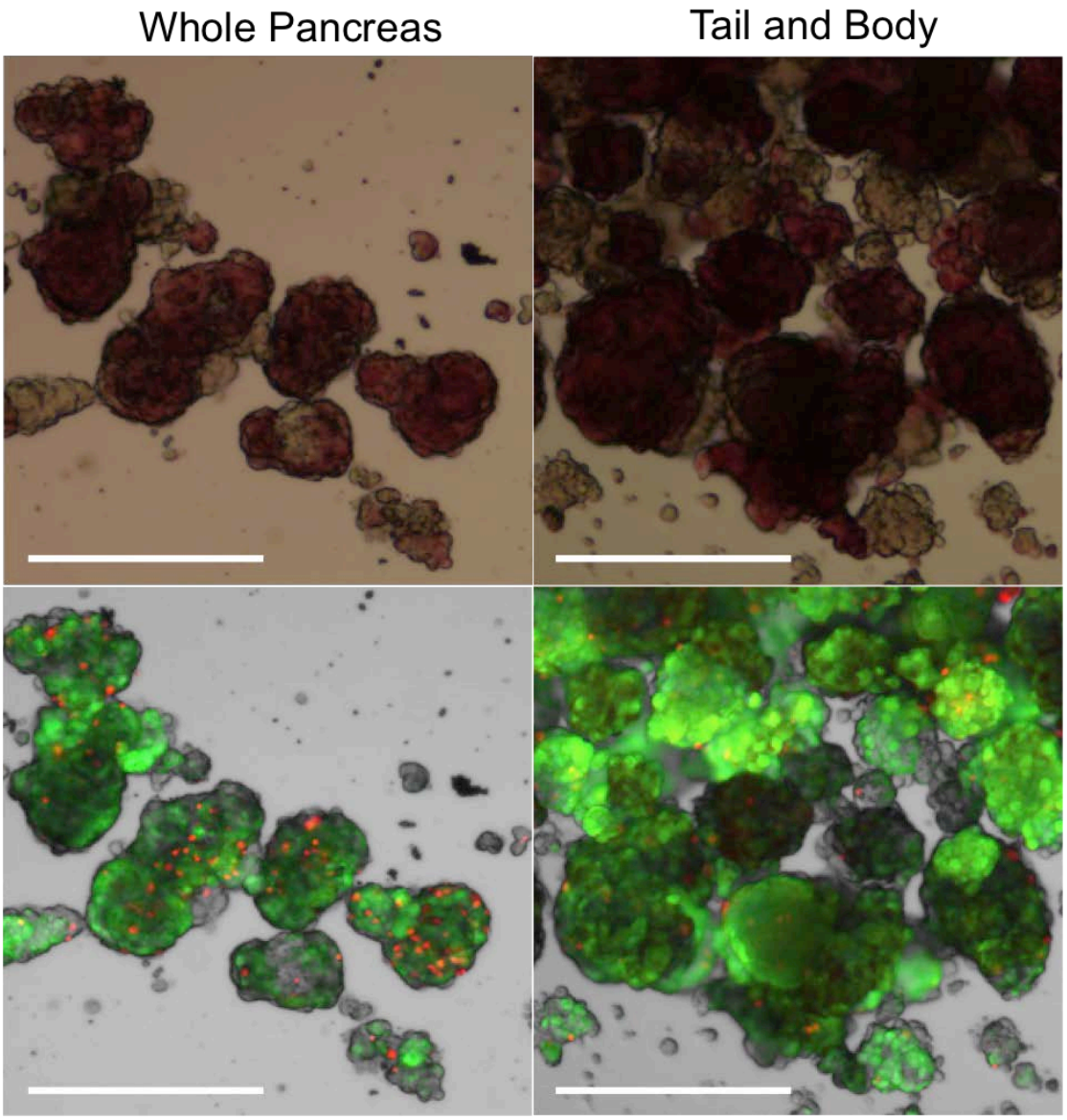

Figure 3.5. Morphology and viability of isolated islets.
Morphology and viability of isolated islets were evaluated. Islets isolated from both groups (whole pancreas or tail/body only) had healthy capsules and stained deep red with dithizone, which binds to insulin within the islet (*top row*). Islets were co-stained with a live (green fluorescence) and dead (red fluorescence) stain (*bottom row*). Islets showed strong green fluorescence and sparse red fluorescence, indicating highly viable islets. Scale bars = 200 μm.

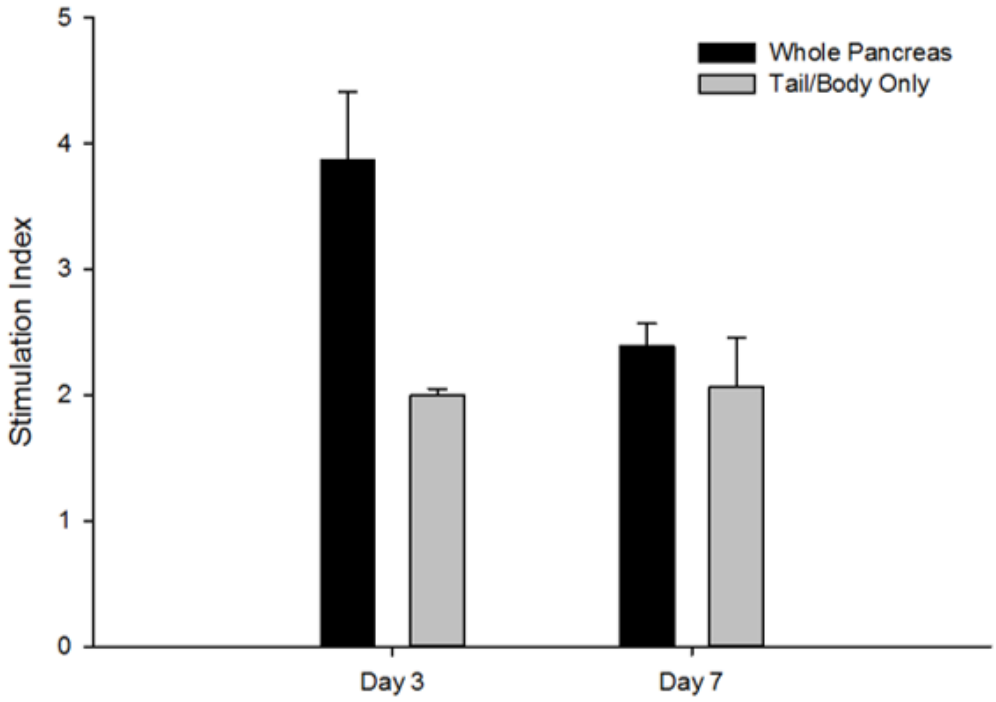

Figure 3.6. Glucose stimulated insulin secretion.
Islet function was evaluated over time via glucose stimulated insulin secretion assay. Islets were exposed to low then high glucose, and the secreted insulin in each condition was quantified to calculate a stimulation index, or SI (high secretion/low secretion). SI's were calculated separately for tail/body isolations and for whole pancreas isolations. Differences in SIs between the groups were not significant at either time point (N=2 per group).

Animal ID	*Breed*	*Gender*	*Age(years)*	*BW(kg)*	*WIT(minutes)*	*CIT(minutes)*
			Whole Pancreas			
W1	Lab/Pitbull	M	N/A	21	17	90
W2	Hound	M	2	25	7	86
W3	Pitbull Mix	M	2	20	13	72
Average	***-***	***-***	***-***	***22.0***	***12.3***	***82.7***
SE	-	-	-	*1.7*	*2.9*	*5.5*
			Tail and Body			
TB1	Shepherd Mix	M	1	21	23	75
TB2	Hound	M	2	31	10	72
TB3	Wheaton Terrier	M	2	20	23	87
Average	***-***	***-***	***-***	***24.0***	***18.7***	***78.0***
SE	-	-	-	*3.5*	*4.3*	*4.6*
			No Heparin/Ductal Flush			
NH1	Pitbull Mix	M	0.5	10	28	77
NH2	Pitbull/Shar Pei Mix	F	2	23	25	72
NH3	Shepherd Mix	F	5	20	20	90
NH4	Chow Mix	M	4	10	20	150
Average	***-***	***-***	***-***	***15.9***	***23.2***	***97.2***
SE	***-***	***-***	***-***	***3.3***	***2.0***	***18.0***
			Histological Study			
IHC1	Boxer	F	8	27	20	85
Combined Average (All Donors)	***-***	***-***	***-***	***20.7***	***18.7***	***86.9***
SE	-	-	-	*1.9*	*1.9*	*6.7*

Table 3.1. Pancreas donor information.
Abbreviations: W, whole pancreas; TB, tail and body; NH, no heparin/ductal flush; IHC, immunohistochemistry; N/A, not available; BW, bodyweight; WIT, warm ischemia time; CIT, cold ischemia time; SE, standard error

Animal ID	Tissue Mass Digested (g)	Total IEQ	Purity (%)
	Whole Pancreas		
W1	40	29,014	76
W2	57	39,134	63
W3	40	36,283	73
Average	***45.7***	***34,810***	***70.7***
SE	*5.7*	*3,012*	*3.9*
	Tail and Body Only		
TB1	12	16,964	67
TB2	35	49,335	74
TB3	23	62,626	74
Average	***23.3***	***42,975***	***71.7***
SE	*6.6*	*13,559*	*2.3*
Combined Average (All Isolations)	***34.5***	***38,892***	***71.2***
SE	*6.3*	*6,474*	*2.1*

Table 3.2. Islet isolation outcomes by pancreas region
Abbreviations: W, whole pancreas; TB, tail and body; IEQ, islet equivalents; SE, standard error

CHAPTER 4: Evaluation of a Hyaluronic Acid Hydrogel as an Alternative to Alginate for Immunoprotected Islet Transplantation[‡]

Abstract

Alginate has long been the material of choice for immunoprotection of islets for its low cost and ability to easily form microspheres. Unfortunately, this seaweed-derived material is notoriously prone to fibrotic overgrowth *in vivo,* resulting in premature graft failure. The purpose of this study was to test an alternative hyaluronic acid and denatured collagen hydrogel (HA-COL), for *in vitro* function, viability and allogeneic islet transplant outcomes in diabetic rats. *In vitro* studies indicated that the HA-COL gel had diffusion characteristics that would allow small molecules like glucose and insulin to enter and exit the gel, while larger molecules (70 and 500 kDa dextrans) were impeded from diffusing past the gel edge in 24 hours. Islets encapsulated in HA-COL hydrogel showed significantly improved *in vitro* viability over unencapsulated islets and retained their morphology and glucose sensitivity for 28 days. When unencapsulated allogeneic islet transplants were administered to the omentum of out-bred rats, they initially were normoglycemic, but by 11 days returned to hyperglycemia. Immunohistological examination of the grafts and surrounding tissue indicated strong graft rejection. By comparison when using the same out-bred strain of rats, allogeneic transplantation of islets within the HA-COL gel reversed diabetes long-term and prevented graft rejection in all animals. Animals were sacrificed

[‡] In Press as **Harrington, S.**, Williams, S., Rawal, S., Ramachandran, K., Stehno-Bittel, L., "Hyaluronic Acid/Collagen Hydrogel as an Alternative to Alginate for Long-Term Immunoprotected Islet Transplantation," *Tissue Engineering: Part A*, **2017**

at 40, 52, 64, and 80 weeks for evaluation, and all were non-diabetic at sacrifice. Explanted grafts revealed viable islets in the transplant site as well as intact hydrogel with little or no evidence of fibrotic overgrowth or cellular rejection. The results of these studies demonstrate great potential for HA-COL hydrogel as an alternative to sodium alginate for long-term immunoprotected islet transplantation.

Introduction

Islets transplantation will most likely remain an experimental treatment while immunosuppressive therapy is required. The reality is that, for the majority of type-1 diabetics, the health risks of chronic immunosuppression may outweigh the potential enhanced quality of life granted by an islet transplant. Indeed, between 1999 and 2007, less than 400 islet transplantations were performed in the United States, while prevalence of this disease stands at approximately 1.25 million cases of type-1 diabetes nationwide.[138,139] Extensive effort has been put forth to address this striking treatment gap. Numerous strategies have been employed toward eliminating the requirement of chronic immunosuppression, including immunomodulation via antigen-specific regulatory T cells, patient specific stem cell-derived autologous beta cells, and a trove of immunoprotective devices, capsules, and coatings.[76,140,141] Of these, immunoprotection by hydrogel encapsulation has received the greatest consideration as one of the most readily translatable approaches for the clinic.

Immunoprotection by gel encapsulation, in general, provides two key advantages. First, the extensive body of research surrounding this concept spans more than three decades, providing a wealth of fundamental knowledge and robust evidence of safety and efficacy to better facilitate translation.[47,54,142] Second, immunoprotection enables transplantation of allo and xenogeneic (e.g. porcine) islets, the latter a promising approach to the critical barrier of donor scarcity.[143,144] To this point, immunoprotective hydrogel systems could have tremendous future utility in the safe delivery of stem cell-derived islet surrogates.[145] Scharp and Marchetti recently published an extensive review summarizing numerous

immunoprotection strategies along with several attempts to commercialize them.[76] Of the various strategies, hydrogel encapsulation remains a leading approach to achieving widespread clinical success of islet transplantation.

Inexpensive alginate hydrogel microcapsules have dominated the islet encapsulation realm since their introduction in 1980.[47] The nearly instantaneous gelation mechanism of these seaweed-derived alginate polymers enables simple fabrication of microcapsules that can be easily injected into a patient. Furthermore, these capsules have been established as both durable and non-toxic to host organisms.[55,101,142] However, due to the foreign nature of the material, they are notoriously prone to fibrotic overgrowth, ultimately leading to necrosis of encapsulated cells and premature graft failure.[48,55,56] Some progress has been made with the development of ultra-purification processes, surface treatments, co-encapsulated materials, and more stringent control of capsule microstructure, but despite these advances, the performance of alginate microcapsules still does not meet the clinical needs for islet transplants.[48–50,101,146]

Recently, native, “raw”, and biomimetic materials have been gaining attention as improved cellular scaffolds and delivery systems.[147,148] Such materials are intrinsically biocompatible with lower probability of inducing fibrosis, and may better sustain or direct cellular function of encapsulated tissues. Lim et al. demonstrated enhanced *in vitro* function and survival of rat islets within a self-assembling biomimetic peptide gel.[89] Liao et al. achieved similar results using an injectable saccharide-peptide gel.[149] In yet another study, a “biosynthetic” hydrogel loaded with VEG-F reversed diabetes in

syngeneic mice at a 40% reduction in islet dose.[88] However, these advanced, bioinspired hydrogels typically degrade too quickly to be effective for long-term immunoprotection of islet transplants.

Another material of particular interest for this application is hyaluronic acid (HA). Hyaluronic acid-based hydrogels have been steadily gaining recognition as an interesting class of biomaterial for tissue engineering and cell therapy applications due to their unique mechanical and biological properties.[90–92] In 2009, Vanderhooft et al. described the versatile rheological characteristics and tunable durability of a hydrogel system comprised of thiolated HA and denatured collagen (COL) and a polyethylene glycol diacrylate (PEGDA) cross-linker.[93] These HA-COL derived hydrogels are easily prepared under physiological conditions with shear moduli ranging from 11 to 3500 Pa. A commercially available version of this gel, sold under the brand HyStem-C, has recently been used *in vivo* for myocardial infarct repair in SCID mice and for osteochondral defect repair in rabbits.[94,95]

In light of the properties of this HA-COL derived hydrogel, the present study sought to evaluate this biomaterial as a replacement for alginate hydrogels in encapsulated islet transplantation, particularly with regard to graft failure related to fibrosis. Unlike previous work, the animal studies were designed to test duration of the islet transplant.

Methods

Canine Islet Isolation

Pancreata were obtained from canine donors at local veterinary clinics from animals scheduled for euthanasia for other purposes and with no known pancreatic disorders. Euthanasia was performed by the licensed veterinarian overseeing the care of each animal, and the clinical veterinarian confirmed death with loss of heart function. Collection of the donor pancreata after death from animals euthanized for reasons other than tissue procurement, was determined to be exempt from review by the Institutional Animal Care and Use Committee of the University of Kansas Medical Center. Canine islets were isolated from donors using a method adapted from Vrabelova et al. [103] Pancreata were removed after euthanasia at the clinic and transported to the laboratory on ice for islet isolation. Pancreata were digested with Liberase T-Flex (Roche Custom Biotech, Indianapolis, IN) and purified by discontinuous density gradient centrifugation with an iodixanol/HTK based density gradient medium (OptiPrep, Cosmo Bio USA, Inc., Carlsbad, CA), as is reported elsewhere. [111] The isolated canine islets were cultured in CMRL (Connaught Medical Research Laboratories) 1066 media supplemented with 10% fetal bovine serum, 2 mM glutamine, and an antibiotic-antimycotic at 37 °C and 5% CO_2. Islets were quantified by conversion to islet equivalents (IEQs) using standard methods. [23] Islet purity was evaluated via dithizone staining (0.2 mg/mL dithizone in PBS), and islets had to have a purity 60% or higher to be included in the studies.

Rat Islet Isolation

The use of rats for islet isolation and transplantation was approved by the Institutional Animal Care and Use Committee of the University of Kansas Medical Center. Islets were isolated from pancreata were procured from male and female Sprague-Dawley rats by collagenase digestion followed by discontinuous density gradient centrifugation with a Ficoll-based density gradient medium (Histopaque 1119 and 1077, Sigma Aldrich) as previously described. [17,18,150] Islets were quantified and cultured as described above.

Molecular Diffusion in HA-COL Gels

For diffusion studies, HA-COL hydrogels (HyStem-C, ESI Bio, Almeda, CA) were prepared according to the manufacturer's instructions with PEGDA as the cross-linker and poured into standard 24-well plates using custom silicone dividers to create gels with a single exposed vertical edge to facilitate uniform lateral diffusion. Gels were stored in phosphate buffered saline (PBS) overnight prior to testing to allow hydrogel swelling. Gels were approximately 5 mm in height at equilibrium swelling.

Molecular diffusion into HA-COL hydrogels was examined via fluorescein isothiocyanate (FITC) labeled dextrans of increasing molecular weight (dextran-fluorescein 3, 70, and 500 kDa, Molecular Probes, Eugene Oregon). Wells were loaded with FITC-dextran solution (0.1 mg/mL in PBS), and fluorescence at the gel/liquid interface was monitored for 24 hours in a Cytation 5 Cell Imaging Multi-Mode Reader (Biotek Instruments, Inc). Care was taken that the FITC-dextran solution did not cover the top of the gels to prevent diffusion from the z-direction. Diffusion was further analyzed by generating plot profiles of

the fluorescent micrographs using NIH ImageJ (black = 0 intensity) to quantify fluorescence intensity at given x coordinates within the gels. Specifically, the x coordinates were chosen to represent 200, 500 and 1000 μm from the edge of the gel with y values representing the average (line analysis) across the gel. Data are the average gray value of all pixels in the y-direction at a given x coordinate along the micrographs. Data were normalized to the average gray value of the surrounding medium outside the gel.

HA-COL Gel Encapsulation

HA-COL hydrogels were prepared according to the manufacturer's instructions for encapsulating cells (HyStem-C, ESI Bio, Almeda, CA). Canine islets were suspended in HA-COL gel precursor at approximately 5000 IEQ/mL. IEQ (islet equivalent) is the standard measure of islet volume with 1 IEQ equating to a spherical islet of 150 mm in diameter. [23] The cross-linker solution (PEGDA, MW 3,400 in PBS) was added and the suspension was thoroughly mixed. Finally, the gel precursor containing islets was distributed in 5 µL aliquots into 24-well non-tissue treated plates. Each well contained one 5 µL gel/islet construct with approximately 25 IEQ per gel. Gels were allowed to cross-link for 60 minutes. Subsequently, 500 µL of CMRL culture media (described above) was added to each well. Final constructs contained 1% gel polymer by weight.

Alginate Encapsulation

Ultrapure, sterile "RGD" conjugated sodium alginate (Novatech MVG GRGDSP peptide coupled alginate, FMC Biopolymer, Sandvika, Norway) was reconstituted in sterile

deionized water containing 300 mM mannitol (to maintain isotonicity) at a concentration of 1% by weight to match that of the HA-COL gels. Islets were suspended in the alginate solution at approximately 5000 IEQ/mL, and 5 µL droplets were added to individual wells of 24-well non-tissue treated plates containing 2.0 mL of cross-linking solution (100 mM calcium chloride, 5 mM barium chloride, and 5 mM HEPES at pH 7.4). Spherical gels formed upon contact with the cross-linking solution, and were allowed to cross-link for 10 minutes under mild orbital agitation. Gels underwent a 10-minute hardening phase in HBSS with 10 mM calcium chloride. Finally, the hardening solution was removed from each well and replaced with 500 µL of CMRL islet culture medium. All islets were encapsulated between two and four days after isolation and incubated at 37°C and 5% CO_2 in the aforementioned CMRL-based islet culture medium. Media was exchanged 50% by volume 3 times/week in all groups, including non-encapsulated controls.

Islet Morphology, Viability, and Survival

Color micrographs of dithizone (DTZ)-stained islets were taken to evaluate islet morphology over long-term culture (Axio Vert.A1 Inverted Microscope, Zeiss International).

Encapsulated islet viability and long-term survival was assessed in all groups at 3, 7, 14, and 21 days after encapsulation via propidium iodide staining and fluorescence microscopy (Cytation 5 Cell Imaging Multi-Mode Reader, Biotek Instruments, Inc). [118] Percent viability, or viable cell fraction, was calculated using procedures reported

elsewhere. [19] Results shown are the average viable cell fraction of at least 25 individually analyzed islets pooled from two separate islet donors for each group at every time point.

Glucose Stimulated Insulin Secretion

Glucose stimulated insulin secretion (GSIS) was tested on days 3, 7, 14, 21, and 28 using a method adapted from the standard Integrated Islet Distribution Program protocol. [151] Unencapsulated (control) islets were tested in Transwell inserts (8.0 um pore size). The islets within the inserts were moved between glucose solutions using sterile forceps after each incubation step. Conversely, islet gels remained in their original wells and glucose solutions were exchanged with a micropipette.

Glucose solutions were made in an EBSS (Earl's Balanced Salt Solution) buffer with 0.1% BSA and sodium bicarbonate added, pH 7.4 at 37 °C. Incubation in different glucose concentrations was done at 37 °C and 5% CO_2. Islets were first equilibrated to the basal medium with 2.8 mM glucose for one hour then exposed to fresh 2.8 mM (low) glucose and 22.4 mM (high) glucose for 90 minutes each. Supernatant media was collected after each incubation and stored at -80 °C until insulin quantification was performed. Tests were performed in triplicate on islets from three different canine donors for all experimental groups. Insulin concentration was quantified via Perkin Elmer alphaLISA insulin assays in conjunction with a Perkin Elmer EnSpire® plate reader. All assays were performed in triplicate according to the manufacturer's instructions using a 12-point standard curve fit to a 5-parameter logistic curve. Insulin concentration data were normalized to IEQ and reported as microIU/mL/IEQ.

Diabetic Rat Models

Outbred streptozotocin-induced diabetic (immune-competent) Sprague-Dawley rats were generated as allogeneic islet transplant recipients as described previously. [118] Diabetes was defined as an average non-fasting blood glucose (NFBG) above 300 mg/dL over three consecutive daily readings. Four diabetic rats received immunoprotected (encapsulated) islet transplants within the HA-COL gel and two received islets without gel as controls to validate allo-rejection in the present model.

Three diabetic rats were given sham surgeries (i.e. without islets) as diabetic controls. Three non-diabetic rats were also included to monitor long-term blood glucose levels in aging rats.

Islet Transplantation in HA-COL Hydrogel and Non-encapsulated Controls

Rat surgeries followed our previously published protocols. [17,18] Briefly, animals were anesthetized by ketamine/xylazine and isoflurane (as needed), positioned in dorsal recumbency, and abdominal fur was shaved and surrounding skin sterilized with iodine. A vertical midline incision was made through the abdominal muscle, and the stomach and greater omentum were gently exteriorized and placed on a small sterile pad. A thin layer of HA-COL gel precursor solution containing the PEGDA cross-linker was applied to the entire omentum and was allowed to cross-link until the gel solution was no longer fluid. Islets, suspended in approximately 200 µL of gel precursor, were applied to the omentum on top of the base gel layer. Care was taken that the islets were located near large blood vessels to maximize nutrient exchange. The islet/gel layer was given

sufficient time to cross- link and the omentum was folded into a pouch-like structure and sutured onto the stomach wall. Finally, the stomach/gel/omentum construct was gently returned into the peritoneal cavity and the abdominal incision was closed.

Islets were transplanted at a minimum dose of 10,000 IEQ/kg into the omentum for all recipients. For encapsulated transplants, a thin layer of blank HA-COL gel was applied to the omental surface, followed by deposition of the islets suspended in HA-COL gel precursor. After gelation was complete, the omentum was sutured to the stomach wall to secure the transplant. For animals receiving transplants without hydrogel, islets were mixed with a sterile microfribrillar collagen hemostat (INSTAT MCH, Ethicon, Inc. Somerville NJ) to form a paste-like substance to hold the islets in place.

Animal Monitoring

Non-fasting blood glucose (NFBG) measurements were taken daily for the first 14 days post-transplant or until graft failure was observed, in which case the animals were sacrificed. Over time, the frequency of glucose readings was reduced to a minimum of once per week. Graft failure was defined as a return to a diabetic state as described above.

Graft Explantation and Evaluation

Upon sacrifice, the omenta of transplant recipients were removed and preserved for histological evaluation. The preserved tissues were embedded in paraffin and sectioned at 7 μm thicknesses. A total of forty total sections were collected and stained with either

H&E or a triple fluorescent stain for insulin, glucagon, and somatostatin as described previously. [113] Micrographs were examined to assess islet health, morphology, and cell composition at the transplant site, and to evaluate biocompatibility and durability of the HA-COL gel. For cell composition analysis, every fifth section was evaluated to ensure that cells were not counted multiple times, and a total of 70 unique islet sections were counted. When a potential overlapping islet was identified, its cells were not analyzed.

Data Analysis

Viability data were evaluated for significant differences by two-way repeated measures ANOVA. Pairwise comparisons were evaluated via the Holm-Sidak test for significant differences between individual group means. Significance was defined as $p<0.001$ for these comparisons as the data did not pass assumptions of normality or equal variance. Insulin secretion data was evaluated for significant differences by two-way repeated measures ANOVA because tests were repeated at each time point on the same sets of islets. Pairwise comparisons were not evaluated for insulin secretion data as the primary ANOVA was not significant.

Results

Diffusion in HA-COL Hydrogels

Micrographs of diffusion using fluorescent dextrans were acquired over a 24-hour period (**Figure 1**). Diffusion of the 3 kDa probe was very rapid, with significant penetration into the gel after just two minutes. Little diffusion of both 70 kDa and 500 kDa probes was observed at the two-minute time point. Diffusion of the 500 kDa probe appeared minimal

even after 24 hours of incubation. Interestingly, accumulation of the 70 kDa probe near the gel edge was observed and appeared to increase with time, as indicated by more intense fluorescence relative to the surrounding medium. Some accumulation of the 500 kDa probe near the gel edge also appeared to be present at later time points, but was minor. Edge accumulation was not observed with the 3 kDa probe.

Images were further analyzed by quantifying the relative fluorescence intensity (pixel intensity) at various distances from the gel edge over time, normalized to the fluorescence of the liquid medium. **Figure 2** provides histograms of the fluorescence intensities of the probes over time at 200, 500, and 1000 μm from the gel edge. All probes eventually showed substantial diffusion to 200 μm after 24 hours, with the 3 kDa probe reaching equilibrium with the medium by the 90-minute time point. At 5 and 24 hours, the 70 kDa dextran intensities were 125% and 166% of the medium at 200 μm, respectively, corroborating the fluorescence accumulation observed near the interface. By comparison, the 500 kDa probe showed 68% and 90% relative fluorescence at the same time points. Fluorescence of 3 kDa probe at 1000 μm was detected quickly at only 10 minutes, surpassed 50% relative intensity by 90 minutes, and was equal to that of the liquid medium at the 24-hour time point. There was negligible fluorescence measured from the 70 and 500 kDa probes at 1000 μm until the 60-minute time point, and relative fluorescence intensity reached 41% and 33% at 24 hours, respectively.

Viability and Survival of Encapsulated Islets

The percentage of viable canine islet cells on day 3 was consistent across all groups as no significant differences were detected and all were between 97 and 98%. Differences in cell survival were non-significant through day 7 of the study period, though the HA-COL gel groups showed a slight increase in the viable cell fraction over day 3 values (**Figure 3**). On days 14 and 21, cell viability was statistically higher in both gel groups compared to the controls, though viability was still over 97% for each group.

Encapsulated Islet Morphology

Figure 4 displays representative micrographs of encapsulated and non-encapsulated control islets stained with dithizone at 3 and 21 days in culture. Images of alginate-encapsulated islets were cloudy due to the optical properties of the alginate material. Islets in all groups appeared healthy and showed robust dithizone staining over the duration of the study. In the gel groups, islets generally remained separated from one another as well as from exocrine and ductal tissue carried over through the islet isolation process. However, in the control unencapsulated group, islets (dark red stained) were more likely to fuse to remnant ductal and/or exocrine tissue (brown, unstained) present in the culture dish, as seen in the left column of **Figure 4.** By day 21, cells appeared to be sloughing off from unencapsulated (control) islets but not the islets in gel (**Figure 4, bottom row**), which is consistent with the increased cell death observed in the control group at later time points. While single cells were also seen in the HA-COL images, they were, most likely, small tissue debris/fragments generated during the islet isolation process that subsequently became trapped in the gel. In the control group, this small

debris was removed during media exchanges. Thus, on day three, the control islets appeared clean compared to the gel groups. At day 21, however, cells in the control group appeared to originate directly from the islets, where in the HA-COL group, single cells were isolated and appeared similar to those in the day 3 images.

Glucose Stimulated Insulin Secretion

A common measure of islet function is the “stimulation index” (SI): the ratio of secreted insulin at high (22.4 mM) to low (2.8 mM) glucose. The SI values were between 2 to 6 throughout the study, indicating that the islets were able to sense glucose and release insulin appropriately (**Figure 5**). Due to substantial variation in the data within and between groups, no statistically significant differences in SIs were detected at any time point.

Novel Method of Encapsulated Islet Transplantation

While *in vitro* work with the hydrogel was conducted using canine islets, transplantation studies into diabetic rats were designed to determine the degree of graft rejection within animal species, because xenotransplantation adds additional confounding complications [152] even when encapsulated. [153,154] Thus, rat islets were encapsulated to be transplanted into diabetic rats. Due to the slow-hardening properties of the HA-COL gel, a new method of bulk encapsulation had to be developed. As described in more detail in the Methods section, a thin layer of HA-COL gel precursor solution containing the cross-linker (PEGDA) was applied to the entire omentum and given time to harden (**Figure 6A**). Islets suspended in the precursor gel were applied to the top of the base layer (**Figure 6B**),

locating the islets near clearly visible blood vessels to maximize nutrient exchange. The islet gel layer was again given time to crosslink so that islets were attached to the base later of gel. Next the omentum was folded and sutured to the stomach wall, creating a pouch (**Figure 6C**), which was then returned to the peritoneal cavity.

Allogeneic Rejection Model Validation (non-encapsulated islet transplants)

In order to validate the presence of graft rejection in the outbred rat model, diabetic rats received allogeneic islet transplants without hydrogel. Recipients were non-diabetic within 2 days following transplantation and displayed normal NFBG, shown in **Figure 7.** On day 8, NFBG levels began to sharply increase in the control animals and by day 11 the rats were overtly diabetic. By comparison, diabetic sham rats failed to have a single blood glucose reading within the normal range (**Figure 7**).

Non-encapsulated omental transplants were recovered after graft failure was confirmed. Tissue from a healthy, non-diabetic rat omentum, stained with H&E, is also shown for comparison, predominantly composed of acellular fat deposits and blood vessels (**Figure 8A**). A representative image of the explanted tissue, is displayed at low and high magnification (**Figure 8B & C**, respectively)**.** Explanted grafts contained areas with large populations of densely packed nuclei with very little cytoplasm, indicative of a massive infiltration of lymphocytes and associated graft rejection. Furthermore, no islets could be identified in any of the tissue sections analyzed from each animal (six sections per rat).

Encapsulated Islet Transplantation Outcomes

When diabetic rats were transplanted with HA-COL encapsulated islets, all were insulin independent and considered non-diabetic immediately following transplantation. Average NFBG of the encapsulated transplant recipients over 1 year are shown in **Figure 9**. Data beyond 40 weeks include only 3 animals, as one was sacrificed at that time. Three of these rats were well controlled with no measured excursions falling within the diabetic range. The fourth rat had occasional values in the 200-250 range in the first 50 days, but those normalized from that time point forward to termination at 52 weeks.

The HA-COL gel transplanted animals were sacrificed for ethical reasons when indications of poor health, not related to diabetes, were observed. Axillary and mammary tumors were the primary justification for early termination in these studies among other neoplastic lesions. Such tumors are common in this strain when the animals reach advanced ages. [155] When possible, the islet grafts were recovered at the time of sacrifice and preserved for evaluation. No gel was noted in any portion of the peritoneal cavity outside of the omentum pouch.

Histological Evaluation of Explanted Encapsulated Islet Grafts

Explanted islet graft sections stained with H&E revealed intact hydrogel, characterized by light blue/purple acellular regions adjacent to the typical adipose tissue of the omentum (**Figure 10)**. Minimal eosin positive staining around the perimeter of the gel indicated a lack of fibrosis. **Figure 11A** contains representative immunofluorescence images of an encapsulated islet from the explants, containing brightly stained islets comprised of all

three major islet cell types. The average percent composition of the beta/alpha/delta cells from 70 islet sections from the explant is shown (**Figure 11B**).

Discussion

This study evaluated the potential of a HA-COL hydrogel as an encapsulant to improve long-term islet transplantation without immunosuppression. While HA hydrogels are becoming increasingly common in tissue engineering research, they have, to our knowledge, never been used for encapsulation and immunoprotection of pancreatic islets.

Immunoprotective materials must facilitate diffusion of nutrients and signaling molecules (e.g. glucose and insulin) while also preventing direct contact between immune cells and the encapsulated cells. Thus, we evaluated the diffusional properties of the HA-COL gel using fluorescent dextrans. A small 3 kDa dextran diffused rapidly into the hydrogel, suggesting that insulin would encounter little diffusional resistance (MW ~ 5.8 kDa). Interestingly, we observed marked accumulation of the 70 kDa probe at the gel/liquid interface. Thus, the probe was able to enter the gel fairly readily, but there was likely some form of thermodynamically favorable interaction between the large dextran and the hydrogel (e.g. conformational effects or van der Waals forces) that did not exist in sufficient magnitude with the smaller 3 kDa probe. [156] This may suggest that moderately sized proteins, such as albumin (~66.5 kDa) could diffuse into the gel *in vivo*, but with marked attenuation at greater diffusion lengths. The 500 kDa probe exhibited the least extensive diffusion, but was not blocked from the gel matrix entirely. However, it is important to note in considering a “molecular weight cut-off”, that dextrans are flexible

and mostly linear polymers, whereas immunoglobulins and antibodies are rigid, globular structures. Pluen et al. demonstrated that diffusion of linear polymers into hydrogels was substantially greater than globular proteins of similar molecular mass, noting that the latter became quickly entrapped within gel pores. [157] Thus, diffusion of high molecular weight globular proteins through this gel would likely be more limited compared to the FITC-dextran probes. While we did not characterize the average pore size of the hydrogels explicitly, infiltration of the 500 kDa dextran probe suggests that the average pore size of the HA-COL gel is large compared to other common hydrogels like those made from low molecular weight PEGDA. For example, Durst et al. described a 15% PEGDA (MW 3.4 kDa) gel with an average pore size of 5.94 nm. [158] By comparison, the reported hydrodynamic radius of a 500 kDa dextran is 15.9 nm. [46] Furthermore, because porosity and pore size are strongly correlated to cross-link density and polymer mass fraction of the hydrogel, these parameters could be easily controlled, if desired, by simply increasing the concentration of HA/COL, PEGDA (the cross-linker), or both.

When comparing the long-term islet viability, the alginate-RGD gel performed as well as the natural HA-COL gel over 3 weeks. The results were somewhat surprising given the more biocompatible characteristics of HA-COL. This result may be attributable to the RGD motif present in both gels, which has a well-documented benefit to islet viability *in vitro.* [89,159,160] Cheng et al. evaluated cardiosphere-derived cells in the same HA-COL gel with and without the RGD-containing (COL) component, and found that the HA-COL gel led to higher cell survival than the gel with HA alone. [95] While our data did not show a significant difference from the alginate-RGD material in terms islet viability *in vitro*, the

HA-COL gel facilitated a significant reduction in cell death over unencapsulated islets during long-term culture.

Islets in all groups, including controls, remained responsive to glucose stimulation throughout the entire 28-day study. Other publications have shown that cultured islets generally have near or complete loss of GSIS after 14 days, [23,24] but we did not see this in our studies. One difference in our procedure was the presence of acinar or ductal cells in our cultures, which have been shown to possess pro-islet properties, compared to typical *in vitro* studies done with highly pure or handpicked islets. [161] In fact, Murray et al. reported that pancreatic duct-derived epithelial cells improved glucose sensitivity *in vitro* compared to control islets, which lost nearly all response after 10 days. [162] Thus, it is possible that the presence of some non-islet cell types carried over from the isolation process contributed to the unanticipated persistence of islet function in the control groups. Overall, the results of this study may suggest that, at least in vitro, any beneficial effects of encapsulating materials on islet function are much less potent than cell-derived signals. However, additional studies would be needed to confirm this hypothesis.

Allogeneic transplants of islets in HA-COL hydrogels into diabetic rats reversed diabetes and showed no evidence of graft rejection or fibrosis in the recipients for up to 18 months. Immunofluorescence staining of explanted HA-COL grafts revealed healthy islets containing all three major islet cell types in a ratio and spatial distribution that is characteristic of healthy rat islets. [118,163] These results corroborate the excellent glycemic control observed *in vivo*, and demonstrate robust long-term biocompatibility and

immunoprotective capacity of the HA-COL gel. This is encouraging given the long history of biocompatibility issues surrounding alginate-based islet transplants, which are prone early graft failure due to fibrosis [54–59], although some progress has been made in this regard through advanced alginate purification and capsule optimization protocols. [48–53] However, the processes for improving alginate biocompatibility are complex and expensive; thus, an alternative encapsulant for islet transplantation is appealing.

There are clearly differences between the bulk-gel transplantation method described here and alginate microsphere-based transplants. Advantageously, we found that the targeted deposition of islets to the highly-vascularized regions of the omentum produced consistent, high quality transplant outcomes. However, this method is of course more invasive and less convenient than a simple injection of alginate beads, and therefore not ideal for clinical use. Considering this, our lab is currently developing a novel method for producing uniform islet-microspheres using this HA-COL gel, enabling a more clinically relevant delivery of the material.

The bio-stability of encapsulating materials is a critical factor for maintaining long-term immunoprotection of an islet graft. Several extracellular matrix- or bio-inspired hydrogels have been evaluated for islet transplantation, including self-assembling peptide gels and a VEG-F loaded PEG maleimide gel. [88,89,149] While these gels improved engraftment, they degraded much too quickly to be appropriate for long-term function *in vivo.* Conversely, the present HA-COL gel forms more durable covalent cross-links, and can be easily tuned

by modifying the component concentrations to improve gel strength further. For example, Vanderhooft et al. showed that when concentrations of HA and PEGDA were increased from 0.4% and 0.2% (formulation used in this study) to 1.6% and 1.6%, respectively, the shear modulus increased from 37 to 3500 Pa. [93] Even at the relatively low gel concentration used in this study, the HA-COL gel persisted for up to 18 months in the rat omentum.

In conclusion, this study demonstrates the potential of an HA-COL derived hydrogel as an effective alternative to alginate for long-term immunoprotected islet transplantation at a time when clinical outcomes of alginate encapsulated islet transplants have been disappointing. These promising results support further investigation of this HA-COL hydrogel for encapsulated islet transplantation.

Chapter 4 Figures

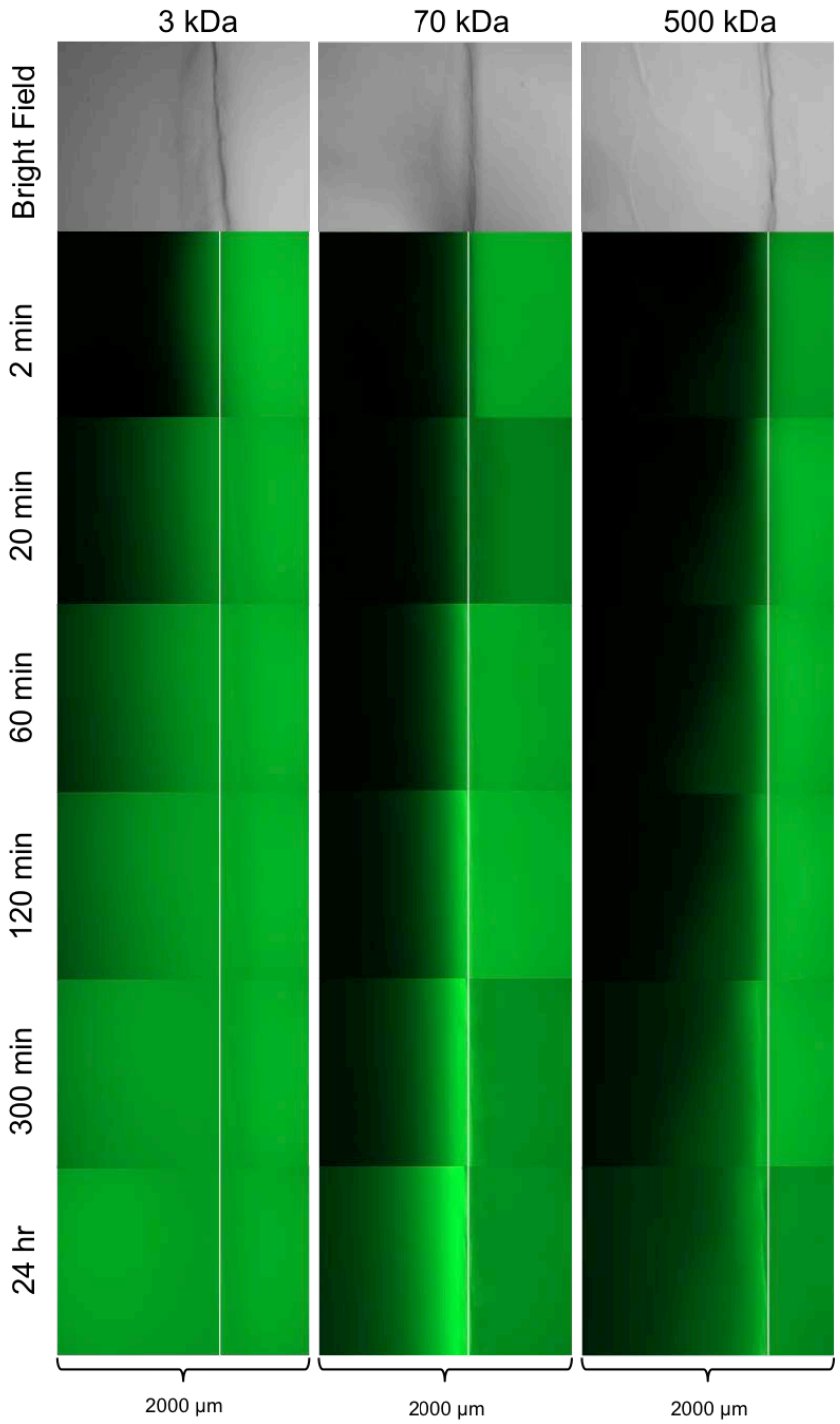

Figure 4.1. Diffusion into HA-COL hydrogels.
Fluorescence micrographs of 3 kDa (*left*), 70 kDa (*center*), and 500 kDa (*right*) FITC-dextran diffusion into HA-COL hydrogels were captured over 24 hours. Bright field images (40X) of the hydrogels are included at the top of each column for reference. Overlaid white lines represent the gel edge for each group. Dimensions of each individual micrograph were 1.4 x 2.0 mm.

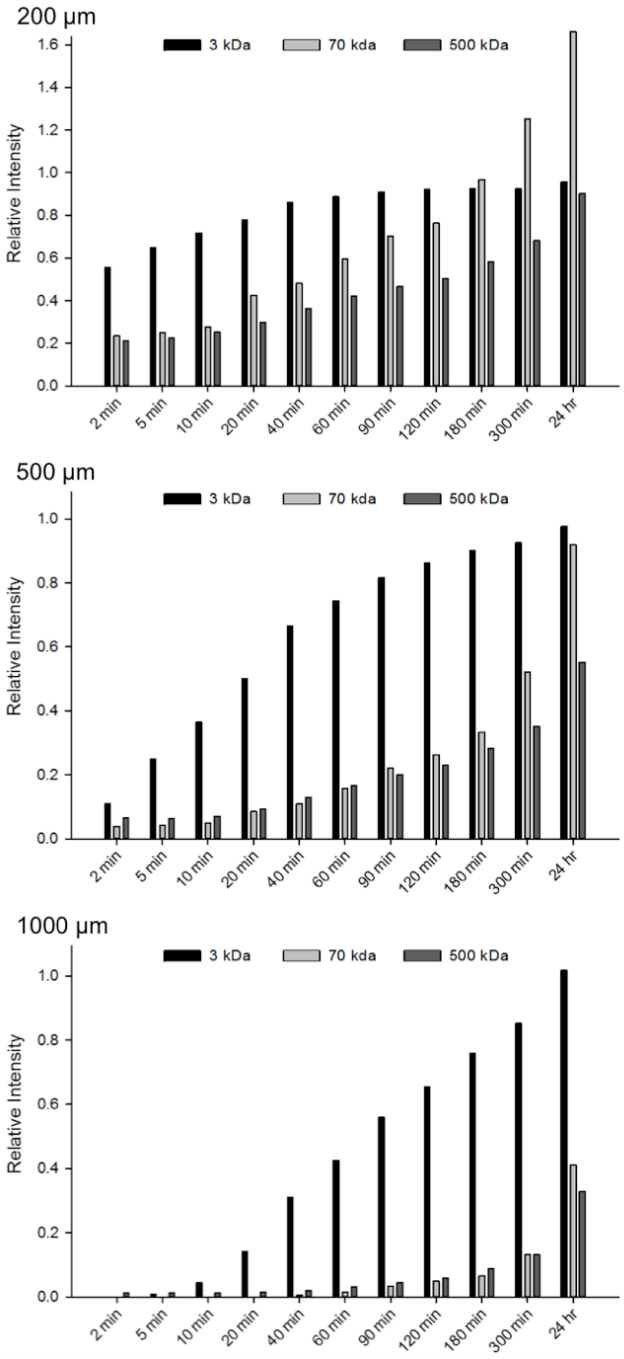

Figure 4.2. Fluorescence intensity of FITC-dextran diffusion into HA-COL gels.
Fluorescence intensities of 3, 70, and 500 kDa FITC-dextran probes were quantified at the x coordinates representing 200 µm (*top*), 500 µm (*middle*) or 1000 µm (*bottom*) from the gel edge and normalized to the surrounding liquid medium at several time points over 24 hours. Fluorescence intensity values were obtained by analyzing the micrographs such as those shown in Figure 1 using NIH ImageJ. The data shown are the average gray value of all pixels in the y-direction of the micrograph at a specified x coordinate (i.e. distance from gel edge).

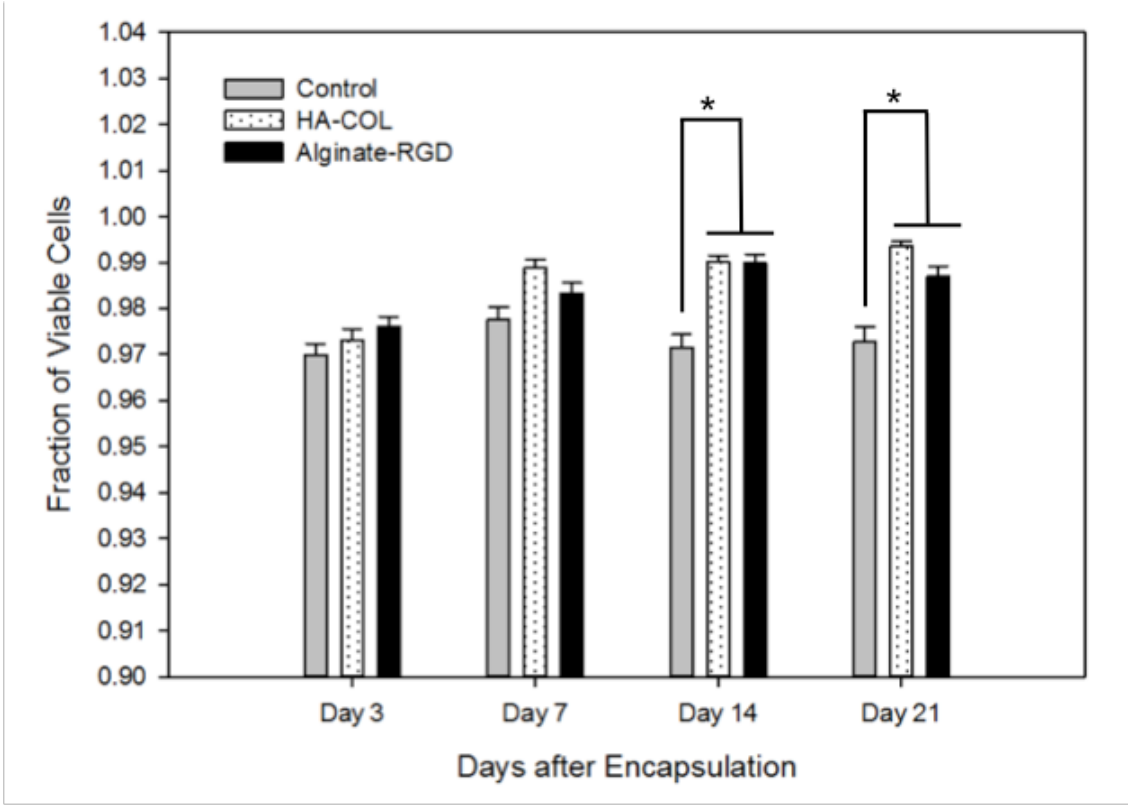

Figure 4.3. Encapsulated canine islet viability over three weeks.
Viability of canine islets was measured at 3, 7, 14, and 21 days after encapsulation in gel with comparison to unencapsulated controls. Values shown are the mean viable fraction of individual islets for each group and time point from two combined donors. Significant differences are denoted with an asterisk (N=25 islets or more group and time point; $p<0.001$).

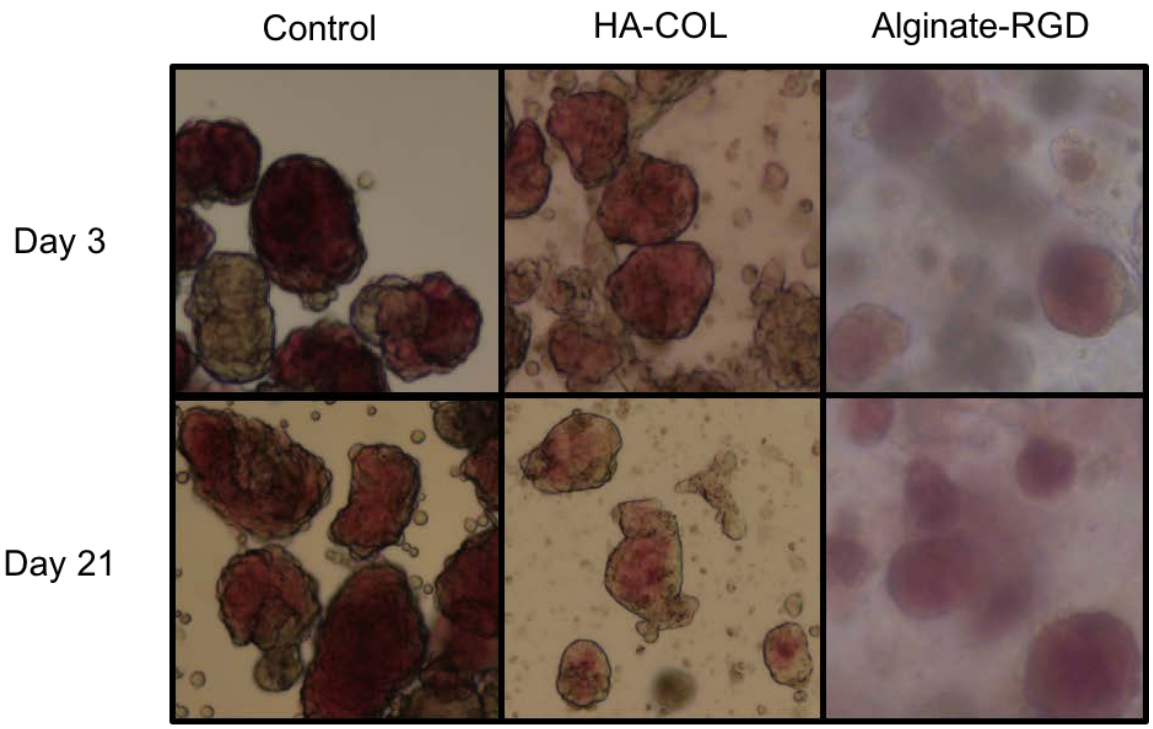

Figure 4.4. Encapsulated canine islet morphology.
Representative micrographs (40X) were taken of encapsulated and control canine islets stained with dithizone at 3 and 21 days for morphological evaluation. Dithizone, red color, indicates the presence of insulin, and thus identifies healthy beta cells. Islets the expected appearance of smooth, rounded edges. In the control group at day 21, however, single cells were seen sloughing off from the islets, which was not observed in the encapsulated islet groups. The cloudy appearance of the islets in alginate is a property of the gel.

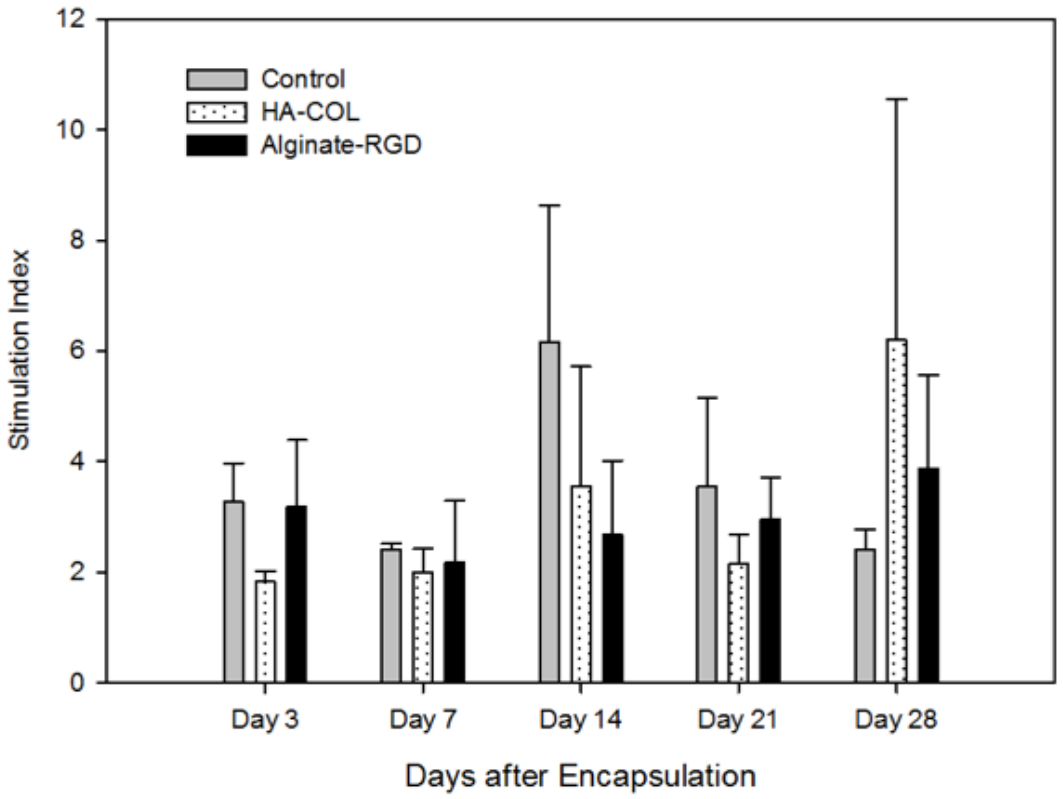

Figure 4.5. Glucose stimulated insulin secretion of encapsulated islets.
Stimulation indices (ratio of high glucose insulin secretion to low glucose secretion) were measured at day 3, 7, 14, 21, and 28 *in vitro* for encapsulated islets in HA-COL and Alginate-RGD hydrogels and for unencapsulated controls. The stimulation index for control cells in media did not change significantly over time, also was true for islet encapsulated in HA-COL and alginate. (N=3 donor animals). ($p<0.05$). Incubation periods were 90 minutes for both low and high glucose conditions.

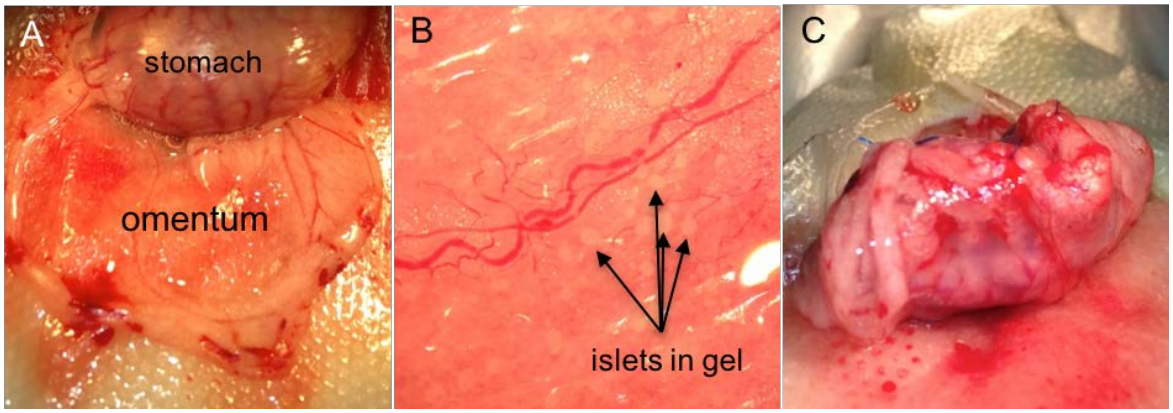

Figure 4.6. Photographs of the surgical procedure for transplantation of islets encapsulated in HA-COL hydrogel.
Islets were encapsulated and transplanted into the rat omentum following a novel three step protocol. The omentum was first exteriorized and a base layer of gel applied and allowed to cross-link **(A)**. Islets, suspended in a HA-COL precursor solution, were applied along large blood vessels for optimum nutrient exchange and the gel solution was allowed to solidify **(B)**. The omentum was then rolled up and sutured to the stomach wall to minimize disturbance of the islet graft **(C)**.

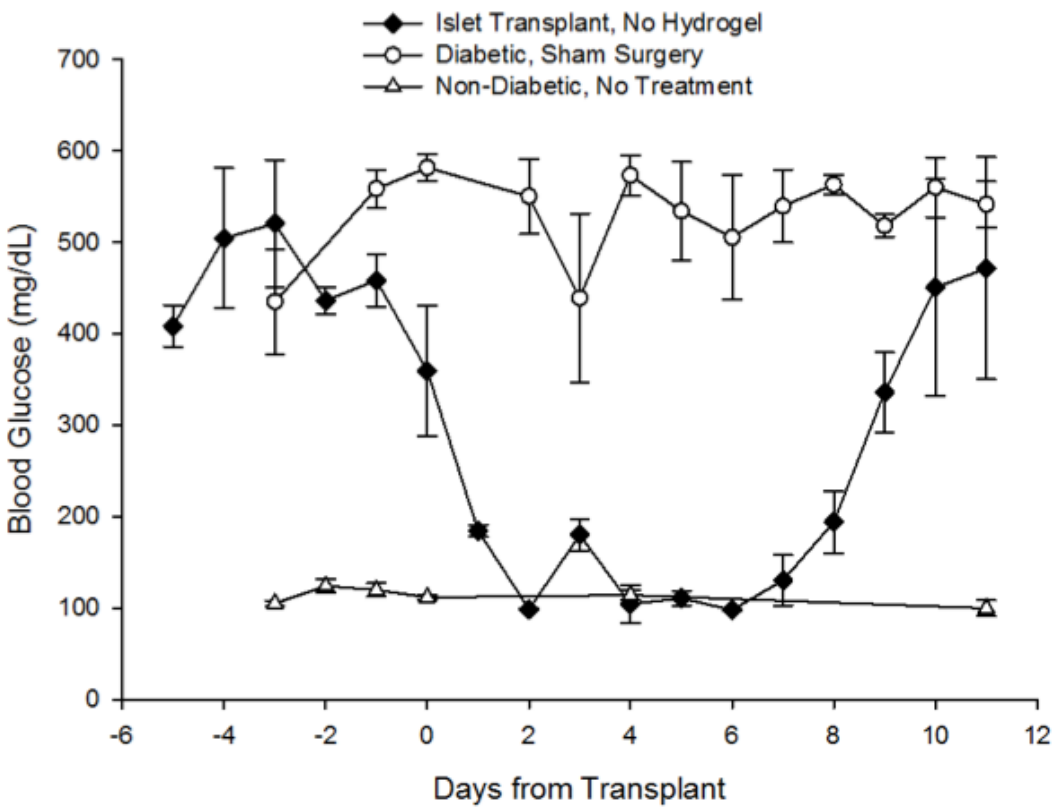

Figure 4.7. Blood glucose levels of control animals.
Non-encapsulated rat islet recipients (*black diamonds, N=2*) achieved normoglycemia initially, but by 11 days returned to a diabetic state after apparent allo-rejection of the transplanted tissue. Diabetic animals receiving sham surgery (*open circles, N=3*) without islets were hyperglycemic throughout the entire study period. For comparison, blood glucose levels of healthy, non-diabetic rats (*open triangles, N=3)* are also shown.

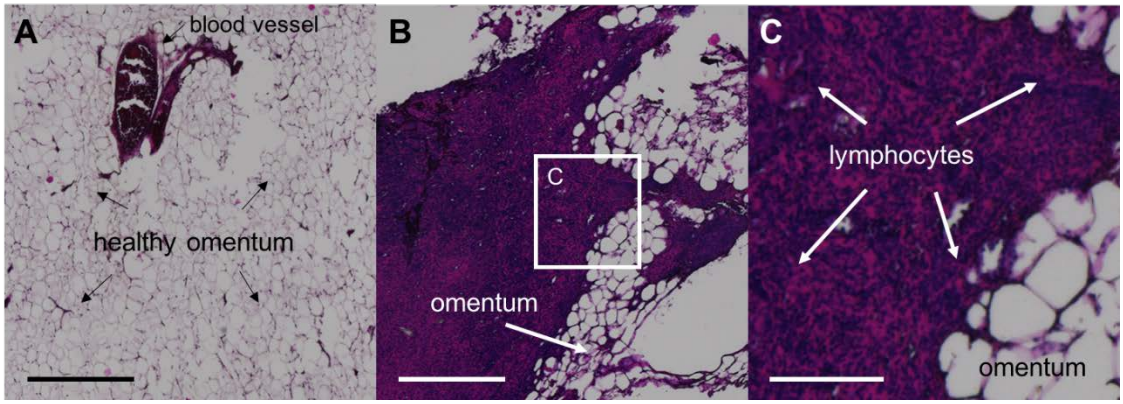

Figure 4.8. Hematoxylin and eosin staining of the omenta of unencapsulated islet transplant controls.

H&E stained section of a typical healthy, untreated rat omentum, shown for comparison **(A)** (scale = 0.5 mm; magnification = 40X). Omentum of rat transplanted with unencapsulated islets, explanted 11 days post-transplant after blood glucose levels indicated graft rejection had occurred **(B)** (scale = 0.5 mm; magnification = 40X). Higher magnification of the center image (white square frame) showing significant lymphocyte infiltration in the region **(C)** (scale = 150 µm; magnification = 200X).

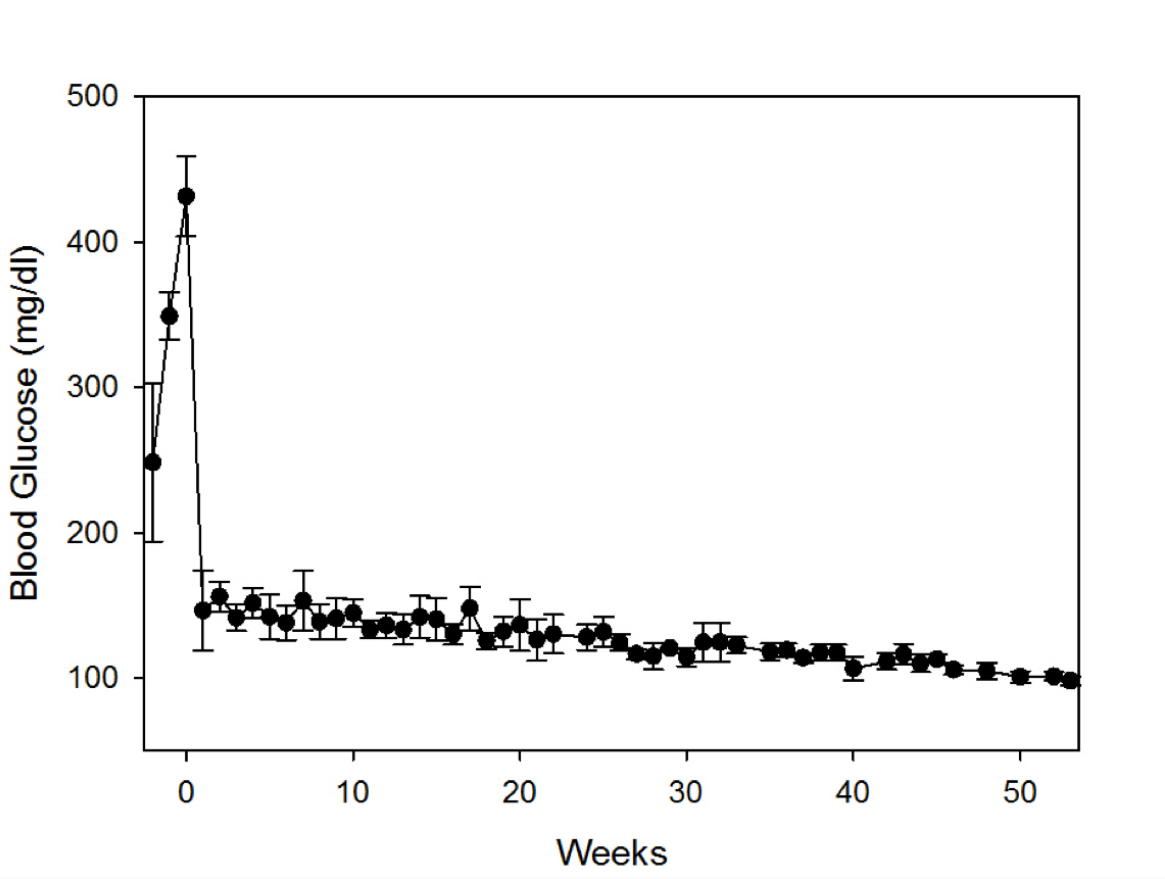

Figure 4.9. Transplantation of islets in hydrogel.
Average non-fasting blood glucose levels of 4 diabetic rats transplanted with islets encapsulated in HA-COL hydrogel over 1 year. “Day 0” marks the day of the islet transplant surgery. Values to the left of “day 0” were taken prior to transplant in order to confirm a diabetic state. All animals showed normal blood glucose levels at sacrifice. Data points beyond 40 weeks are from only 3 animals, as one animal was sacrificed at this time point.

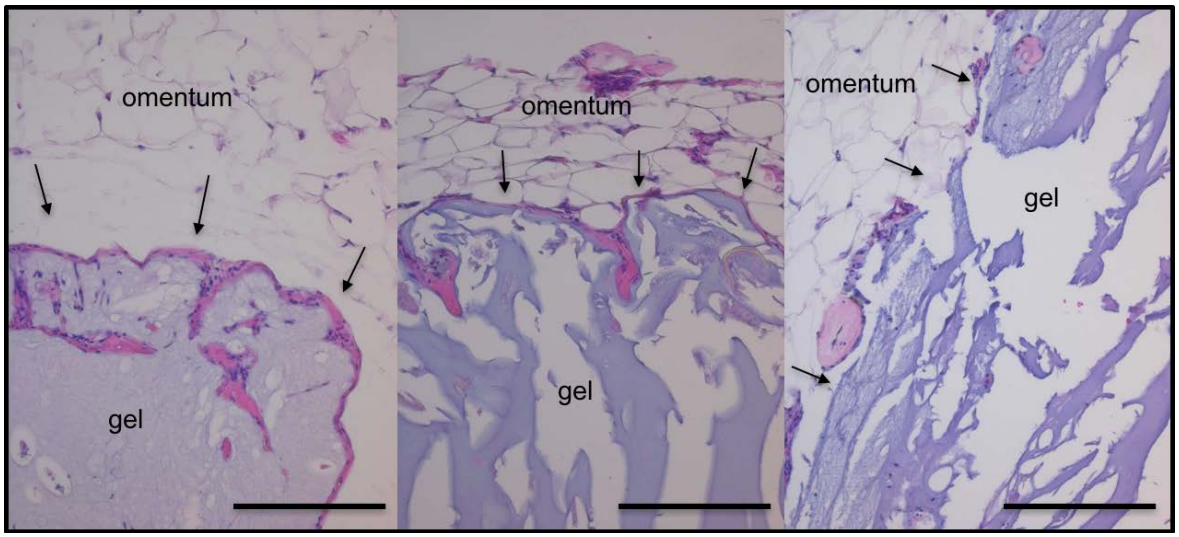

Figure 4.10. Hematoxylin and eosin staining of encapsulated islet transplants. Micrographs (200X) of H&E stained sections from the explanted graft showed intact hydrogel and very little or no fibrosis at the gel/tissue interface, indicated with black arrows. Tissues were explanted from rats that received encapsulated islet transplants at 40 (*left*), 52 (*middle*), and 64 (*right*) weeks post-transplant. The large open spaces around the explanted hydrogel material were due to changes in the gel's physical properties during paraffin embedding because of its high water content, which leaves the gel brittle and difficult to section. Scale bars = 200 μm.

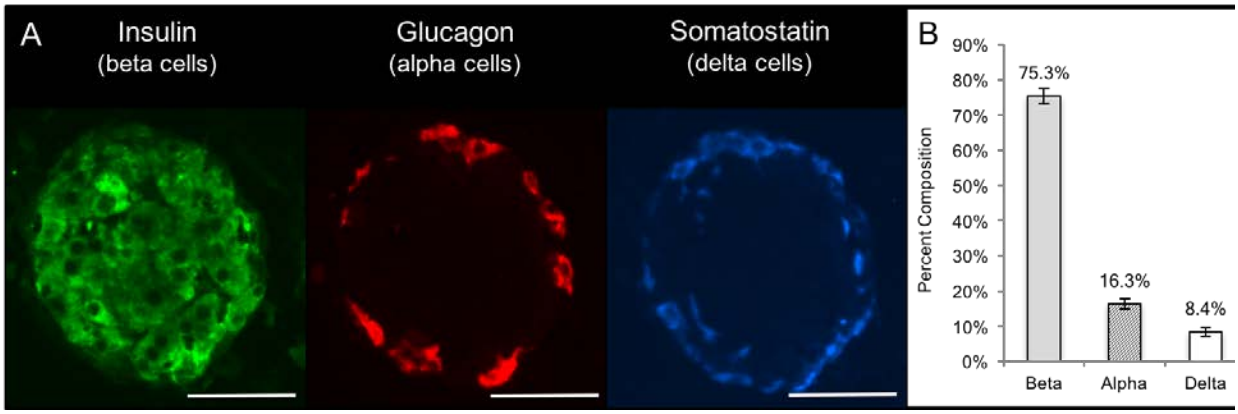

Figure 4.11. Immunohistochemistry of explanted islet graft.
Islets within the recovered graft displayed strong staining for the three major islet cell types – beta, alpha, and delta. Insulin is shown in green, glucagon in red, and somatostatin in blue **(A)**. Histogram of cell composition of islets found in explanted tissue (N=70 islet sections) showing normal distribution of rat islet cell types **(B)**. Scale bars = 50 μm, magnification = 400X.

CHAPTER 5: A Novel and Versatile Method for Producing Hydrogel Microspheres for Islet and Cell Encapsulation[§]

Abstract

Cell encapsulation, while predominantly associated with islet transplantation, is a rapidly expanding field with broad potential utility in stem cell therapies and tissue engineering research. Sodium alginate has dominated this space due to its easy preparation as injectable hydrogel microspheres, but has been historically fraught with poor performance *in vivo*. Furthermore, more advanced hydrogel biomaterials are beginning to emerge including hyaluronic acid (HA), chitosan, and functionalized polymers that offer improved chemical and mechanical performance. Methods for formulating these advanced materials as convenient microspheres are wholly absent, largely due to their typically slow gelation kinetics. Thus, we have developed a novel method to produce hydrogel microspheres compatible with this class of materials. In this study, microspheres were produced using both an HA-based hydrogel and a standard photo-cross-linked polyethylene glycol diacrylated (PEGDA) hydrogel, and then characterized to determine basic physical and chemical properties. HA and PEGDA spheres possessed markedly different properties, demonstrating the versatility of this method, and both were well tolerated *in vivo* in a two-week rodent implantation model.

[§] In preparation as **Harrington, S.**, Ramachandran, K., Stehno-Bittel, L. "A Novel and Versatile Method for Producing Hydrogel Microspheres for Islet and Cell Encapsulation," for *Biotechnology and Bioengineering*, **2017**.

Introduction

The concept of cell encapsulation was first popularized in 1980 by Lim and Sun, who showed that islets embedded in alginate hydrogel microspheres could reverse diabetes in rats without the need for immunosuppression, albeit for a only a few weeks. [47] This initial success, however, was followed by a flurry of research aimed at better understanding and improving this process. [42,49,59,164–176] Though great progress has been made, alginate microspheres have notoriously suffered from issues with long-term biocompatibility. [48,51,52,54–56] Despite these issues, alginate has persisted as the clear material of choice for islet encapsulation on account of its unique, near instantaneous cross-linking kinetics, enabling straightforward and nontoxic fabrication of convenient, injectable microspheres. Conversely, other hydrogels typically can only be prepared as bulk, macroscopic structures due to comparatively slower cross-linking rates. Some protocols have been developed for producing microspheres using alternative hydrogels such as agarose, chitosan, or hyaluronic acid (HA), but are based on oil-emulsions and are unattractive for cell encapsulation and transplantation due to harsh conditions and poor process control.[97,177,178]

Cell encapsulation strategies are gaining attention for other applications as well, including improved stem-cell delivery and three-dimensional (3D) tissue culture. In 2016, Landazuri el al. demonstrated that microencapsulated mesenchymal stem cells (MSCs) dramatically enhanced paracrine-mediated healing in a murine hind-limb injury model, showing increased survival and pro-angiogenic activity compared to unencapsulated MSCs. [179] Furthermore, manipulation of the physical and chemical properties of cell encapsulants

has become a powerful tool for tissue engineering research *in vitro*. [180] For example, Rockwood et al. demonstrated that increasing the stiffness of the encapsulating matrix directed MSC differentiation toward a more osteogenic path versus a chondrogenic path for softer materials. [181] In another study, rat neuronal cells cultured in a 3D collagen hydrogel showed better survival and behaved more like native neuronal networks compared to cells grown in 2D on the same material. [182]

As applications of cell encapsulation continue to grow in number and sophistication, the ability to fabricate convenient, injectable, biocompatible microspheres using advanced biomaterials would be decidedly useful. Here, a novel method is described for producing hydrogel microspheres, termed core-shell spherification. This method was strategically designed for use with hydrogels with much slower gelation rates compared to alginate, thus enabling the production of microspheres with a variety of chemical, physical, and bioactive properties. Furthermore, the method was developed for use with standard, GMP-ready equipment ("good manufacturing practice" e.g. closed, sterile environment, tight process controls, material certificates for all parts) to better facilitate accessibility, scale, and regulatory compliance.

To demonstrate the versatility of this new encapsulation procedure, we tested two different slow-gelation hydrogels, composed of either HA or polyethylene glycol diacrylated (PEGDA), and compared their properties with and without islets. In addition, we conducted a preliminary in vivo compatibility study in rats.

Methods

Isolation, Assessment and Culture of Canine Islets

Canine islets were isolated from pancreas donated locally from euthanized donors as described in Chapter 3 of this dissertation. Isolated islets were converted to islet equivalents, or "IEQ", for quantification purposes and evaluated for purity via dithizone staining. [23] Islets with a purity of < 60% were not used for the following studies. Canine islets were cultured in CMRL 1066 supplemented with 10% fetal bovine serum, 2 mM glutamine, and an antibiotic-antimycotic at 37 °C and 5% CO2.

Cytotoxicity of Calcium and Hydrogel Precursor to Canine Islets

Canine islets were exposed to solutions containing either 100 mM or 200 mM calcium chloride, 10 mM HEPES buffer, (4-(2-hydroxyethyl)-1-piperazineethanesulfonic acid), and 20% PEGDA, MW 3,400 (Laysan Bio, Inc.) for 5, 10, or 15 minutes. A group was also tested that contained 100 mM calcium chloride without the PEGDA component to evaluate the effect of calcium alone. Islets were suspended at approximately 5,000 IEQ/mL in the test solutions to reflect the high cell loading density associated with the encapsulation process. At the end of the test periods, the islets were washed twice with supplemented CMRL 1066 islet media and then incubated at 37 °C and 5% CO_2 for three hours prior to assessment.

Islet cytotoxicity was evaluated via propidium iodine staining and fluorescence microscopy. Fluorescence micrographs were captured with a Cytation 5 Imaging Multi-Mode Reader (Biotek Instruments, Inc, 531/647 nm ex/em). Cell death was quantified by

calculating the ratio of red (dead) pixels to total islet pixels using Adobe Photoshop as described previously.[19] Twenty-five individual islets were analyzed per group. Results are reported as the average viable cell fraction and normalized to islets from the matched, untreated controls.

Cytotoxicity of Ultraviolet Light Exposure and Photoinitiator to Canine Islets

Canine islets were suspended in Dulbecco's phosphate buffered saline (DPBS) containing 0, 0.025, or 0.05% (w.v) Irgacure 2959. Islets were loaded into wells of a 24-well plate and irradiated with long-wave ultraviolet (UV) light for 3, 5, or 10 minutes. Approximately 50 islets were in each test well in two mL of DPBS. A PortaRay 400 UV lamp was used for irradiation in low-power mode at a distance of 6", which corresponds to approximately 40 mW/cm^2 according to manufacturer data (Uvitron International). After exposure, islets were washed twice with supplemented CMRL 1066 islet media and then incubated at 37 °C and 5% CO_2 for three hours prior to assessment. Cell death was evaluated via propidium iodide staining and quantified as described in the previous section.

Fabrication of Hyaluronic Acid Hydrogel Microspheres

Hyaluronic acid hydrogel precursor was prepared by dissolving a thiolated HA (HyStem, Biotime Inc) at 1.2% (w/w) in a custom buffer containing 100 mM calcium chloride, 15 mM HEPES, and 20% (w/w) OptiPrep (CosmoBioUSA, Inc) as a density modification agent. The viscosity of the precursor solution was measured with a Cannon-Manning Semi-Micro calibrated glass capillary viscometer (size 200) at room temperature. The precursor was

extruded via automated droplet generator into a stirred bath of 0.15% (w/v) sodium alginate (Protanal LF 10/60, FMC Corp.) containing 300 mM mannitol, 0.1% Tween 20, 0.4% (w/v) PEGDA 3,400 (Laysan Bio, Inc), and adjusted to pH 7.6 using a custom 15 mM HEPES buffer. The droplet generation system utilized was a Buchi 395-Pro Encapsulator (Buchi Corporation, Newcastle, DE) equipped with an air jet nozzle system and a 400-micron diameter inner fluid nozzle within a 1.5 mm concentric air nozzle. The precursor solution was extruded at 1.5 mL/min with an airflow rate of 2.2 L/min using compressed nitrogen as the air source. Core-shell constructs formed upon contact with the bath that contained the hydrogel precursor in the spherical core. The constructs were stirred gently for 5 minutes in the original bath solution, then the bath was diluted by half with DPBS, which reduced the solution pH to 7.4. The bath was stirred for an additional 30 minutes to continue cross-linking of the HA precursor within the core. The core-shell constructs were next rinsed in a 25 mM citrate buffer in DPBS for 5 minutes under mild stirring to dissolve the alginate shells, collected using a steel mesh screen and suspended in DPBS. A second rinse in 50 mM citrate for 5 minutes was performed to ensure complete dissolution and removal of the alginate shell. Final HA microspheres were stored in DPBS. A general schematic of the hydrogel microsphere fabrication process, termed core-shell spherification, is provided for clarity in **Figure 5.1**.

Fabrication of PEGDA Hydrogel Microspheres

PEGDA hydrogel precursor solution was prepared by dissolving PEGDA 3,400 and 20,000 (Laysan Bio, Inc.) at 18% and 12% (w/w), respectively, in a custom buffer containing 100 mM calcium chloride, 10 mM HEPES, and 0.025% (w/v) Irgacure 2959.

The solution was filtered using a 0.22-micron syringe filter and the viscosity was measured as described above. The precursor was extruded as described above into a stirred alginate bath containing 0.15% (w/v) sodium alginate (Protanal LF 10/60, FMC Corp.), 300 mM mannitol, 0.1% Tween 20, 0.025% (w/v) Irgacure 2959, and adjusted to pH 7.4 using a custom 15 mM HEPES buffer to form core-shell constructs. All solutions for PEGDA microsphere fabrication were prepared in water degassed by sonication to eliminate excess oxygen, which can inhibit photo-cross-linking.[183–186] The bath containing the core-shell constructs was irradiated with long-wave UV light such that the irradiance at the center of the bath was approximately 40 mW/cm^2 (PortaRay 400, Uvitron International). Irradiation was applied at all times during extrusion of the precursor solution and for one minute after extrusion to ensure complete cross-linking of all core-shell constructs. Constructs were processed further as described above to dissolve the alginate shells.

Encapsulation of Canine Islets in PEGDA Microspheres

The PEGDA precursor solution was prepared as described above at 1.1X concentration (i.e. 110 mM calcium, 33% total PEGDA, etc) and later combined with a slurry of canine islets in CMRL 1066 media at volumetric ratio of 10:1 just prior to extrusion. Core-shell constructs were generated and cross-linked as described above using a fully enclosed sterile reaction vessel designed specifically for the Buchi 395-Pro Encapsulator to maintain tissue sterility. Alginate shells were removed as described above with the exception that Hank's Balanced Salt Solution (HBSS) was used in place of DPBS for all steps. Islet-PEGDA microspheres were transferred to supplemented CMRL 1066 islet

media and incubated at 37 °C and 5% CO_2. Media was exchanged completely one hour after fabrication.

Physical Properties and Size Distribution of Hydrogel Microspheres

Representative samples of the hydrogel microspheres were dispensed into a 24-well plate and imaged using a Cytation 5 Imaging Multi-Mode Reader (Biotek Instruments, Inc). Diameters of 100 individual microspheres were measured to determine the average microsphere diameter and size distribution for each microsphere type.

Hydrogel microspheres were further characterized by determination of the swelling ratio, “Q”, for each microsphere type, which is the ratio of the swollen hydrated mass to the dry mass. Several hundred microspheres were placed on a Kimwipe to remove excess surface moisture and then weighed on a pre-weighed watch glass. The spheres were then dried overnight at 60 °C and reweighed to obtain the dry mass.

Diffusion Characteristics of Microspheres

Hydrogel microspheres were incubated overnight in 0.1 mg/mL solutions of FITC-labelled dextrans in DPBS with average molecular weights of 10, 40, 70, and 500 kDa (Molecular Probes). Microspheres were then rinsed with DPBS and imaged via fluorescence confocal microscopy to monitor efflux of the probes (Olympus Fluoview 300). Fluorescence micrographs were captured between three and 150 minutes after removing removal from the FITC-dextran incubation solutions.

Implantation of Hydrogel Microspheres into Rat Omentum

Healthy Sprague-Dawley rats were used to evaluate the safety and initial biocompatibility of the microspheres produced by the core-shell spherification method (N=2 per microsphere type). Microspheres were implanted to the omentum following the protocol described in Chapter 4 of this dissertation with the exception of the delivery of the biomaterial. For these surgeries, microspheres were delivered via syringe as a suspension in DPBS. Approximately 1 mL of loosely packed microspheres were deposited directly to the omentum of the rat, which was subsequently sutured to the stomach wall to hold the microspheres in place for easier retrieval. Photographs of the surgery can be seen in **Figure 5.2** for additional clarity. Rats were monitored and scored for pain and activity levels for the 10 days following implantation of the microspheres.

Necropsy and Histological Evaluation of Implanted Microspheres

Rats were sacrificed 14 days after implantation for evaluation of the implantation site for signs of gross inflammation and tissue abnormalities. Tissue samples were collected and preserved in neutral buffered formalin, embedded in paraffin and sectioned at 7 micron thicknesses. Sections were stained with H&E and evaluated microscopically. Color micrographs of the stained sections were taken on a Zeiss Axio Vert.A1 inverted microscope.

Data Analysis

Cytotoxicity data were analyzed for significant differences by two-way ANOVA. Pairwise comparisons were evaluated using the Holm-Sidak method. Due to the high variability

associated with islets, cytotoxicity data were in violation of the normality and equal variance assumptions. For this reason, pairwise comparisons were denoted as significant at $p < 0.05$ or $p < 0.001$ for added clarity in interpreting the results.

Results

Islet Cytotoxicity Studies

Critical components of the core-shell spherification process were evaluated to identify thresholds for cytotoxicity to islets, specifically high levels of calcium ion and high intensity UV irradiation. **Figure 5.3** depicts the effects of calcium concentration and exposure time to canine islets with or without the PEGDA precursor component. At the shortest measured exposure time of 5 minutes, no significant difference in cytotoxicity was observed for any group, which were 200 mM calcium, and 100 mM calcium with and without PEGDA. All groups were above 97.5% viability compared to controls. However, a strongly significant drop in viability was seen in the 200 mM calcium group at each subsequent time point compared to the 5-minute measurement. Further, viability in the 200 mM group was significantly lower than the two 100 mM groups at both 10 and 15 minutes. No differences were observed in either of the 100 mM groups through 10 minutes. However, at 15 minutes, the 100 mM group containing PEGDA showed a significant decrease in viability compared to the 5- and 10-minute time points and to the 100 mM group without PEGDA at 15 minutes. Interestingly, no significant change in viability was observed at any time point within the 100 mM group without PEGDA, which was 97.6% viable at 15 minutes compared to controls.

The effects of photoinitiator concentration and UV light exposure time are shown in **Figure 5.4**. Canine islets were subjected to ~40 mW/cm^2 long-wave UV exposure for 3, 5 and 10 minutes at Irgacure 2959 concentrations of 0, 0.025, and 0.05% (w/v) and evaluated for cytotoxicity. Little cytotoxicity was observed in either of the groups containing Irgacure at any time point, as no significant difference in viability was detected within groups across the three time points. Interestingly, the group containing no photoinitiator showed the highest degree of cytotoxicity of all groups. Viability in the 0% group was significantly lower at 5 minutes and 10 minutes with respect to the 3-minute exposure time. Further, the 0% group was significantly less viable at 5 and 10 minutes compared to both Irgacure groups. The only significant difference detected between the 0.025 and 0.05% groups was at 10 minutes with viable cell fractions of 94.5 and 87.2%, respectively.

Physical Properties and Size Distribution of Hydrogel Microspheres

Hydrogel microspheres were fabricated using a novel core-shell spherification method. **Figure 5.5** depicts the core-shell constructs just after fabrication and prior to crosslinking. Alginate shells were characterized by a concentric ring-link morphology, and core diameters were typically between 600-800 μm. Microspheres composed of HA or PEGDA were characterized to determine size distribution and swelling ratio. **Table 5.1** provides some physical properties of the hydrogel formulations before and after cross-linking, as well as the average diameter and diameter range. HA microspheres were markedly smaller than PEGDA microspheres despite having been fabricated using the same droplet generation equipment and parameters. Furthermore, HA microspheres increased

in total polymer mass fraction after cross-linking while PEGDA microspheres dramatically decreased from the starting levels. However, PEGDA gels still exhibited a much lower swelling ratio “Q”, indicating a more compact overall hydrogel. The incorporation of islets into the PEGDA microspheres resulted in a slightly larger average diameter, but, interestingly, also resulted in a narrower diameter range. This is illustrated further in **Figure 5.6**, which contains scatter plots depicting the diameters of 100 representative microspheres composed of HA, PEGDA, or PEGDA with islets. Indeed, PEGDA spheres with islets had a much tighter band compared to empty PEGDA microspheres, which exhibited relatively broad size distribution and comparatively low clustering compared to the other two groups. HA microspheres were much smaller in size than both PEGDA groups, and had a relatively small size distribution, similar to the PEGDA-islet group.

Diffusion Characteristics of Microspheres

Figure 5.7 illustrates diffusion characteristics of the HA and PEGDA hydrogel microspheres fabricated by the core-shell spherification method. Microspheres were incubated in fluorescent probes of varying molecular weight, rinsed, and then examined by confocal microscopy to characterize the extent of diffusion into the microspheres and monitor efflux of the probes. Fluorescence micrographs were taken at the equator of the microspheres at 3, 10, 30, and 150 minutes after rinsing the spheres in blank DPBS. The HA microspheres (**Figure 5.7A**) showed strong fluorescence signal from all probes, indicating that all were able to penetrate the gel matrix. Signal from the 10 kDa probe diminished quickly compared to the larger probes, and was near equilibrium at the 30-minute time point. This is expected given the much smaller size of the probe. Signal from

the 40 and 70 kDa probes was stronger within the area of the microsphere compared to the surrounding medium at the latest time point of 150 minutes, which was not observed with the other two probes, suggesting that the probe had either not completely diffused out of the sphere or had become adsorbed to the matrix due to favorable thermodynamic interactions. PEGDA microspheres (**Figure 5.7B**) displayed comparatively weak fluorescence to the HA spheres. While strong signal was detected from the 10 kDA probe in the PEGDA group, efflux of the probe appeared less rapid than in the HA group. The 40 kDa probe displayed some positive fluorescence from within the PEGDA spheres, but was much less extensive than in the HA group. The 70 kDa and 500 kDa probes did not appear to penetrate to any appreciable extent as indicated by the very weak, granular fluorescence signal. Interestingly, fluorescence distribution between the microsphere and surrounding medium appeared to reach near or complete equilibrium in the in these two groups at the 30-minute time point, which was not seen in the HA gels, a possible indication that the probes had weakly adsorbed to the surface of, but not penetrated into, the microsphere matrix.

Encapsulation of Canine Islets in PEGDA Microspheres

Canine islets were encapsulated to demonstrate the compatibility of the core-shell spherification process for cell encapsulation. **Figure 5.8** shows representative images of canine islets encapsulated in PEGDA microspheres after 14 days in culture. Islets displayed strong red dithizone staining, which confirms the presence of insulin and suggests good viability and function of the islets. Islets also possessed smooth, round

edges, another indication of viability. Unstained tissue is exocrine pancreas tissue that was carried over from the original islet isolation process.

Evaluation of Safety and Initial Biocompatibility of Microspheres

HA or PEGDA microspheres were implanted into the omenta of healthy Sprague-Dawley rats (N=2 per group) to evaluated the safety and biocompatibility of microspheres produced using the core-shell spherification method. Animals were monitored for 10 days post-op for signs of pain and reduced activity, which were scored daily between 0 and 3, with 0 being normal and 3 being severe abnormalities. All pain and activity scores were 0 for all 10 days in all four rats. No observations of porphyria, poor grooming, skin discoloration, pica, weight loss, self-mutilation or decreased activity were made in any of the animals. Necropsies were done after 14 days and no signs of acute inflammation, pus, excess fluid, or tissue abnormalities were observed throughout the abdominal cavity, though some tissue adhesions were identified, particularly where the omentum was sutured to the stomach wall. Photographs of the implantation sites during surgery are provided in **Figure 5.2,** for reference. Both HA and PEGDA microspheres were found intact in the omentum, and were visually translucent, and appeared to be surrounded by a very thin film-like layer, which can be seen in **Figure 5.9.** In one of the PEGDA implanted rats, microspheres were found adhered to the surface of the liver, evidently having escaped from the omental pouch after implantation (**Figure 5.9B)**. Hematoxylin and eosin staining of the explanted tissues is shown in **Figure 5.10** for both microsphere groups. Microspheres generally appeared intact, as was expected from the necropsy observations, but many appeared to have been crushed or deformed during processing.

It was common to find microspheres possessing a thin layer of cells around their perimeters, often two or three cells thick, and all were devoid of cells in the interior. As microspheres were randomly distributed into the omentum, some single microspheres were isolated, surrounded by normal omental tissue (**Figure 5.10A-D**), while some were surrounded by a large population of what appeared to be primarily fibroblasts and some lymphocytes, characterized by either an elongated or near absent cytoplasm, respectively (**Figure 5.10EF**). These large populations of cells were typically associated with large clusters of microspheres in close proximity to one another, where isolated spheres tended to have very few “non-omental” cells nearby. In many cases, newly formed blood vessels were identified in the tissues near the microspheres, examples of which can be seen in **Figure 5.10EF** denoted by white arrows.

Discussion

We have developed and evaluated a new method for fabricating hydrogel microspheres for cell encapsulation and delivery. Current methods for cell micro-encapsulation are mostly based on alginate spheres [42,45,47,49,56,175,187–190], and others utilize harsh oil-emulsion techniques. [97,178,191,192] Alternatively, our method, termed core-shell spherification, could be used for a wide variety of hydrogel materials and is compatible with standard, commercially available and GMP-ready equipment and requires minimally cytotoxic conditions. Though primarily considered for islet or islet-like cell transplantation for diabetes, cell microencapsulation has also shown promise as a useful tool for stem-cell therapies and *in vitro* 3D tissue culture systems for drug development and disease modeling. [180,193,194] As the benefits of cell encapsulation continue to gain attention and

sophistication, our novel method for producing convenient cell-laden hydrogel microspheres from a variety of biomaterials could be of broad potential value for these applications.

Because islets do not replicate *in vitro*, low cytotoxicity is a critical feature for islet encapsulation strategies. Thus, we evaluated some of the key enabling components of the core-shell spherification method for cytotoxic effects using canine islets. Specifically, high levels of calcium are required for core-shell construct formation, particularly at small droplet sizes, or exposure to high intensity UV light is required for effective crosslinking of photo-initiated hydrogels such as PEGDA. Not surprisingly, 200 mM calcium was very quickly and significantly cytotoxic to islets. However, we found that islets tolerated 100 mM calcium very well even in a highly concentrated and viscous PEGDA solutions for at least 10 minutes. Furthermore, when PEGDA was not present, canine islets in 100 mM calcium showed no significant reduction in viability for up to 15 minutes.

Exposure to 40 mW/cm^2 long-wave (~365 nm) UV light was, overall, minimally cytotoxic to canine islets for at least 10 minutes. Unexpectedly, the group without photoinitiator, Irgacure 2959, displayed the most cell death after UV exposure. This is in contrast to results reported in several other studies that examined toxicity of the same photoinitiator.[195–198] However, these studies involved much lower UV intensity, between 4-10 mW/cm^2, and the photoinitiator concentration used herein were comparatively low. Thus, it appears that, at least at very high UV intensity, the photoinitiator may actually offer a protective effect up to a certain point perhaps by preferentially absorbing UV photons. Regardless,

a concentration dependent increase in cytotoxicity was still observed in the groups containing Irgacure, which is in agreement with the studies cited above. Further, the UV irradiation conditions utilized herein for microsphere production (40 mW/cm^2, 0.025% Irgacure) produced no significant decrease in islet viability for at least 10 minutes, and had a minimum viable cell fraction of 94.5% compared to controls. Advantageously, a maximum capacity production run with the present encapsulation equipment required a UV exposure time of about six minutes.

Microsphere diameter is an important factor for downstream applications of encapsulated cells, particularly islet transplantation. [142] Because a sizeable number of cells are required to reverse diabetes (e.g. ~10,000 IEQ/kg) [63,67], microsphere volume becomes a major concern. Furthermore, smaller spheres are more convenient to handle *in vitro* and are easier to deliver via syringe for transplantation. Despite being fabricated under the same conditions, the HA and PEGDA microspheres described in this study were vastly different in size, with average diameters of 637 and 904 μm, respectively. These diameters correspond to an average microsphere volume of 135 and 386 nanoliters, roughly a 3-fold difference in total volume per sphere.

The difference in size between the HA and PEGDA is most likely a result of the swelling behavior of the two hydrogel materials. Hydrogel swelling is governed by a number of variables, but is strongly related to the overall concentration of polymer and the density of cross-links within the gel, with changes in either of these two having opposite effects on swelling. [199,200] More specifically, cross-links serve to resist swelling by strengthening

the gel matrix, while an increase in polymer concentration tends to promote swelling by increasing the affinity of the matrix to bind water. A major difference between the HA and PEGDA gels was the initial polymer concentration of the hydrogel precursor solutions, which were 1.2% and 30% by mass, respectively. Thus, a high degree of post-fabrication swelling in the PEGDA spheres is likely a primary factor contributing to their much larger size. This is corroborated by the massive reduction in polymer mass fraction measured for the final constructs, which was only 5.8%, though it is also likely that some of this decrease in mass fraction was due to diffusion of some of the precursor out of the alginate shell before cross-linking was complete. Conversely, the final mass fraction of the HA spheres was triple the initial value (3.6% vs 1.2%). This is likely due in part to the incorporation of the cross-linking molecule (PEGDA 3,400) as it diffused into the core through the alginate shell and reacted with the HA polymers. However, it is also possible that as a result of the very low initial polymer concentration, the HA spheres may have contracted, as cross-link density continued to increase after the initial core-shell constructs were formed. Though not included in this chapter, evidence of this HA gel contraction is provided in Appendix B of this dissertation.

Diffusion properties were also considerably different between the HA and PEGDA microspheres. HA microspheres were highly permeable to dextran probes up to 500 kDa in size, while PEGDA spheres appeared to severely limit diffusion of dextrans above 70 kDa. Indeed, the degree of gel swelling is likely a key contributor these phenomena. The swelling ratio “Q” (the ratio of the equilibrium hydrated mass to the dry mass of the gel), is strongly correlated to the permeability of the hydrogel, though a wide array of factors

can affect this property. [156,200] The HA and PEGDA microspheres in this study had Q values of 27.7 and 17.3, respectively. Durst et al. published an excellent report in 2011 correlating the swelling ratio of a number of PEGDA hydrogel formulations to their average pore size. In this report, gels with similar Q values to those reported here (26.4 and 17.7) corresponded to an average pore size of 17.2 and 11.7 nm, respectively. Further, the hydrodynamic radius of a 500 kDa dextran has been reported as 15.6 nm. [46] Thus, the permeability of the 500 kDa dextran into the HA microspheres is well in line with other observations, at least in terms of its swelling ratio.

Results of the diffusion studies were less straightforward for the PEGDA microspheres than for HA. Of particular note was the marked attenuation of fluorescence signal near the center of the sphere for both the 10 kDa and 40 kDa probes, and the near absent penetration of the 70 kDa probe. The hydrodynamic radius of a 40 kDa and 70 kDa dextrans are reported to be 4.78 and 6.49 nm, respectively. [46] Thus, given the Q value for the PEGDA gels and corresponding estimated mesh size, penetration of these probes would be expected, though it should be reiterated that mesh size is dictated by many factors other than swelling ratio. A likely explanation for the unexpected fluorescence patterns in the PEGDA gels two-fold. First, as mentioned above, it is possible and even likely that some of the PEGDA molecules diffused out of the alginate shell before cross-linking was complete. This phenomenon would, in theory, produce a polymer concentration gradient within the core and therefore in the resulting gel microsphere once cross-linked. This could in turn produce a permeability gradient such that diffusivity increases at distances further from the center of the sphere. Secondly, the higher overall

polymer density of the PEGDA compared to HA microspheres (5.8% vs. 3.6% mass fraction) could have led to optical effects during imaging. Because the constructs are spherical, the amount of material light must penetrate increases toward the center of the construct, potentially leading to a shadow-like artifact, which would be more pronounced in the more concentrated PEGDA microspheres. Furthermore, a “shadow” artifact such as this would in theory be exacerbated if the spheres indeed possessed a polymer density gradient as discussed above. However, such hypotheses would require additional experimentation to confirm. Overall, it is clear that the PEGDA microspheres were far less permeable compared to the HA microspheres.

Finally, hydrogel microspheres intended for cell transplantation and immunoprotection must accomplish the following three things: 1) induce no negative effects to the host organism, 2) prevent the infiltration of host lymphocytes into the encapsulating matrix, and 3) avoid severe foreign body reaction resulting in an avascular fibrous capsule around the microsphere, which would lead to necrosis of the encapsulated cells. To explore these points, HA and PEGDA microspheres were implanted into healthy rats for a two-week period. All animals displayed no classical signs of pain or reduced activity [201] after implantation of the spheres even despite undergoing open abdominal surgery. Necropsies showed no internal signs of tissue abnormality or necrosis, providing further confirmation that the presence of the microspheres was well tolerated by the host. Microspheres appeared intact and were translucent in appearance. Histological analysis of the implantation site revealed a thin layer of cells around many of the microspheres, which were situated in what appeared to be normal omentum tissue. There were also

several regions in which spheres were surrounded by a dense population of cells primarily consisting of fibroblasts, and no cells appeared to have penetrated into the microspheres. Evidence of neovascularization was also identified in these more cellular regions. Interestingly, the incidence of fibroblast proliferation appeared to be largely associated with regions containing large numbers of spheres in close proximity to each other. These observations are indicative of an early stage/mild foreign body reaction, which is expected in response to the implantation of a biomaterial. [202] However, signs of advanced stage foreign body reactions associated with fibrous encapsulation are typically not observable after only two weeks, and are initiated by a number of physiological and material-based factors. [203–206] Thus, more comprehensive and longer-term *in vivo* studies will be required to fully characterize the extent of foreign body responses elicited by the HA and PEGDA microspheres.

In conclusion, the novel method presented herein for producing hydrogel microspheres is a promising new tool for cell transplantation and tissue engineering research. This method, termed core-shell spherification, could be applied to a wide variety of hydrogel materials, thereby enabling broad control of microsphere properties for application specific purposes. In the present study, microspheres were produced with markedly different size, structural, and mass transport properties with minimal modifications to the fabrication protocol. Furthermore, microspheres evoked no negative effects *in vivo* and appeared to be well tolerated, though long-term biocompatibility studies are needed. Other future studies will incorporate additional hydrogel materials and seek to expand

control of construct microstructure, including generation of gradiential gel spheres or liquid-core capsules.

Chapter 5 Figures and Tables

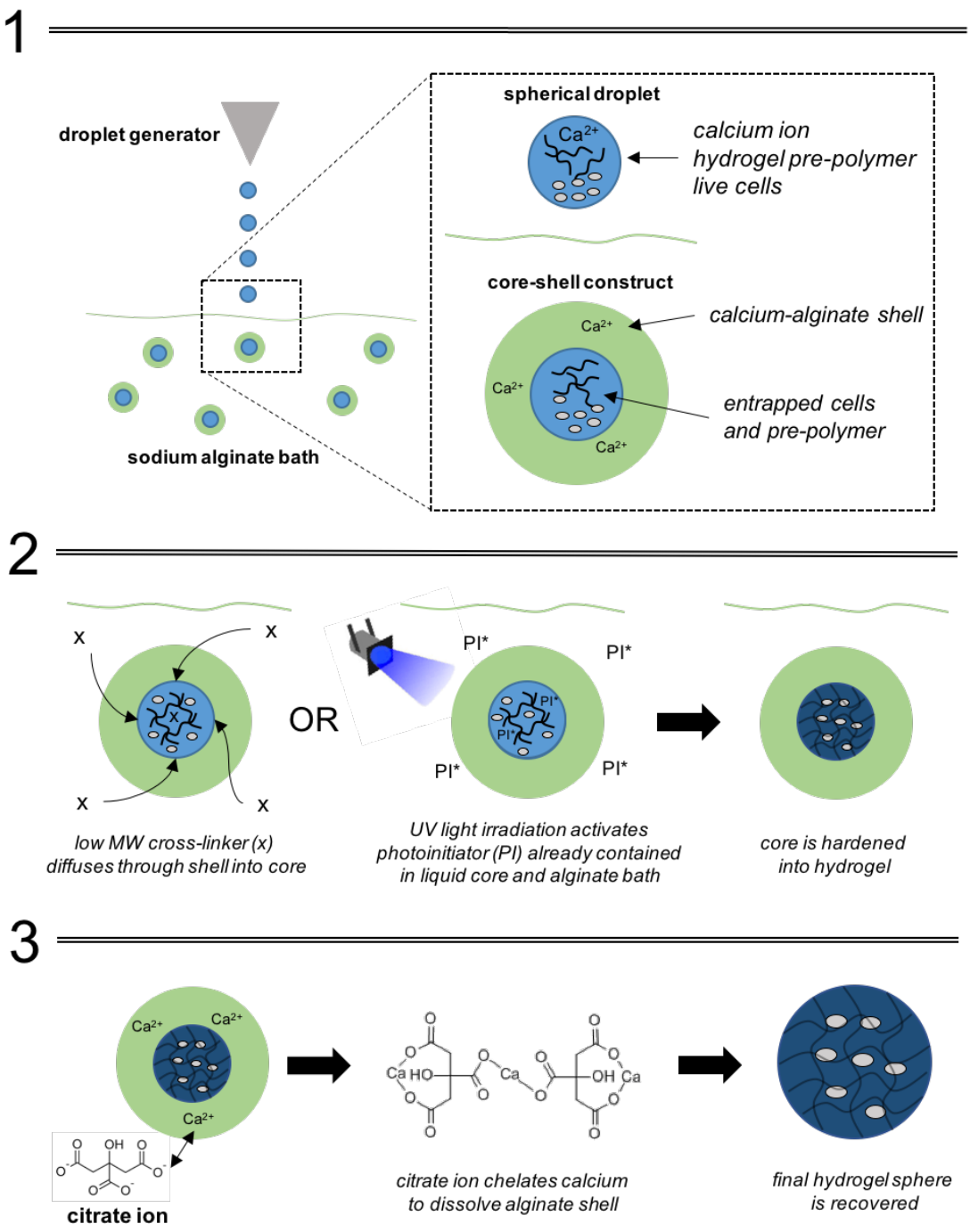

Figure 5.1. Schematic of core-shell spherification method.
Hydrogel precursor solution is prepared with calcium chloride and mixed with cells. The precursor is then extruded into an alginate bath to generate spherical core-shell constructs in which the hydrogel precursor and cells are entrapped within the shell **(1)**. The precursor is cross-linked by diffusion of a small cross-linker through the shell, or by irradiation with activating UV light **(2)**. The alginate shell is finally dissolved with citrate, leaving only the cross-linked hydrogel microsphere **(3)**.

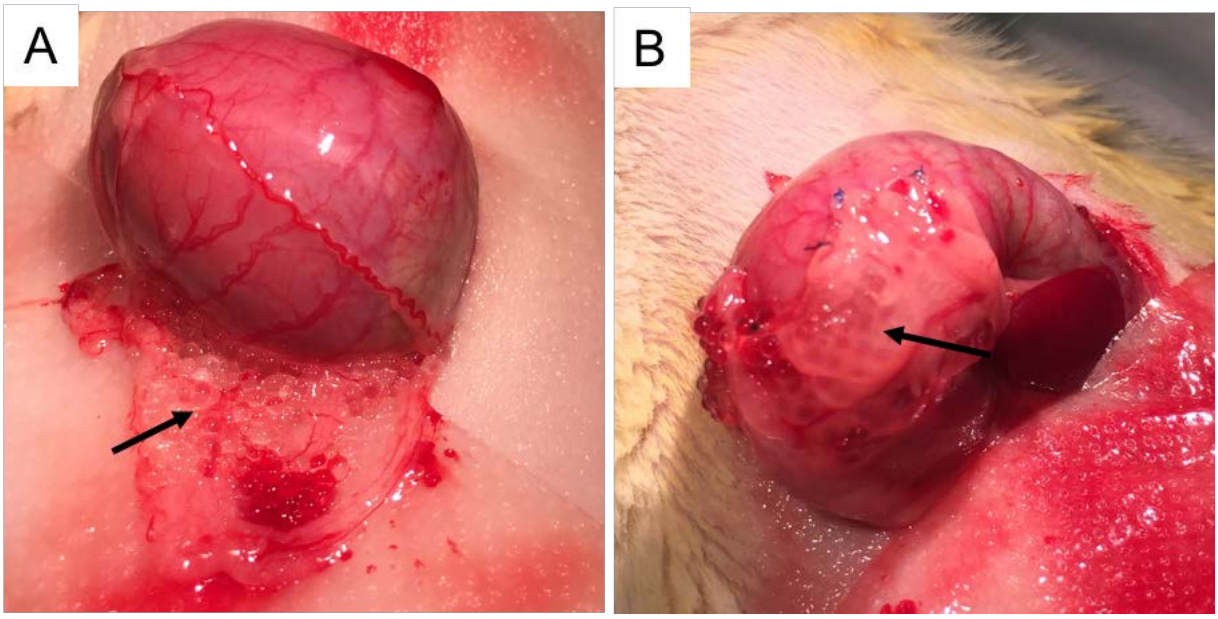

Figure 5.2. Photographs of microsphere implantation surgery.
Hydrogel microspheres were implanted into healthy Sprague-Dawley rats to evaluate initial biocompatability and safety. A small midline incision was made in the abdomen and the stomach and greater omentum were exteriorized. Microspheres were deposited via syrine in a DPBS suspension on the surface of the omentum **(A)**. The omentum was subsequently sutured to the stomach wall to hold the microspheres in place for easier retrieval **(B)**. The stomach and "omental pouch" were replaced into the abdominal cavity and the wound was closed.

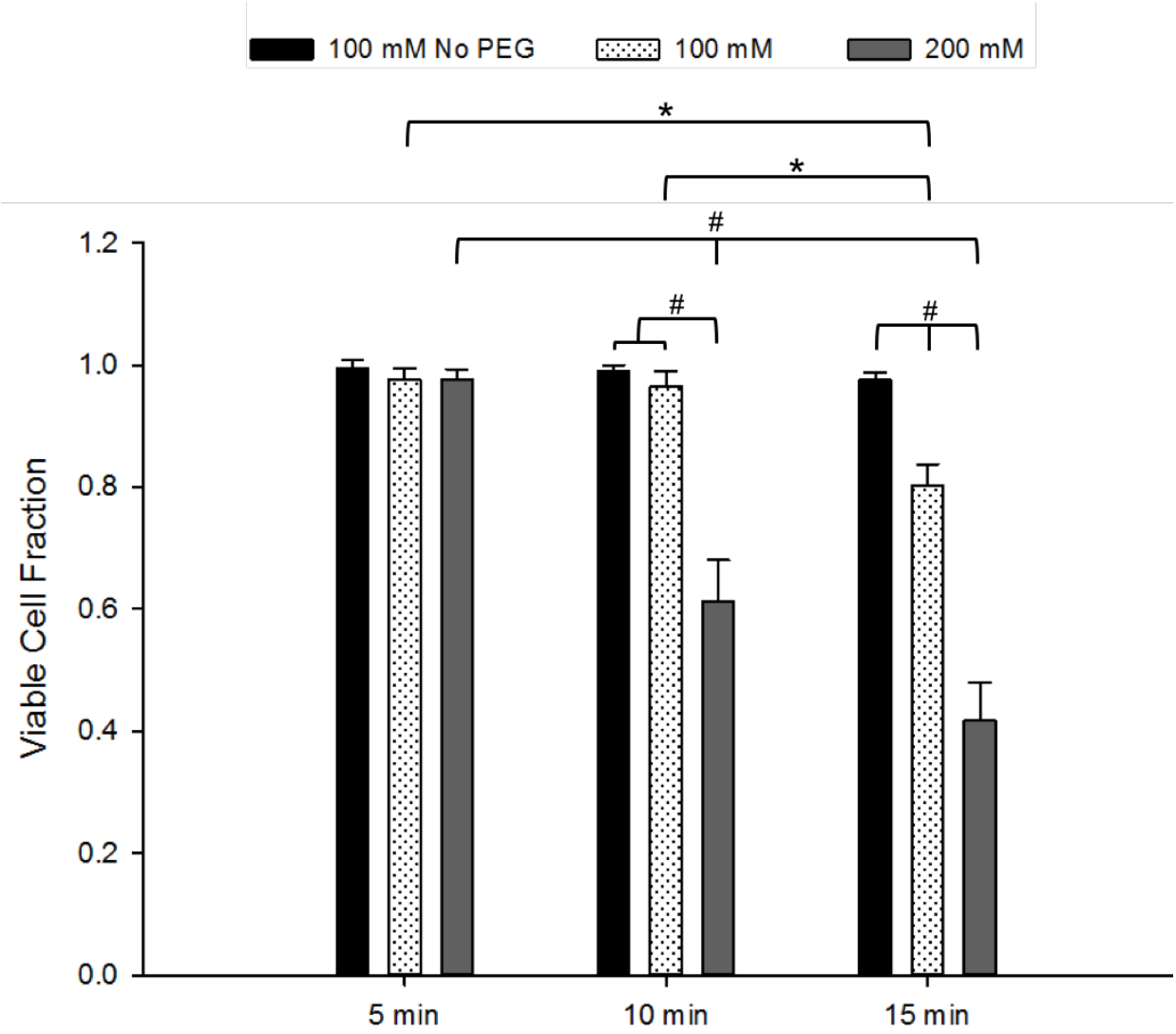

Figure 5.3. Cytotoxicity of calcium exposure in hydrogel precursor.
Canine islets were exposed to elevated calcium levels similar to those encountered during microsphere fabrication and evaluated for cytotoxicity at 5, 10, and 15 minutes. A group without the PEGDA precursor (*100 mM No PEG*) was also evaluated to better illustrate the effects of calcium alone. Cytotoxicity was evaluated using propidium iodide fluorescence staining and results are shown as the average viable cell fraction of 25 individually analyzed islets. Data were normalized to untreated controls. Significant differences are denoted either by an * ($p < 0.05$) or # ($p < 0.001$).

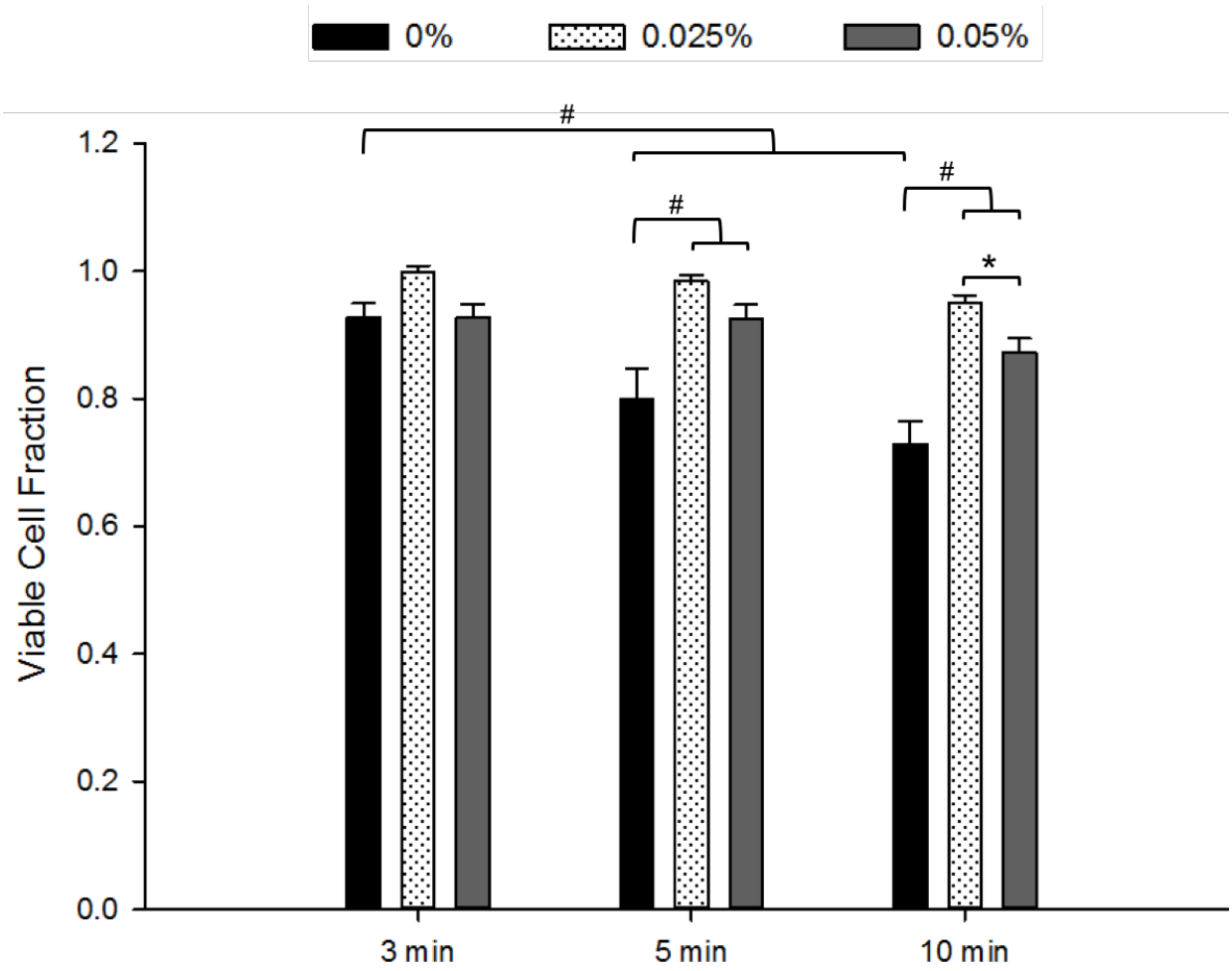

Figure 5.4. Cytotoxicity of photoinitiator and UV exposure.
Canine islets were exposed to long-wave UV light in DPBS solutions containing 0, 0.025, or 0.05% Irgacure 2959 to evaluate the cytotoxicity of the photo-cross-linking process. Islets were irradiated at approximately 40 mW/cm^2 for 3, 5, or 10 minutes. Cytotoxicity was evaluated using propidium iodide fluorescence staining and results are shown as the average viable cell fraction of 25 individually analyzed islets. Data were normalized to untreated controls. Significant differences are denoted either by an * ($p < 0.05$) or # ($p < 0.001$).

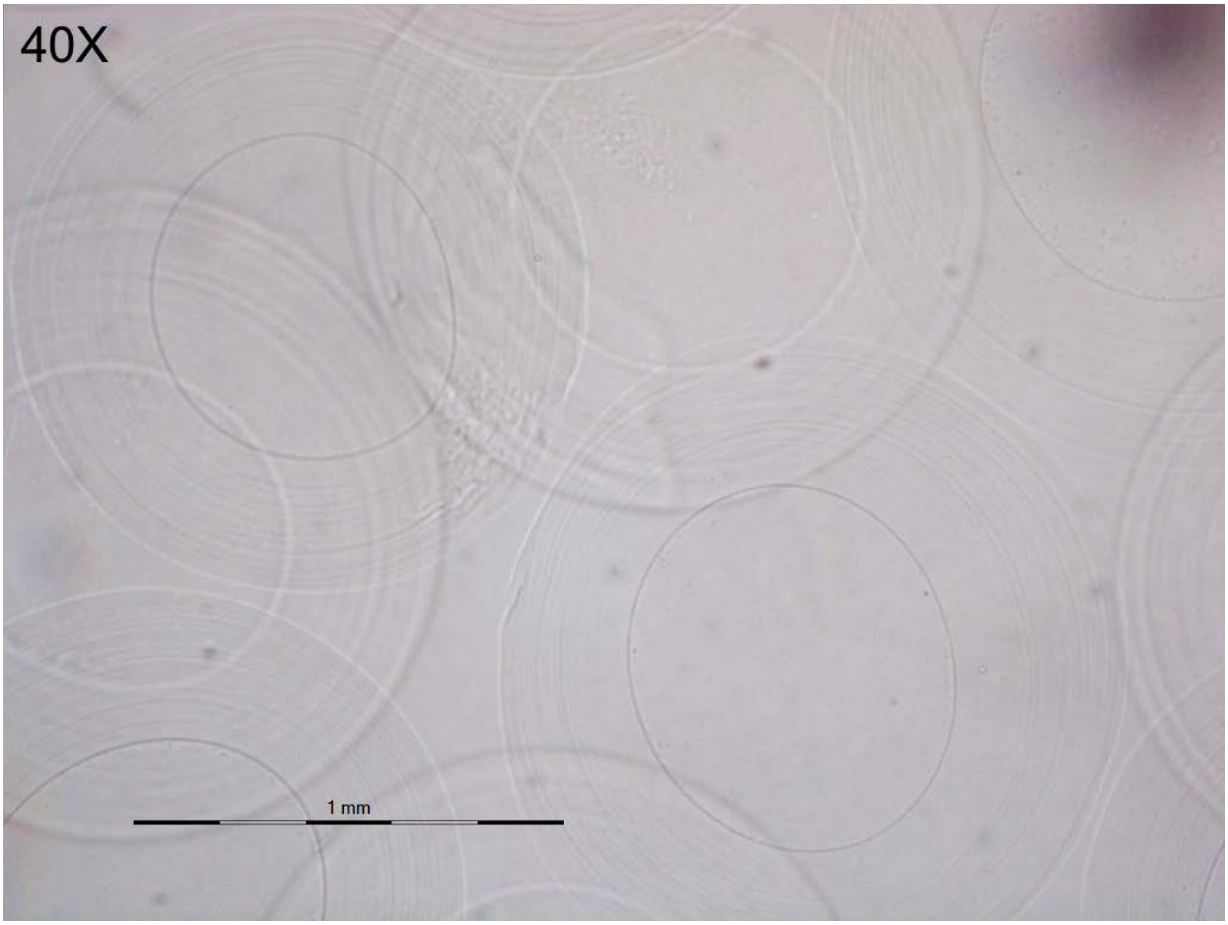

Figure 5.5. Example of core-shell constructs.
Core-shell constructs had spherical cores and wide, diffuse alginate shells. Alginate shell had a concentric ring-like appearance. Core diameters of constructs produced with the current method were generally between 600-800 microns. Scale bar = 1 mm.

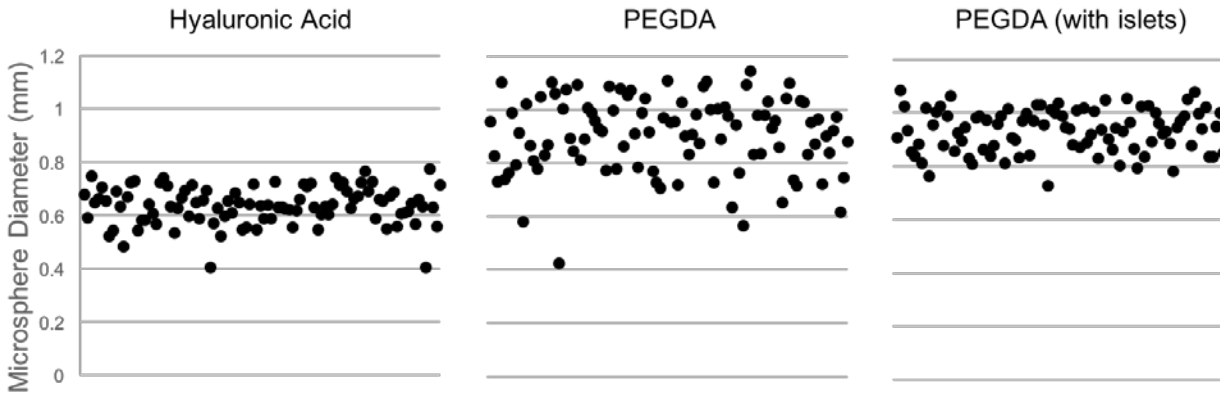

Figure 5.6. Size distribution of hydrogel microspheres.
The diameters of a representative sample of 100 microspheres of each material type were measured and displayed in a scatter plot to visualize the size distribution. All microspheres were produced using a 450-micron air jet nozzle system under the same production parameters. The data above are plotted on the same y-axis for better comparison of between the groups.

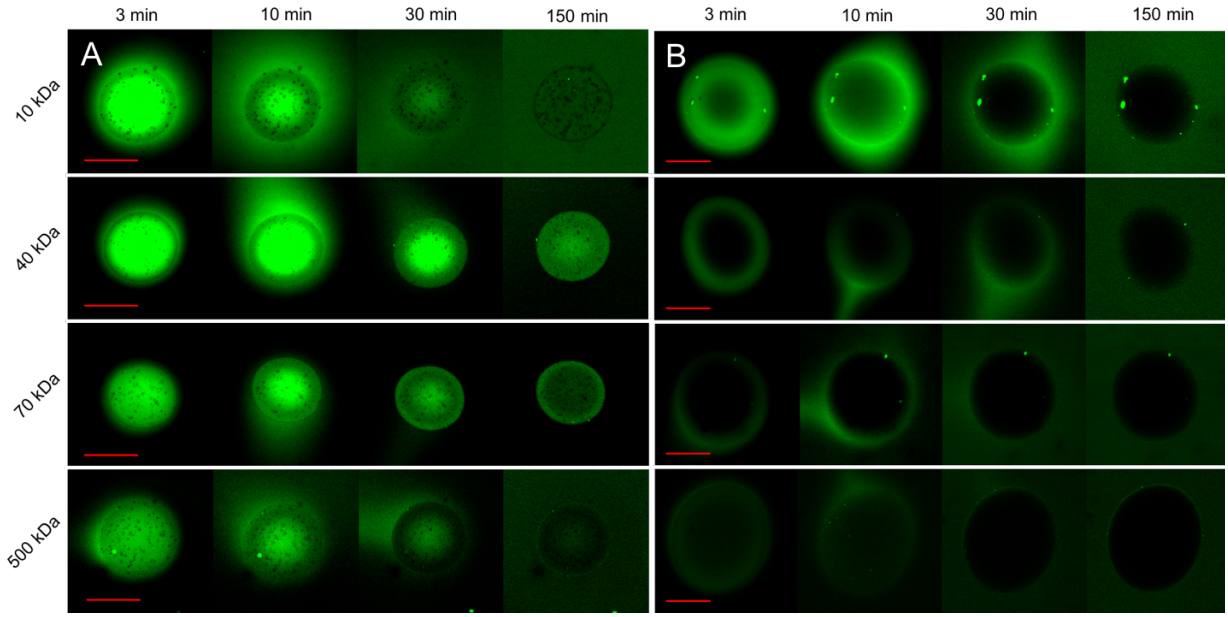

Figure 5.7. Diffusion of FITC-dextrans in hydrogel microspheres.
Hydrogel microspheres were incubated for 24 hours in solutions containing FITC-dextrans of increasing molecular weight. After incubation, the FITC-dextran solutions were exchanged with blank DPBS and the microspheres were monitored via confocal microscopy for 150 minutes to visualize efflux of the dextran probes. Images of the HA **(A)** and PEGDA **(B)** microspheres captured at the sphere equator are displayed for each condition at 3, 10, 30, and 150-minute time points. Scale bars = 500 microns.

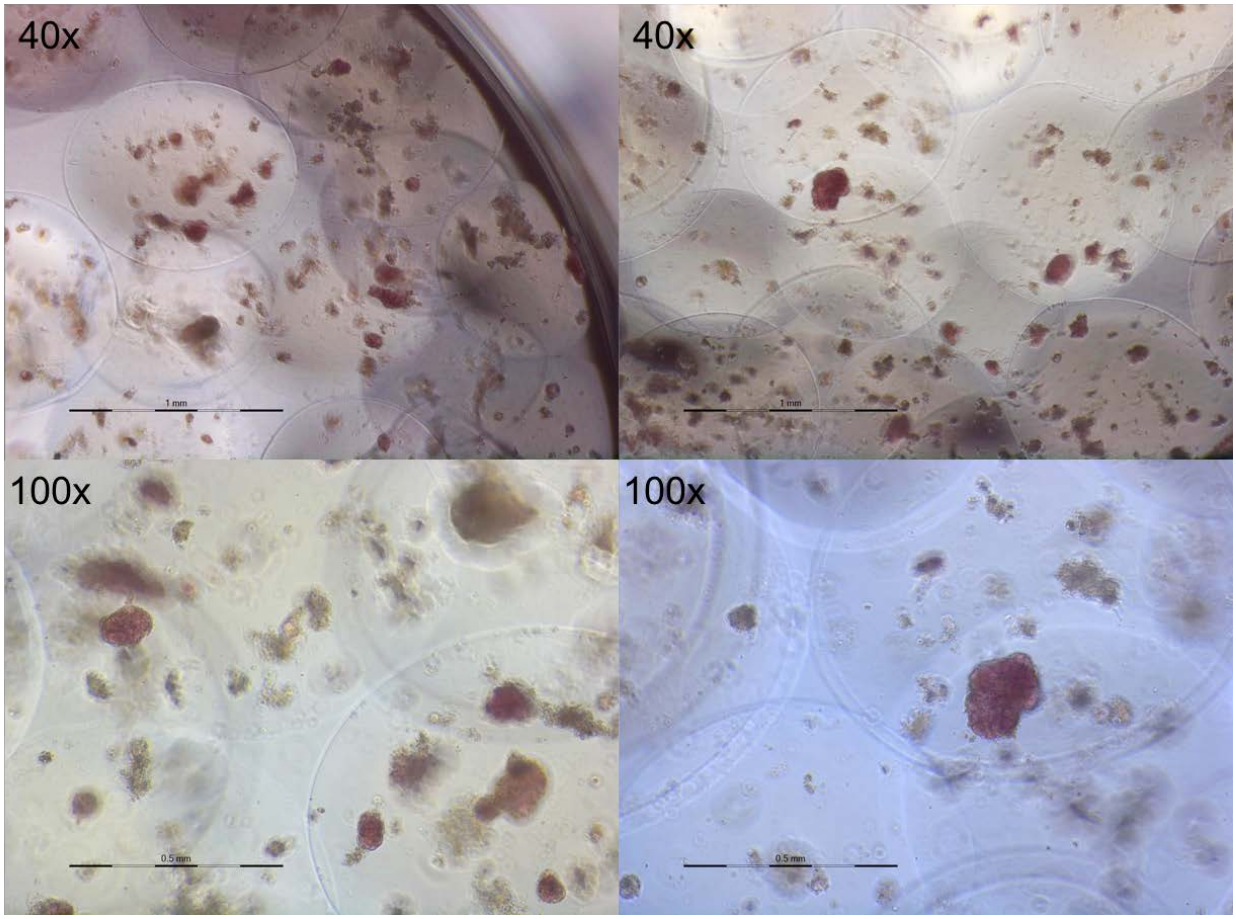

Figure 5.8. Canine islets encapsulated in PEGDA microspheres.
Canine islets were encapsulated in PEGDA hydrogel microspheres and cultured for 14 days to evaluate islet survival. Islets within the spheres were stained with dithizone, a common islet stain, which binds to insulin within the islets. Islets showed strong staining after two weeks in culture and possessed smooth, rounded edges, which are both signs of good islet health. Unstained tissue is remnant exocrine tissue that remained trapped in the hydrogels. Scale bars at 40X = 1 mm, and scale bars at 100X = 0.5 mm.

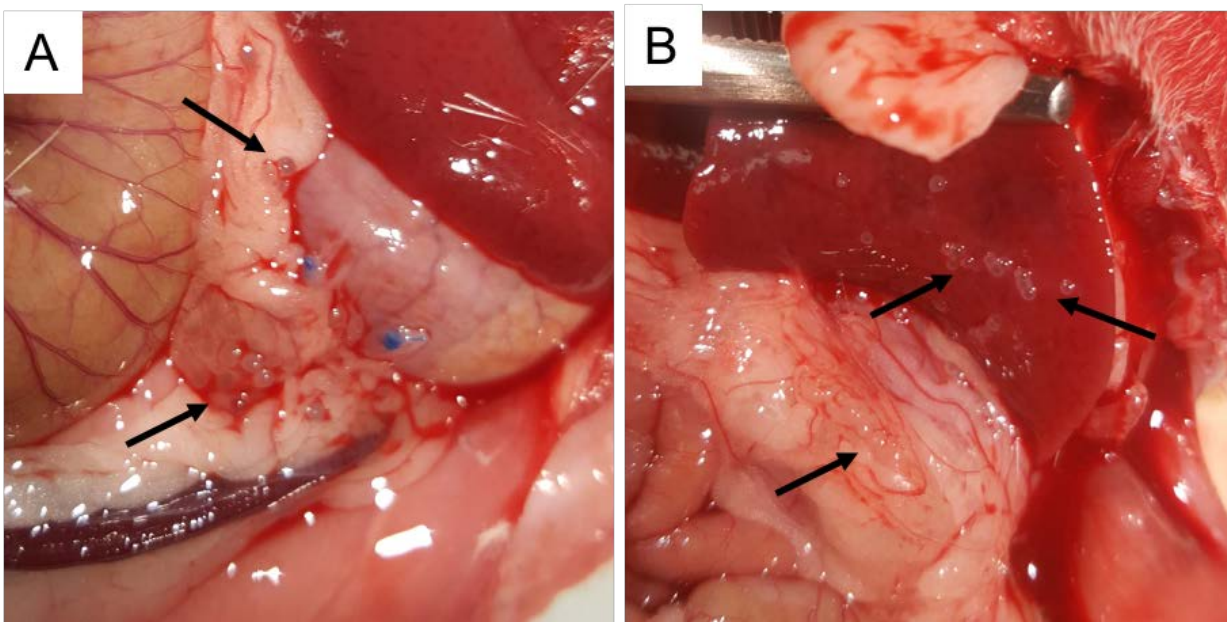

Figure 5.9. Photographs of microspheres at necropsy.
Healthy Sprague-Dawley rats were implanted with empty HA or PEGDA microspheres. Microspheres were deposited onto the greater omentum of the rat and sutured to the stomach wall. Necropsies were performed 14 days after implantation of HA **(A)** or PEGDA **(B)** microspheres. Microspheres are denoted by black arrows for easier identification.

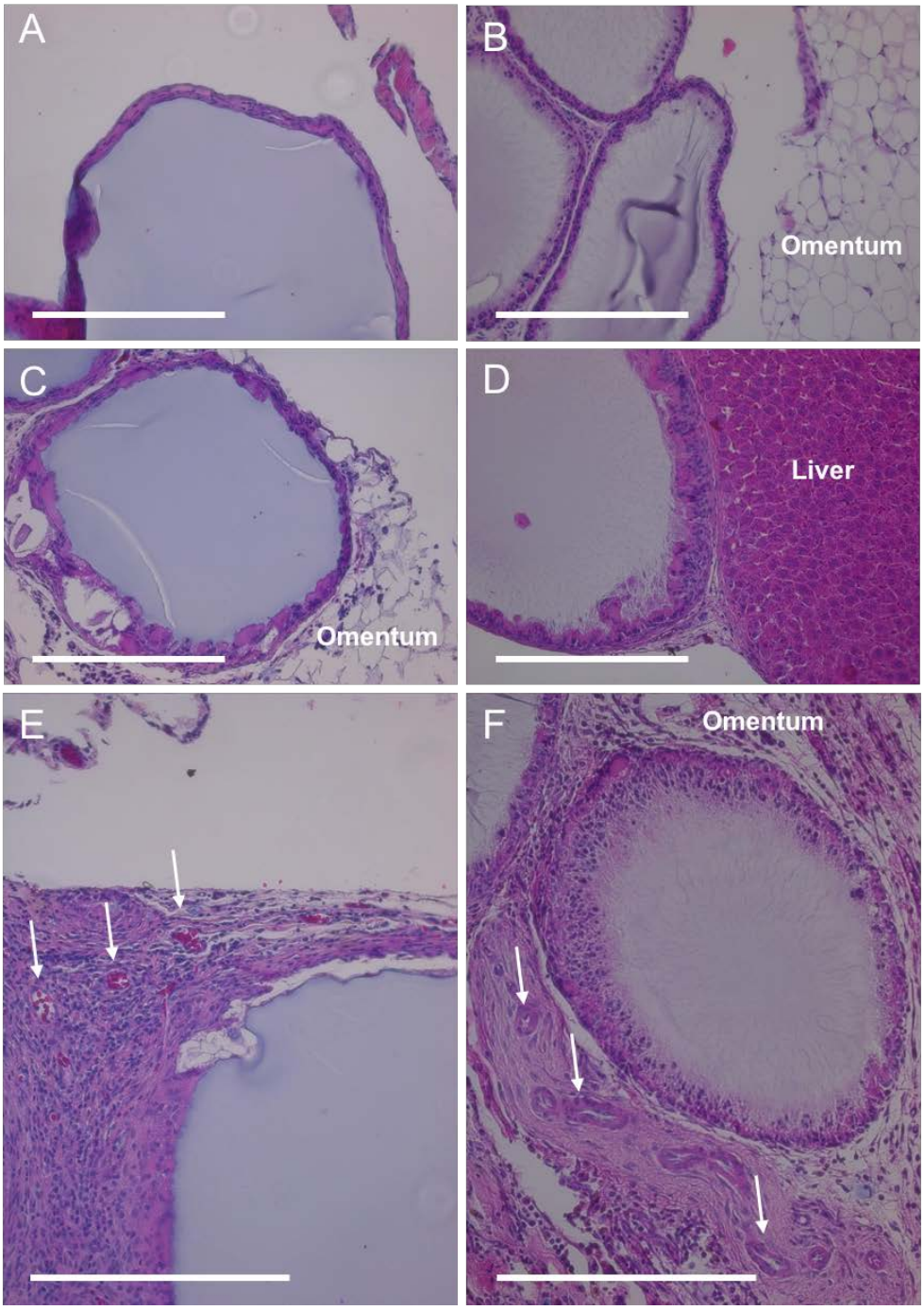

Figure 5.10. H&E staining of microspheres explanted after 14 days.
Implanted microspheres and surrounding tissues were recovered at 14 days and stained with H&E. Cellular deposition and host tissue response to HA **(A,C,E)** and PEGDA **(B,D,F)** microspheres were similar. In some regions, microspheres were identified surrounded by only thin layer of cells, often 2-3 cells thick **(A-D)**, and were surrounded by normal, healthy omental tissue. In other regions, microspheres were surrounded by a dense population of cells, primarily fibroblasts, and newly formed blood vessels, which are denoted by white arrows **(E,F)**. Scale bars = 300 microns in all images.

	HA spheres	PEGDA spheres	PEGDA spheres (with islets)
polymer mass fraction in gel precursor	*1.2 %*	*18% PEGDA 3.4k 12% PEGDA 20k*	*18% PEGDA 3.4k 12% PEGDA 20k*
precursor viscosity	*90 cSt*	*60 cSt*	*not measured*
polymer mass fraction in final swollen spheres	*3.6%*	*5.8%*	*not measured*
mass swelling ratio "Q"	*27.7*	*17.3*	*not measured*
sphere size range (in 100 sphere sample)	*406 – 776 μm*	*424 – 1146 μm*	*729 – 1085 μm*
average final swollen diameter (+/- SD)	*637 μm (+/- 7.1 μm)*	*904 μm (+/- 14.2 μm)*	*938 μm (+/- 7.9 μm)*

Table 5.1. Physical characteristics of gel precursor and final microspheres.

CHAPTER 6: Conclusion

Summary of Experimental Work

Islet transplantation is approaching a point of saturation as a treatment for human type-1 diabetes. Limited donor tissue and mandatory immunosuppression ultimately preclude the availability of this treatment to the overwhelming majority of diabetics. Therapies based on renewable, stem-cell-derived islet replacements, which are in need of substantial breakthroughs, are now the only foreseeable path toward mainstream application of this treatment in humans. Meanwhile, canine diabetes, which is strikingly similar to human diabetes and rapidly increasing in prevalence, is treated with outdated and marginally effective therapies. Despite an extensive history of islet transplantation research in canines for human application, it has never been seriously explored as a veterinary treatment option for diabetic pets and their owners. As such, the primary goal within this dissertation was to address the key challenges facing the translation of islet transplantation to veterinary medicine. As a corollary to this goal, I developed and patented a useful cell encapsulation technique applicable not just to canine islet transplantation, but to the broader field of cell therapy and regenerative medicine.

The first and most obvious component needed for canine islet transplantation is a source of canine islets. In research, canine islet tissue was routinely sourced from laboratory animals with little regard to cost. However, when progressing from a laboratory setting to the clinic, the use of purpose-bred canines would be ethically and economically unacceptable. Chapter 3 of this dissertation addressed this concern by examining the

process of islet isolation under the deleterious conditions inherent to organ donation from canines previously euthanized at veterinary clinics or shelters, without the benefits of heart-beating organ procurement and negligible ischemia afforded in experimental research. Furthermore, studies were also targeted at optimizing process efficiency specifically for the canine pancreas, which varies tremendously in size depending on donor bodyweight. Of particular note, I demonstrated that roughly one third of the pancreas could be effectively discarded without significantly impacting islet yield, which led to commensurate savings in both processing time and material costs. Overall, this work led to a reliable, cost-efficient protocol for isolating transplant quality canine islets from ethically obtained donor pancreas, a critical step in bringing clinical islet transplantation to diabetic canines.

Canine and human islet transplantation have a common enemy in the requirement of immunosuppression to prevent graft rejection. I address this problem in Chapters 4 and 5 of my dissertation in the examination of more advanced biomaterials for islet encapsulation and delivery. Despite great improvement in standard alginate-based technologies, a new wave of smarter and more biomimetic materials are beginning to emerge as alternatives to alginate hydrogels for cell encapsulation. One such example, and the primary focus of my research, are hydrogels derived from hyaluronic acid (HA), a natural and abundant component of native extracellular matrix. HA hydrogels have been employed successfully *in vivo* in several previous studies [91–94,207], but never as an immunoprotective matrix for islet transplantation. Encouragingly, I demonstrated that a commercially available, cGMP-ready HA hydrogel system could be used to prevent long-

term immune rejection of transplanted allogeneic islets in rats, which remained cured of diabetes for the entire duration of the study.

While effective in the laboratory, the surgical procedure used in the initial rat studies was invasive, required specialized training to properly prepare the islet-laden hydrogels *in situ*, and therefore unlikely to be adopted clinically. Thus, I began to explore techniques to fabricate injectable microspheres composed entirely of this promising HA hydrogel material. My primary objective with this project was to design a process that would easily translate into a commercial setting. So, I incorporated only readily accessible materials, and developed the procedure using standard commercial equipment designed for sterile operation and cGMP compliance. As the new fabrication process started to take form, it became apparent that it was not limited the HA hydrogel, but potentially compatible with a wide variety of biomaterials and thereby a wide variety of applications. The second iteration of this new method was fabricating PEGDA microspheres on account of the well-established biocompatibility and commercial availability of this material. Ultimately, these studies led to a United States Patent covering the method, now termed core-shell spherification, which was officially issued in 2017.

Future Directions

Though a donor-based clinical program has far more room to grow in canine diabetes than in humans, the supply of islets will most likely fall exceedingly short of demand in veterinary medicine as well. Eventually, a stem-cell derived islet surrogate will be needed to reach the broad population of diabetic canines, and a successful islet encapsulation

system will be crucial to ensure the safe delivery and long-term survival of these new cells. To this point, future application of this work will largely lie in the continued development of the core-shell spherification protocol. Initial *in vivo* studies were conducted, but a long-term evaluation both of microsphere biocompatibility and the fate of encapsulated islets/cells within will need to be completed. Furthermore, as 3D tissue culture is gaining popularity for both tissue engineering and disease modeling, the ability to microencapsulate cells within a broad variety of hydrogels could have great value outside of cell therapy as well.

The conditions of the core-shell spherification method present some interesting opportunities for development, namely, the potential for producing gradiential microspheres or even liquid-core capsules. For example, in the case of the HA hydrogels, the cross-linking molecule diffuses inward from the surrounding bath. Presumably, given enough time, the cross-linker equilibrates within the core area and produces a uniform gel. However, the cross-linker used here, PEGDA, reacts relatively slowly with the HA polymers, causing gelation in 10-30 minutes, in general. Another cross-linker for this hydrogel, PEG-dimaleimide (PEGDMal), reacts much more rapidly, on the order of just several seconds. If PEGDMal were used instead of PEGDA, cross-linking would occur much more rapidly near the core-shell interface, and early termination of the reaction could enable generation of liquid-core capsules. In contrast, for photo-cross-linkable gels such as PEGDA, the opposite could be done by removing the photoinitiator from the surrounding bath or decreasing its concentration to induce a chemical gradient. In this scenario, cross-linking would occur more rapidly at the center of the core-shell construct,

resulting in hydrogel microspheres that decrease in stiffness and diffusivity toward the exterior of the gel. This type of microstructure could be useful to control degradation profiles in applications where permanent residence of the hydrogel is not desired, such as in stem-cell assisted wound healing. [179] Beyond these examples, incorporation of additional hydrogel materials into the method such as chitosan [87,96] or functionalized smart polymers [88,192] should be explored in future studies as well.

In summary, this work has laid the groundwork necessary to expand the exciting option of islet transplantation to a growing population of diabetic dogs and their owners that have long awaited a better solution. Beyond this, the novel method for microencapsulation of cells developed in pursuit of this goal has potential as a versatile platform for a variety of applications in regenerative medicine. As cell therapies and 3D tissue culture continue to expand their role in medicine and research, tools for implementing these new strategies, including the method introduced herein, will be increasingly useful. In this light, the present approach of translating this new technology first into veterinary medicine could facilitate a shorter time to market with less overall risk, and potentially create a strategic advantage for human translation in the future.

APPENDIX A: Evaluation of a Simplified "*ex vivo*" Vascular Preservation Method of Canine Pancreas for Islet Isolation after Overnight Shipping

The following data were presented in poster format at the National AALAS 2015 Annual Meeting in Phoenix Arizona under the title "Successful Islet Isolation from Canine Pancreas Procured Post-Circulatory Death and After Extended Cold Ischemia".

Introduction

Diabetes mellitus is one of the most common endocrine disorders of dogs and cats and is characterized by a failure to adequately control blood glucose due to loss or dysfunction of pancreatic beta cells. Over 1 million dogs and cats have been diagnosed with diabetes in the United States and the prevalence of diabetes in dogs has doubled since 2007. [73,98] Diabetes mellitus is a chronic disease requiring lifelong treatment and monitoring. Typical treatment involves the administration of twice daily insulin injections in addition to diet modification and frequent monitoring of blood glucose levels. Islet transplantation would offer a markedly improved treatment option for owners of diabetic pets.

Widespread availability of this treatment will greatly depend on the accessibility of donor tissue from which to isolate islets. Pancreas obtained in local clinics where total cold ischemia times are limited to about 90 minutes can be successfully processed without internal preservation (i.e. vascular flushing) of the pancreas. However, potential donor pancreas may often come available in remote locations where transport times would be excessive and may include overnight shipping. Unfortunately, current pancreas preservation protocols, which are designed for human application, are highly complex and

require extensive flushing of the entire peritoneal vasculature *in situ* with high-priced preservation solutions. This practice is prohibitively complex and expensive to be feasible in veterinary medicine. Thus, we sought to develop a simplified "*ex vivo*" vascular flushing procedure specific to the canine pancreas with respect to the unique conditions associated with veterinary practice. Such a procedure would enable collection in remote sites and therefore increase the pool of available donor pancreas.

Methods

Pancreas Harvest and Perfusion

The canine donor was administered at least 300 IU/kg heparin intravenously 10 minutes prior to euthanasia. Euthanasia solution (Euthasol® Virbac, Ft. Worth, TX) was then administered at 0.22 mL/kg intravenously. The abdominal cavity was exposed by gross resection of the ventral body surface. The pancreas was identified and positioned to clamp the portal vein, caudal vena cava, and splenic and pancreaticoduodenal vessels. The duodenum was double clamped and cut at the pylorus and at the distal edge of contact with the pancreas. The pancreas and duodenum were removed *en bloc* and placed on a sterile metal pan atop a frozen ice pack, and then the duodenum was resected and discarded. Clamps were removed and the vessels cannulated with a sterile 20 g catheter. A modified HTK (histidine-tryptophan-ketoglutarate) preservation solution prepared with 5% (w/v) polyethylene glycol, M.W. 8000, was used to perfuse the pancreas until all blood was visibly removed by visual inspection.

The perfused pancreas was then immersed in povidone iodine solution for two minutes for surface decontamination, rinsed with sterile saline solution and placed in a sterile container filled with the modified HTK supplemented with gentamycin, a broad spectrum antibiotic, for overnight shipment.

Pancreas Dissection and Digestion

Upon receipt, the pancreas was immersed in povidone iodine solution for two minutes, rinsed thoroughly with saline solution, trimmed of excess non-pancreatic tissue, and then weighed on a sterile pan. The accessory pancreatic duct was located and the branch leading into the body/tail region of the pancreas was cannulated with a sterile catheter. Enzyme solution (Liberase® T-Flex, Roche Custom Biotech) in HBSS with added calcium and HEPES buffer was perfused into the ductal system until the gland was significantly distended with a target collagenase activity of 10 Wunsch Units and 0.6 mg of thermolysin per gram of pancreas digested. The head of the pancreas was neither perfused with enzyme nor included in further processing. Next, the distended pancreas was cut into several pieces and transferred to sterile flasks containing silicon nitride beads to aid in mechanical disruption. Regions not well preserved prior to cold storage were identified and discarded. Undigested tissue was weighed to determine the final mass of digested tissue.

The flasks were filled with additional digestion buffer and clipped into a 38 ˚C shaking water bath at 120 rpm. Tissue dissociation and islet liberation were monitored by dithizone staining and microscopic examination. Digestion was stopped when the majority of islets

had been released from the extracellular matrix by adding cold media containing calf serum, which deactivated the enzyme.

Islet Isolation and Purification

The tissue digest was rinsed several times with fresh, cold RPMI cell culture medium with calf serum to remove remaining enzyme and cool the tissue. Islets were then purified from the digested tissue via density gradient centrifugation. Islets were suspended in a custom density gradient medium comprised of iodixanol and the modified HTK preservation solution adjusted to approximately 1.110 g/mL, and deposited beneath RPMI medium in 50 mL centrifuge tubes to create a two-layer discontinuous gradient. Tubes were centrifuged and islets were collected from the supernatant. The majority of exocrine tissue, being denser than islets, migrated to the pellet and was discarded.

Islet Yield and Purity Quantification

Islet yield was calculated according to the standard method of conversion to islets equivalents, or "IEQ," which accounts for the extreme size variation of native islets.[23] One IEQ is defined as a spherical islet with a diameter of 150 microns, which contains approximately 1000 individual islet cells. Essentially, IEQs are calculated by measuring the individual diameters of a representative aliquot of islets and applying standard conversion factors for each diameter range. Due to the size disparity of canine pancreas, islet yield is also expressed on a per gram basis, rather than total IEQ per pancreas.

Islet purity was evaluated by dithizone staining. Dithizone is a deep red-purple dye that strongly chelates zinc, which is highly concentrated in the beta cells of islets in association with insulin molecules. As such, islets stained with dithizone appeared bright red or purple (depending on incubation time, dithizone concentration, etc), whereas exocrine and ductal tissues were not stained. Five representative samples of the islet preparations were stained with dithizone and examined with a bright field microscope. The percent purity was estimated visually for each sample and averaged.

Viability Assessment

Islet viability was evaluated using a live/dead fluorescence assay that utilizes calcein AM and propidium iodide. Caclein AM itself is non-fluorescent, but, when taken up by living cells is modified such that it exhibits green fluorescence. Propidium iodide is a red fluorescent dye that is only able to enter dead cells and binds strongly to DNA. When bound to DNA, the fluorescence intensity of propidium iodide increases sharply, thus staining dead cells bright red. Islets stained with these dyes were imaged by fluorescence microscopy. The percentage of dead cells was calculated by taking the ratio of red pixels per islet to the total islet pixel area. Viability was expressed as the percentage of live cells.

Glucose Stimulated Insulin Secretion Assessment

Glucose stimulated insulin secretion was measured by incubating islets in media containing a range of glucose concentrations. The relative amount of insulin released by the islets into the surrounding medium was measured using Perkin Elmer alphaLISA insulin assay kits after one hour of exposure to the glucose solutions and compared to a

baseline reading. Insulin assays were prepared and read immediately after glucose stimulation in the same wells following a novel all-in-one method developed in our laboratory. Four replicates were tested for each glucose concentration for each individual donor, averaged, and normalized to the baseline secretion signal, which was 2.8 mM glucose. Insulin secretion was expressed as a percent change in signal from baseline secretion.

Results

"Ex vivo" vascular flushing for pancreas preservation

Figure A1 displays photographs of two canine pancreas after preservation with the *ex vivo* vascular flushing method. The pancreas from donor 3 was well flushed and displayed thorough removal of blood as indicated by the pale-white appearance of the pancreas tissue throughout the majority of the organ. The pancreas from donor 4 is an example of incomplete vascular flushing, where large regions of the pancreatic tissue retained a pink color. However, the distal tail region of the pancreas from donor 4 was very well preserved (right side of image).

Islet Isolation Outcomes

Procurement variables and islet isolation outcomes for four separate canine pancreas are displayed in **Table A1**. Our method yielded an average of 49,560 IEQ per pancreas with a purity of 71%. **Figure A2** shows representative color micrographs of dithizone stained islet immediately following islet isolation for all four donor pancreas. Islets appeared morphologically intact and all showed good dithizone staining. As can be seen in **figure**

A2, islets from donor 3 were the least pure. Notably, this pancreas was exposed to the longest period of cold ischemia of the four pancreas included in this study at 20 hours.

Islet Assessment

Islet viability was evaluated using a live/dead fluorescent assay. **Figure A3** shows a representative fluorescence micrograph of islets stained with calcein (green) and propidium iodide (red). A color micrograph of the same tissue co-stained with dithizone is included for reference to distinguish islet tissue from exocrine. Viability was quantified by determining the ratio of dead (red) pixels to the total number of pixels for individual islets, with a minimum of 25 islets evaluated per isolation. The average viability for the method was 94.8 +/- 2.8 % (N=3 isolations).

Islet function was evaluated by glucose stimulated insulin secretion assay over a range of glucose conditions using an alphaLISA insulin assay to quantify insulin release. **Figure A4** shows the average relative signal (N=4 isolations, tested in quadruplicate) at each glucose condition relative to a baseline reading of islets in prior to glucose stimulation. Islets generally secreted more insulin as glucose concentration increased, an indication of proper islet function.

Discussion

We have developed a technique that enables isolation of healthy canine islets under extreme conditions. To our knowledge, we are the first to report successful isolation of islets from canine pancreas with extended periods of cold storage between 16.5 and 20

hours. Our method yielded on average 1487 islet equivalents (IEQ) per gram of digested tissue with a purity of 71%. Islets were approximately 95% viable and showed dose dependent glucose stimulated insulin secretion. By comparison, Vrabelova et al. reported an average yield of about 800 IEQ per gram from canine pancreas obtained post-circulatory death, and had lower viability (~85%) but higher purity (~86%). [103] Furthermore, their results were obtained with only nominal cold storage time. Thus our method improves total islet yield and viability over current techniques, but even more advantageously, enables donor pancreas to be procured in remote locations and shipped to the processing center overnight.

We found that our method produced encouraging results in comparison to more complex and expensive human organ preservation techniques. Kuhtreiber et al. conducted a study in 2010 on human pancreas processed after extended cold ischmia times, and reported an average yield of 4278 IEQ/gram of pancreas. [109] While our yields were considerably lower at 1487 IEQ/gram, the average cold ischemia time in our study was much higher at 18.6 hours compared to 13.2 hours in the human study. Cold ischemia has been shown to have a profoundly negative impact on islet yield even when high quality vascular flushing and preservation is performed. [134]

Interestingly, we obtained a higher islet yield per gram when only the distal tail of the pancreas was processed (donor 4) vs. the entire tail and body. This corroborates previous histological studies that revealed a higher number and larger size of islets in the tail of the pancreas compared to the head and body, which is unique to the canine pancreas. [21]

This is further confirmed by the results presented in this dissertation in chapter 3 that compared the effects of processing only the tail and body regions of the pancreas vs. the entire organ. Due to the high cost of tissue processing, particularly digestive enzymes and density gradient media, maximizing islet isolation efficiency will be critical in translating this treatment into the clinic.

In conclusion, this study demonstrates a simple, cost effective method for canine pancreas preservation that enables the isolation of highly viable islets from pancreas procured under sub-optimal conditions in remote locations. Furthermore, our method tolerated extreme periods of cold ischemia, allowing the use of standard overnight shipping services rather than expensive custom express couriers. This method could therefore be employed to significantly increase the pool of potential donor pancreas available for islet transplantation in diabetic canines.

Appendix A Figures and Tables

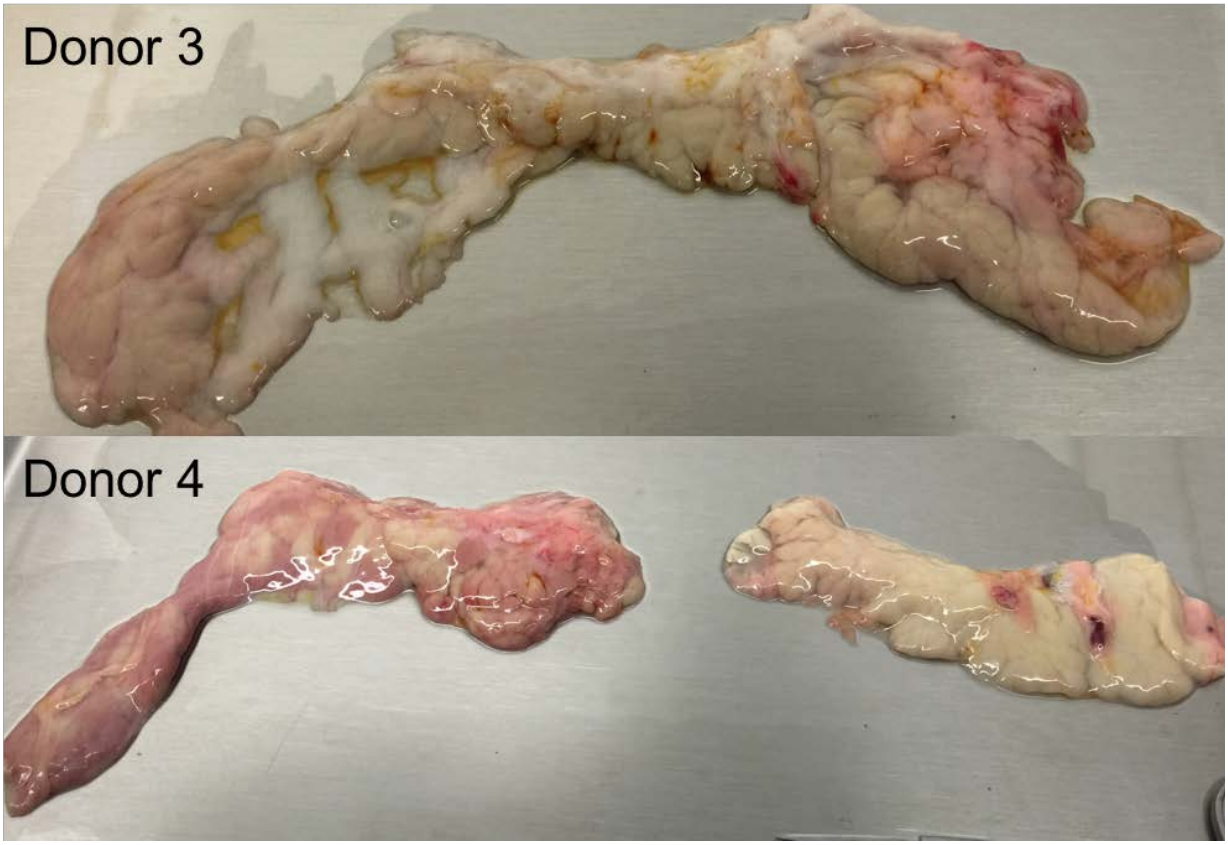

Figure A1. Canine pancreas preservation.
Shown here are photographs of pancreas preserved by our simplified “ex vivo” vascular flushing method. The pancreas from donor 3 (top image) was well flushed throughout the majority of the organ, indicated by the pale-while color of the pancreatic tissue. The pancreas from donor 4 (bottom image) was flushed well only in the distal tail region shown in the right side of the image. The head and body of the pancreas, seen in the left side of the image, were poorly flushed with several regions still remaining pink in color as a result of blood remaining in the tissue. Poorly flushed regions are not viable after long periods of ischemia, and are therefore not processed for islet isolation.

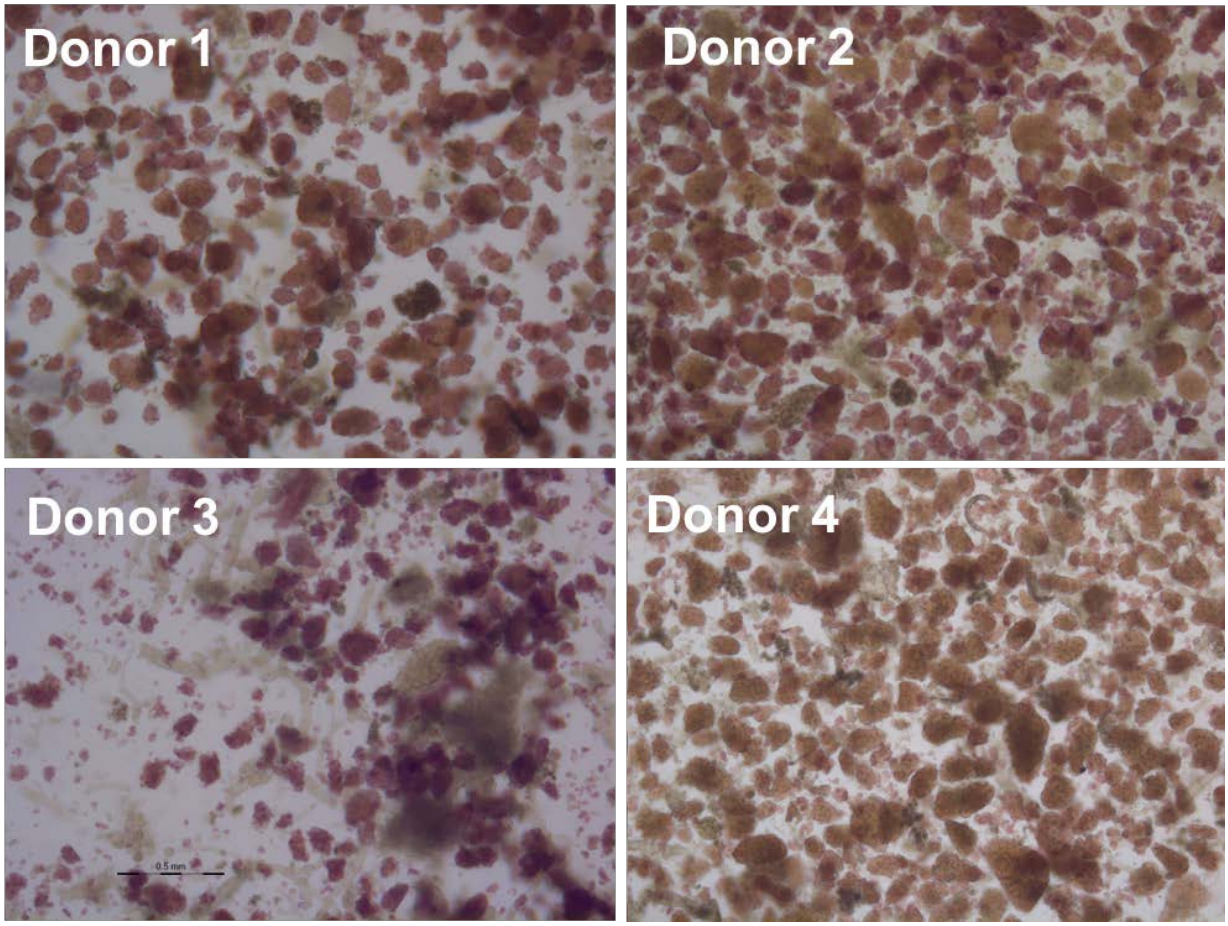

Figure A2. Dithizone staining of isolated canine islets.
Islet tissue from four separate canine pancreas immediately after isolation were stained with dithizone to evaluate islet quality and estimate purity. Islets from donor 3 contained a much higher percentage of non-islet tissue compared to the other isolations, as seen above. Islets all showed good dithizone staining and typical morphology, indicating good islet quality.

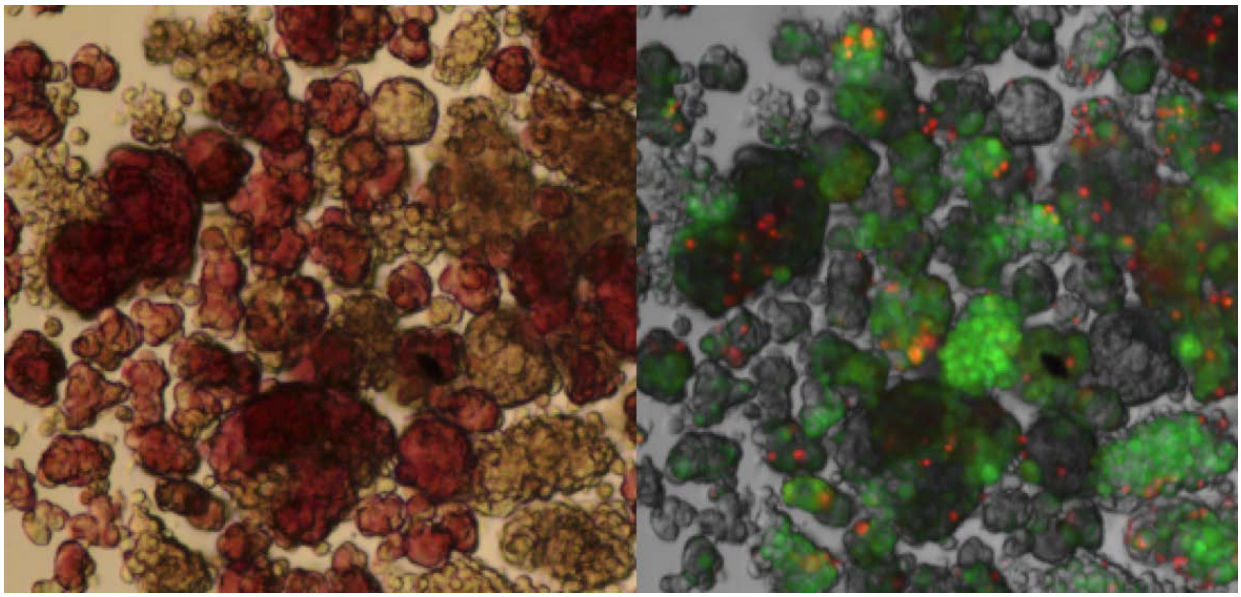

Figure A3. Islet viability.
Islet preparations were evaluated using a live/dead fluorescence assay to determine the viability of islets isolated after extended cold ischemia. Shown above are islets stained with dithizone (*left*) and calcein/propidium iodide (*right*) for a representative sample of isolated canine islets. Dithizone was used for differentiation of islet and exocrine tissues. Calcein (green) fluorescence indicates live cells, where propidium iodide (red) fluorescence indicates dead cells. Completely non-fluorescent tissue is mostly acellular debris. Some tissues, while actually alive, fluoresce very dimly which is often due to poor penetration of the calcein dye through the tightly packed cellular aggregates.

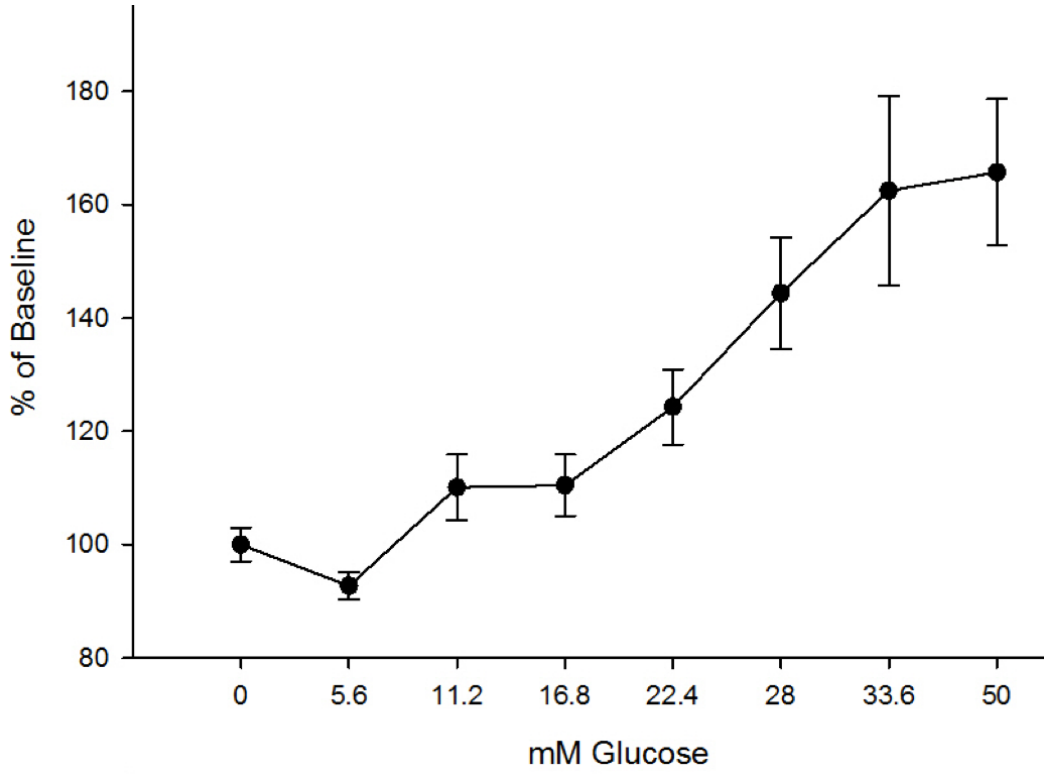

Figure A4. Glucose stimulated insulin secretion.
Isolated islets were incubated in various concentrations of glucose and secreted insulin was measured by alphaLISA insulin assay. Shown here are the average responses of islets from four separate isolations. Islets were tested in quadruplicate for each glucose condition for all islet isolations. Data are the alphaLISA signal intensity normalized to baseline intensity, which was obtained from islets in 2.8 mM glucose. Islets generally exhibited increased insulin secretion as glucose concentration increased, an indication of proper islet function.

Donor ID	CIT (hours)	Mass Digested (grams)	IEQ Total	IEQ/Gram	Purity (%)
1	*19*	*50*	*41500*	*830*	*78*
2	*19*	*40*	*62266*	*1557*	*72*
3	*20*	*50*	*45814*	*916*	*61*
4	*16.5*	*18*	*48659*	*2645*	*73*
Average	***18.6***	***39.5***	***49560***	***1487***	***71***
St. Dev	*1.5*	*15.1*	*8967*	*837*	*7.2*

Table A1. Islet isolation outcomes and procurement variables.
Shown here are data for four islet isolations performed canine pancreas shipped to our laboratory overnight after vascular flushing with organ preservation solution. Yields are listed as total IEQ as well as IEQ per gram of digested pancreas to better account for the variability in size of the canine pancreas between donors. Only the distal tail region of the pancreas from donor 4 was processed due to incomplete flushing of the main body. For all other isolations, the body and tail of the pancreas were included. The head of the pancreas was not included in any isolations.

APPENDIX B: Developmental Studies Toward the Core-shell Spherification Method (Chapter 5)

Introduction

This appendix is provided in support of Chapter 5 of the dissertation, which describes a novel method for producing cell-laden hydrogel microspheres, dubbed “core-shell spherification”. Several experiments are documented herein that were integral to the developmental of this new protocol, beginning with the initial proof of concept continuing through optimization for commercial deployment for islet transplantation. The current method was originally developed using a thiolated hyaluronic acid (HA) hydrogel system, sold commercially as “HyStem”, that was cross-linked via a Michael-type addition reaction between the thiol moieties and a polyethylene glycol diacrylate (PEGDA, MW ~3,400) cross-linker. This HA hydrogel was initially attractive from a commercial perspective as it had a well-established biocompatibility record and was already available in a cGMP compliant format. However, it became apparent over time that the method would potentially be compatible across a variety of hydrogel systems. For example, microspheres composed of PEG alone can also be fabricated from PEGDA polymers using the core-shell spherification method, which is described in in detail in Chapter 5.

Experimental Work

B1: Early Attempts and Proof of Concept

B.1.1 PEG dimaleimide as a cross-linker for increased reaction kinetics

The commercial version of this hydrogel includes a PEGDA cross-linker to initiate gel formation, and results in cross-linking times between 3-60 minutes depending on a number of variables including component concentrations and pH. However, in a discussion with the manufacturers of the product, it was learned that cross-linking times could be significantly reduced using a maleimide functionalized PEG in place of the standard acrylate. This was due to the greatly increased reactivity of maleimides toward the thiol groups on the HA polymers, which could reduce gelation time to a matter of seconds. The hypothesis was that with significantly increased reaction kinetics, the HA gel could be prepared as microspheres in a manner analogous to that of alginate, where droplets of the pre-polymer are simply extruded into a bath of cross-linker.

PEG dimaleimide, (PEGDMal, MW 3,400 LaysanBio Inc., Arab, AL) was dissolved at 1% or 5% wt in PBS and adjusted pH 7.5. The HA precursor solution was added dropwise through a 27G needle into the stirred PEGDMal bath. Gelation of the HA was observed and occurred very rapidly. However, through several iterations of the experiment, all of the resulting gels were highly amorphous and possessed fiber-like protrusions dangling from the main gel structure. It was concluded that, despite the markedly increased cross-linking kinetics, gelation was still too sluggish to produce uniform, spherical microspheres in this manner.

B1.2 Hybrid alginate/HA hydrogel microspheres

Another approach was to combine the thiolated HA precursor with alginate in solution, utilizing the near instantaneous gelation of alginate to form the initial spherical construct while the HA polymers could be cross-linked slowly within the alginate matrix. Then after allowing sufficient time for the HA cross-linking to proceed, the alginate could be dissolved using by citrate chelation of the calcium ion cross-links.

Initial sphere production using the hybrid solution of alginate and thiolated HA was successful. Also, in order to determine if the HA could even be successfully cross-linked under these conditions, spheres were produced with and without the PEGDA cross-linker. Spheres produced with the cross-linker did exhibit better initial stability as determined by comparing change in mass over time compared to uncross-linked hybrids. However, this strategy quickly proved to be ineffective, as all hybrid spheres began to degrade rapidly after 4 weeks. By comparison, spheres made with alginate alone exhibited relatively little degradation or change in mass over the same time period.

B1.3 Emulsion based strategies for HA microencapsulation

Emulsion-based strategies have been employed in the past for producing hydrogel microspheres, wherein an aqueous hydrogel precursor is rapidly stirred in a hydrophobic liquid, often mineral oil, to create small micro-droplets. [97,178] The micro-droplets are then cross-linked by various mechanisms and subsequently separated from the organic layer. This method was initially considered for islet microencapsulation in the thiolated HA gel, but was ultimately avoided due to poor control of microsphere size and potential

cytotoxicity to islets, which are notoriously vulnerable to mechanical shear, and do not replicate *in vitro*.

B1.4 Proof of concept experiment for "core-shell spherification" method using thiolated HA hydrogel (HyStem)

The following is an account of the initial proof of concept for the microencapsulation method described in Chapter 5 of this dissertation. The method was developed around the concept of liquid core alginate capsules, which have been used for purposes such as controlled release of drugs or proteins and cultivation of yeast or bacteria for biomolecule production, wherein the cells are trapped inside to facilitate easier collection of the target molecule. [208–212] The semi-permeable nature of these capsules gave rise to the notion that if small therapeutic molecules could diffuse out of the alginate shell, a small cross-linking molecule should also be able to diffuse into it while a much larger hydrogel polymer remained trapped within.

B1.4.1 Experimental summary

A 1% (w/v) solution of the thiolated HA precursor was prepared with 25 mM calcium chloride, and added dropwise to a stirred bath containing 0.25% (w/v) low viscosity alginate (Protanal LF 10/60, FMC Biopolymer Inc.). Core-shell constructs formed immediately upon contact with the bath, and were stirred for 5 minutes and then transferred to PBS containing 10 mM calcium chloride for additional shell hardening. Images of the core-shell constructs containing the HA precursor are shown in **figure B1.1A**. Cores diameters were between 2-3 mm, and while generally spherical, many

possessed tail-like features. The core-shells were then transferred to a solution of 0.2% PEGDA dissolved in PBS, and incubated overnight.

After overnight incubation, the core-shells were inspected microscopically. While the alginate shells appeared relatively unchanged, the cores contained what appeared to be hardened gel spheres that were markedly reduced in size, with clear separation between the gel core and the inner wall of the alginate shell **(figure B1.1B)**. Constructs were then incubated in a 50 mM sodium citrate solution with gentle agitation for 45 minutes, collected in a wire screen, and rinsed well with fresh citrate solution. Alginate shells were visibly weakened after 20 minutes of incubation in citrate **(figure B1.1C)** and were completely dissolved upon the final rinsing step **(figure B1.1D)**.

B1.4.2 Discussion

This proof of concept demonstrated the feasibility of using a core-shell approach to produce hydrogel microspheres under biologically compatible conditions. However, some challenges remained to be addressed. First, the overall size of the constructs was much too large for the intended application both in terms of delivery (i.e. injection) and nutrient diffusion. Unfortunately, current protocols for producing liquid-core capsules were limited to these large droplet sizes. Thus, miniaturization studies would need to be conducted. Second, the geometry of these constructs was not ideal, as many possessed tail-like protrusions. This would be undesirable in an any object indented for long-term in vivo residence as sharp or rough surfaces have been well established to be more immunogenic than smooth surfaces. [48,53] Finally, attention would need to be paid to

questions of scale and sterility. These initial studies were carried out manually using a syringe and needle on an open benchtop. For this method to have any kind of clinical relevance for transplantation, it should be compatible with established bead production instrumentation designed for sterile operation.

B2: Fluorescent Labelling of Hydrogel Polymer Core within Alginate Shell

The core-shell spherification method is enabled by the ability of the alginate shell to prevent diffusion of the hydrogel precursor for a sufficient amount of time for cross-linking to occur. The results of the proof of concept experiment described in section B1.2 are evidence that this is largely the case, but it is still possible that some fraction of the HA polymers could diffuse out and potentially change the resulting properties of the gel microsphere from what would be expected given the initial precursor formulation. To investigate if, and to what extent, this occurs, the HA polymers were labelled with a fluorescent probe, prepared as core-shell constructs, and monitored via fluorescence microscopy.

B2.1 Experimental Summary

The thiolated HA was labelled with carboxyrhodamine 110-C5-maleimide, a green fluorescent probe (Biotium Inc., Fremont CA), which bonds to the HA via similar chemistry to the that of cross-linking reaction with PEGDMal. The HA precursor was incubated in the dark for 2 hours with the fluorescent probe at a concentration of 0.02 mg/mL, and then added dropwise into an alginate bath without the PEGDA cross-linker to form core-shell constructs, and transferred to PBS for incubation and evaluation. Fluorescent

micrographs were taken after 2 and 72 hours to identify any loss of the HA precursor **(figure B2.1)**. Two hours after formation of the core-shell constructs, a strong fluorescence signal was still observed in the core area of the construct. There also appeared to be some weak fluorescence emanating from within the alginate shell, suggesting some minor diffusion of the HA into the shell had occurred. At 72 hours, strong fluorescence was still seen in the core, and the alginate shell displayed negligible signal compared to the 2 hour observations.

B2.2 Discussion

The results of this experiment indicated that some diffusion of HA through the alginate shell probably occurs, but at an extremely low rate. Interestingly, loss of the HA polymer in the core area between 2 and 72 hours appeared minimal, yet the fluorescence originating from the alginate shell essentially disappeared during that time. This is most likely explained by autocross-linking of the HA polymers within the core area, which can occur in the presence of oxygen over the course of several hours as a result of disulfide bridge formation between the thiol groups. Thus, gelation likely occurred even in the absence of the more rapid cross-linking reaction with PEGDA, halting further loss of the HA polymers.

The manufacturer of the thiolated HA reports the average molecular weight of the polymers to be in the range of 250 kDa. Thus, smaller hydrogel precursors would likely diffuse out more rapidly, thus shortening the available window for cross-linking and potentially impacting the final properties of the gel. Overall, though it is possible that some

gel precursor can indeed escape the initial core-shell construct, the loss appears to be very minimal and likely has very little impact on the resulting gel structures produced with this particular material.

B3: Optimization for Microscale Production of Core-Shell Constructs

The following section describes the challenges encountered in reducing the size of the hydrogel spheres to within a range suitable for cell transplantation. In light of this objective, a Buchi B-395 Pro micro-droplet generation system was incorporated. The Buchi B-395 Pro was selected as it was specifically designed for sterile operation and cell encapsulation, and is cGMP ready.

B3.1 Early experiences with microscale core-shell spherification

Initial attempts at reducing the size core-shell constructs to the microscale (i.e. below 1 mm) were met with significant challenges. The dramatic reduction in droplet mass and volume was perhaps the most impactful factor. For example, a spherical 2.5 mm droplet corresponds to volume of approximately 8.2 microliters, whereas a 0.5 mm droplet is only 0.065 microliters, a 125-fold decrease. Notably, this also meant the total free calcium, necessary for forming the alginate shell, was reduced by the same factor. Due to these factors, early trials at making sub-millimeter particles produced extremely weak and misshapen constructs, that were unable to withstand even mild stirring **(figure B3.1)**.

B3.2 Calcium concentration

Eventually, increasing the calcium concentration to at least 100 mM was found to be an effective strategy to improve the strength of the alginate shells at the microscale. For particularly small constructs (e.g. < 500 microns), concentrations near 200 mM were necessary to form sufficiently strong shells. Because these elevated calcium levels were later determined to be cytotoxic to islets (chapter 5), efforts were focused on slightly larger spheres between 600-1000 microns produced with 100 mM calcium in the hydrogel precursor solution.

B3.3 Alginate concentration and viscosity differential

A common issue aside from the strength of the alginate shell was the construct morphology. As depicted in **figure B3.1**, cores often had grossly non-spherical geometry, were teardrop shaped, or possessed appendage-like deformities. These issues were determined to be heavily correlated to the viscosity differential between the droplets and the alginate bath, which was several times that of water (~ 5-6 cSt) for formulations being examined at the time (0.25%-0.5% low viscosity alginate). Further experimentation revealed an alginate bath concentration of 0.12 – 0.15% to be a suitable balance between ensuring alginate shell stability and reducing bath viscosity, which for that range was approximately 2.5 -3.5 cSt, as measured by a glass capillary viscometer. At this alginate level, a droplet viscosity of approximately 60 cSt or higher consistently resulted in high quality, sub-millimeter core-shell constructs. Sample images of the optimized core-shell constructs are provided in Chapter 5.

B3.4 Hydrogel precursor solution density

Another consideration for micro-scale production of core-shell constructs was the density of the hydrogel precursor solution. Increased droplet density (~1.05 -1.08 g/mL) was found to improve overall quality of the resulting constructs, particularly for smaller droplet sizes, by preventing the droplets from clinging to the surface of the bath. At lower density, small, thin, tail-like features often formed as the droplets sank slowly into the alginate bath **(figure B3.2)**. Increasing the density of the core solution was also of great value for cell encapsulation, as the cells were more neutrally buoyant in the denser solutions, mitigating settling of the tissue during microsphere production.

B4: Precursor Solution Formulation Development for PEG Microspheres

As discussed in the preceding section, a minimum droplet viscosity was necessary to ensure high quality core-shell constructs and resulting microspheres. When producing PEG microspheres using only PEGDA (described in chapter 5), fairly high concentrations of polymer were needed to meet the viscosity requirement due to the relatively small molecular weight of these polymers. A well-known property of PEGDA gels is the propensity to swell with water after fabrication, and the extent of this swelling is correlated to the polymer concentration and polymer molecular weight. [213–216] However, there was very little published data on the effect of combining PEGDA polymers of different molecular weights on swelling behavior. Thus, a study was conducted to identify a PEGDA formulation that would both meet the viscosity requirements for core-shell spherification and also exhibit the least amount of swelling in order to keep microsphere size as small as possible.

B4.1 Experimental Summary

Several different ratios of PEGDA 3.4 kDa and PEGDA 20 kDa were compared to gels made with PEGDA 10 kDa alone at the same polymer concentration. Cylindrical gels were made using a custom mold at a 30% total PEGDA mass fraction and contained 0.1% (w/w) Irgacure 2959 as a photoinitiator. Gels were weighed immediately after fabrication and again after 24 hours once equilibrium swelling was reached. Swollen gels were dried on a Kimwipe to remove excess water from the surface of the gel. The results of this experiment are summarized in **table B4.1**. The amount of swelling observed in the 10 kDa gels was higher than any of the hybrid formulations tested. This was unexpected given the theoretical average molecular weights of the hybrid gels, which were higher in than 10 kDa for 3 of the 5 formulations.

B4.2 Discussion

The goal of this study was to identify a formulation of PEGDA gel precursor that would both meet the minimum viscosity requirement while exhibiting the least amount of swelling. Swelling was undesirable as it increased the size of the resulting microspheres, limiting their convenience and potentially leading to problems with nutrient diffusion. Based on these results, the 18/12% hybrid formulation was chosen as the optimal core solution due to its viscosity just meeting the target of about 60 cSt and exhibiting a much lower swelling ratio than the 10 kDa formulation, which was also about 60 cSt. While the 20/10% gel exhibited even less swelling than the 18/12% gels, the viscosity of this solution was determined to be too low to produce high quality microspheres.

B5: Development of UV Photo-cross-linking Protocol for PEG Microspheres

A protocol for cell encapsulation in PEG microspheres using PEGDA was desirable due to its long-standing biocompatibility record, wide commercial availability and tight production control. [213–217] However, the relatively small molecular weight of the PEGDA polymers presented a challenge when incorporated into the core-shell spherification method, as the alginate shells were too porous to contain these polymers for extended periods of time. As such, increasing the gelation rate of these gels was critical to retain sufficient concentration of the polymer to form quality microspheres, and is generally achieved in one of two ways, 1) increase UV light intensity (i.e. irradiance, or watts/area) or 2) increase photoinitiator concentration.

Initial trials were conducted using a standard laboratory grade 6W long-wave UV lamp (UVL-56, UVP, LLC.), which was sufficient to cross-link PEGDA gels on the benchtop in 5-15 minutes, and had an irradiance rated at 1.35 mW/cm^2 at a distance of 3 inches according to the manufacturer. However, when used for core-shell spherification, no cross-linking was observed under any conditions with this lamp. The next iteration of the protocol utilized a much higher power 100W lamp (Blak-Ray B-100AP, UVP, LLC) with an irradiance of 21.7 mW/cm^2 at a distance of 2 inches. Cross-linking times using this lamp were rapid enough to produce PEG microspheres, but at the levels of photoinitiator required (0.2%), resulted in excessive cytotoxicity. When photoinitiator concentration was reduced into non-cytotoxic ranges (<0.08%), the resulting microspheres were extremely weak, easily damaged, and swelled markedly such that encapsulated islets often fell out of the gels **(figure B5.1)**.

Because an increase in photoinitiator concentration was not an option due to cytotoxicity, another escalation in UV lamp power was the only apparent alternative. Excellent results were finally achieved with a 400W lamp with an irradiance rating of 200 mW/cm^2 at a distance of 3 inches (PortaRay 400, Uvitron International, Inc.). The full irradiance of 200 mw/cm^2 was found to be unnecessarily high, as gels could be fully cross-linked in under 30 seconds at approximately 40 mw/cm^2 using extremely low photoinitiator concentrations (0.025%). Another advantage of this lamp was its much wider coverage area, resulting in more complete and even irradiance of the cross-linking bath during core-shell spherification.

B6: Evaluation of Bead Generation Technologies for Application Specific Process Optimization

The Buchi B-395 Pro micro-droplet generator is compatible with two different nozzle systems for producing liquid droplets, a vibrational nozzle and an air jet nozzle. The vibrational nozzle system produces droplets via vibrational frequency applied to the nozzle head to disrupt a laminar fluid stream. The size of the resulting droplets is controlled by the nozzle size, fluid flow rate, and vibrational frequency, where smaller nozzles, reduced fluid flow, and higher frequencies produce smaller droplets. The air jet nozzle utilizes an internal fluid nozzle within a larger concentric nozzle for a compressed gas, namely air or nitrogen, which creates a cylindrical jacket of airflow around the central nozzle. As the fluid is pumped through the central nozzle, droplets are blown off by the airflow. In this system, droplet size is strongly correlated to the airflow rate, and also to nozzle size. The higher the airflow, the smaller the droplets.

B6.1 Experimental Summary

These droplet generation technologies were investigated for microencapsulation of islets using the core-shell spherification method. Microspheres were produced using both systems with and without islets. Islets above 200 microns in diameter were removed using a steel mesh prior to encapsulation to avoid clogs. Then, the size distribution of the resulting spheres was analyzed by measuring the diameters of 100 individual spheres from a representative sample of each group, which are displayed in **figure B6.1**. Because the nozzles for the two systems were different sizes, data were normalized to the average bead size of the empty spheres within each group for better comparison of the effects of the different nozzle systems on the microsphere size distribution. Interestingly, a marked relative increase in microsphere diameter and heterogeneity was observed with the vibrational nozzle system when islets were included. This trend was not seen with the air jet nozzle. In fact, the introduction of islets appeared to improve size uniformity in the air nozzle group, as fewer outliers per 100 spheres were observed compared to empty spheres. However, the average diameter did not appear to differ significantly from the empty spheres in this group.

B6.2 Discussion

The vibrational nozzle system was found to be better for fabricating empty spheres, generating the most uniform size distribution of microspheres. However, the air jet nozzle was vastly superior to the vibrational nozzle for encapsulating islets. Microsphere size distribution was extremely heterogeneous when using the vibrational nozzle with islets. A likely explanation for this stark difference is that the air jet nozzle does not rely on the

principle of laminar fluid flow as does the vibrational nozzle. The inclusion of the relatively large islet particles may have disrupted the laminar flow required for proper droplet generation with the vibrational nozzle. In contrast, size uniformity appeared to improve with the inclusion of islets using the air nozzle compared to empty spheres, though the reason for this is unclear. Thus, the air nozzle system was selected for future development in islet encapsulation, while the vibrational nozzle may be preferred for encapsulation of proteins, or smaller, single cells.

General Summary

The fundamental concept of the core-shell spherification method is relatively simple; a temporary, spherical alginate shell holds a desired hydrogel precursor in place long enough for it to cross-linking, and is subsequently dissolved. However, in practice, several variables came to light that required further investigation, particularly with regard to miniaturization of the initial proof of concept to the target microsphere size of < 1mm in diameter. The dynamic environment inherent to this method presented additional challenges when utilizing the photo-cross-linkable PEGDA gel precursor, which diffused out of the alginate shell much more rapidly on account of its low molecular weight compared to the HA polymers. To overcome this, the cross-linking rate had to be significantly increased, but in such a way that cytotoxicity to encapsulated cells was avoided. Ultimately, it was determined that a markedly increased irradiance intensity was necessary to achieve sufficient cross-linking kinetics without increasing photoinitiator concentrations to toxic levels. Furthermore, because a minimal core solution viscosity is required to generate spherical constructs, additional studies were done to identify a

formulation of PEGDA precursor what would meet the viscosity requirement while resulting in the least extensive post-fabrication swelling behavior. Finally, droplet generation technology was also evaluated to elucidate the benefits and limitations of two available nozzle systems. An air jet nozzle system had clear benefit for encapsulation of large cellular aggregates, i.e. islets, while a vibrational nozzle facilitated excellent control of microsphere diameter when islets were not present, indicating that this nozzle system would likely be preferable for encapsulation of much smaller objects like proteins or single cells.

Appendix B Figures and Tables

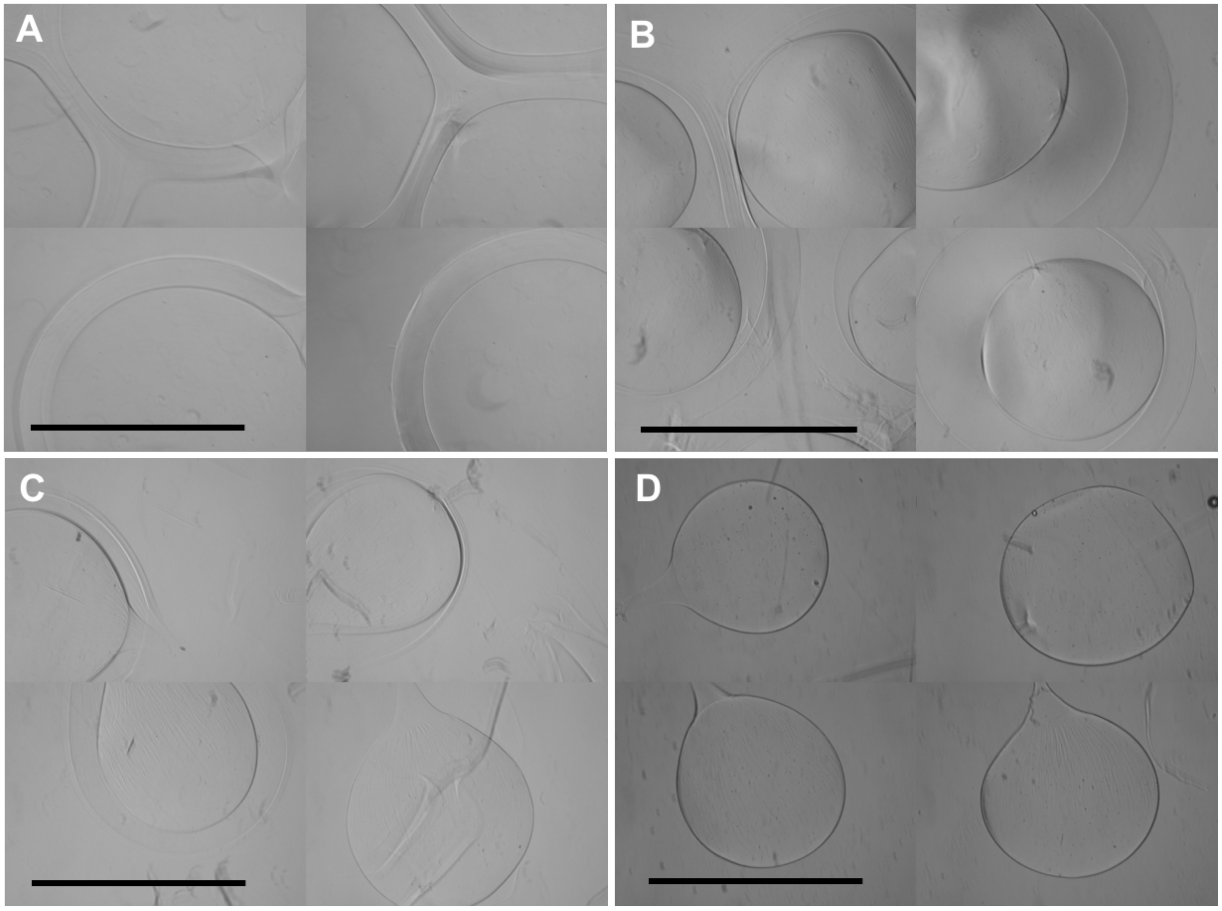

Figure B1.1. Core-shell spherification proof of concept study.
Shown here are photomicrographs taken of the initial proof of concept study for the core-shell spherification method. Core-shell constructs containing the HA precursor trapped within an alginate shell **(A)**. Core-shell constructs after overnight cross-linking **(B)**. Weakened alginate shells after 20 minutes of incubation in 50 mM citrate **(C)**. Final HA spheres after complete alginate shell dissolution **(D)**. Scale bars = 2 mm.

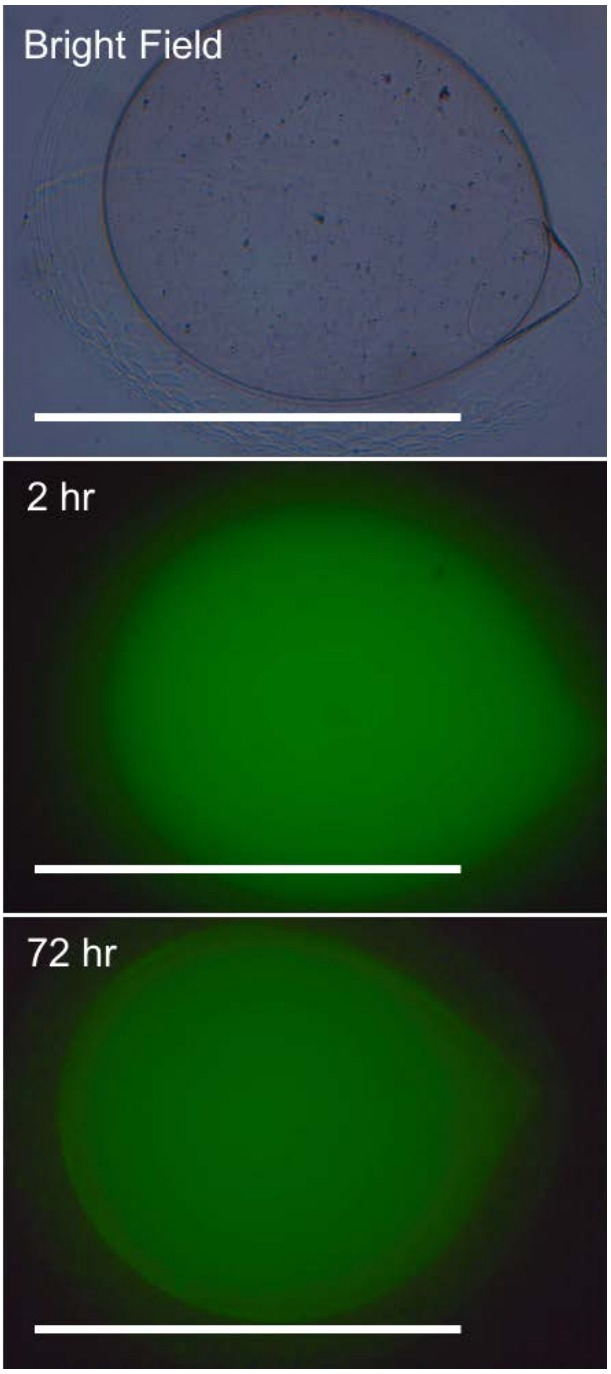

Figure B2.1. Fluorescent labelling of HA precursor.
HA prepolymers were labelled with a green fluorescent probe in order to investigate the effectiveness of the alginate shell for preventing diffusion of the HA out of the core area. Fluorescent images of the core-shell constructs produced with the labelled HA were taken after 2 and 72 hours of incubation in PBS. Scale bars = 2 mm.

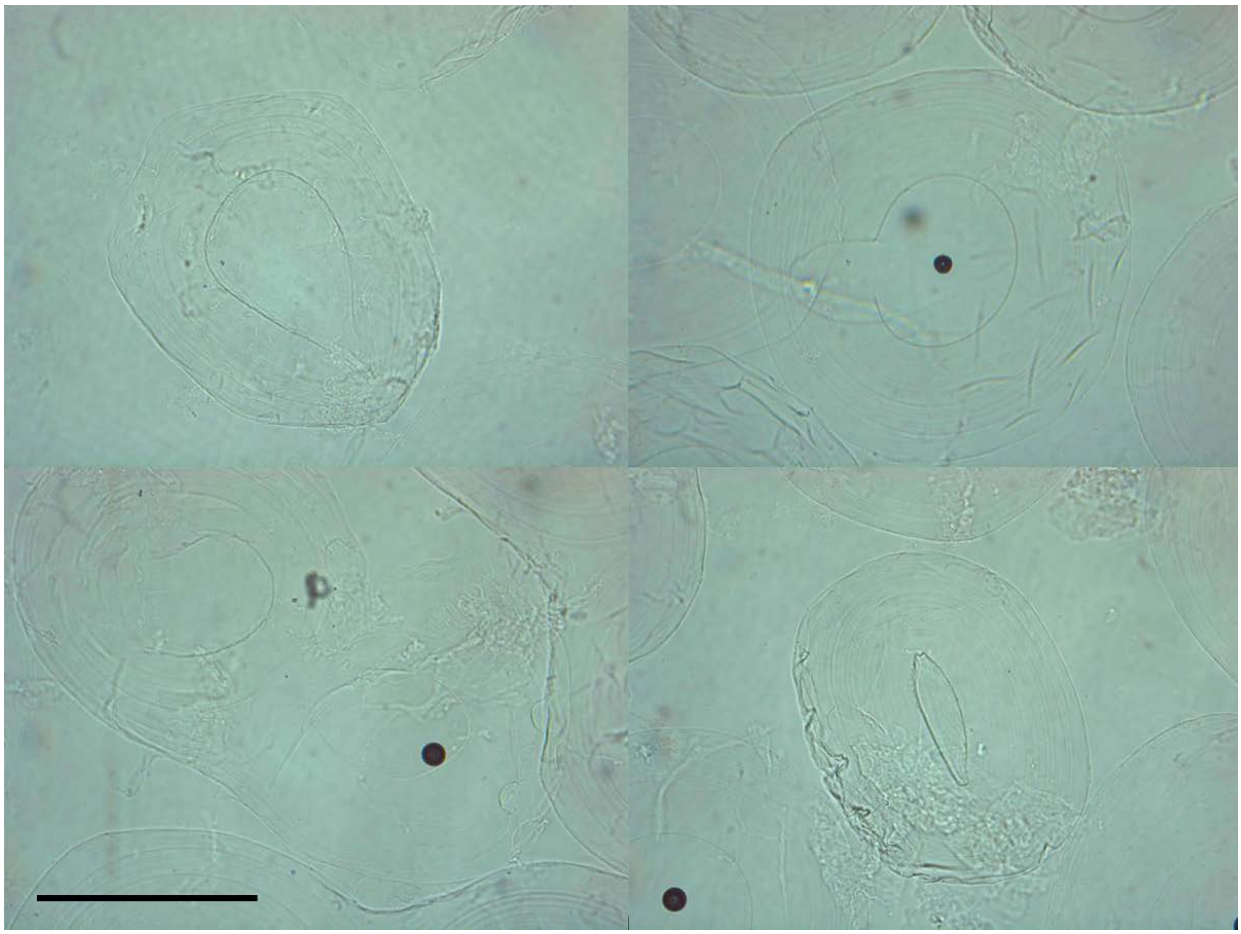

Figure B3.1. Poorly formed core-shell constructs.
Initial attempts to reduce the size of the core-shell constructs were largely unsuccessful. Constructs had very poor sphericity, rough edges, and large protrusions. In many cases, alginate shells were too weak to withstand even mild stirring or handling, and would collapse onto themselves. A collapsed core-shell can be seen in the *bottom right corner* of the figure. Scale bar = 1 mm.

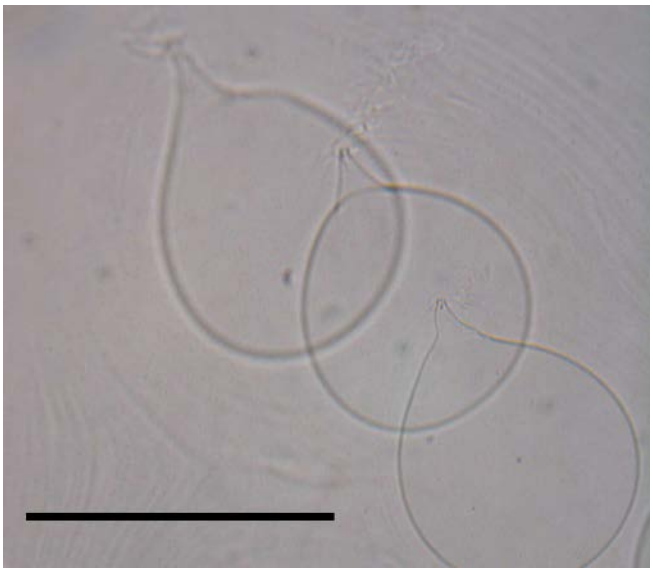

Figure B3.2. Examples of tail-like features in early microspheres.
Smaller, lighter droplets often appeared to linger near the surface of the alginate bath upon contact, resulting in the formation of small, tail-like features extending from an otherwise spherical construct. Increasing the density of the droplet solutions, among other modifications, helped to eliminate these undesired morphological deformities. Scale bar = 1 mm.

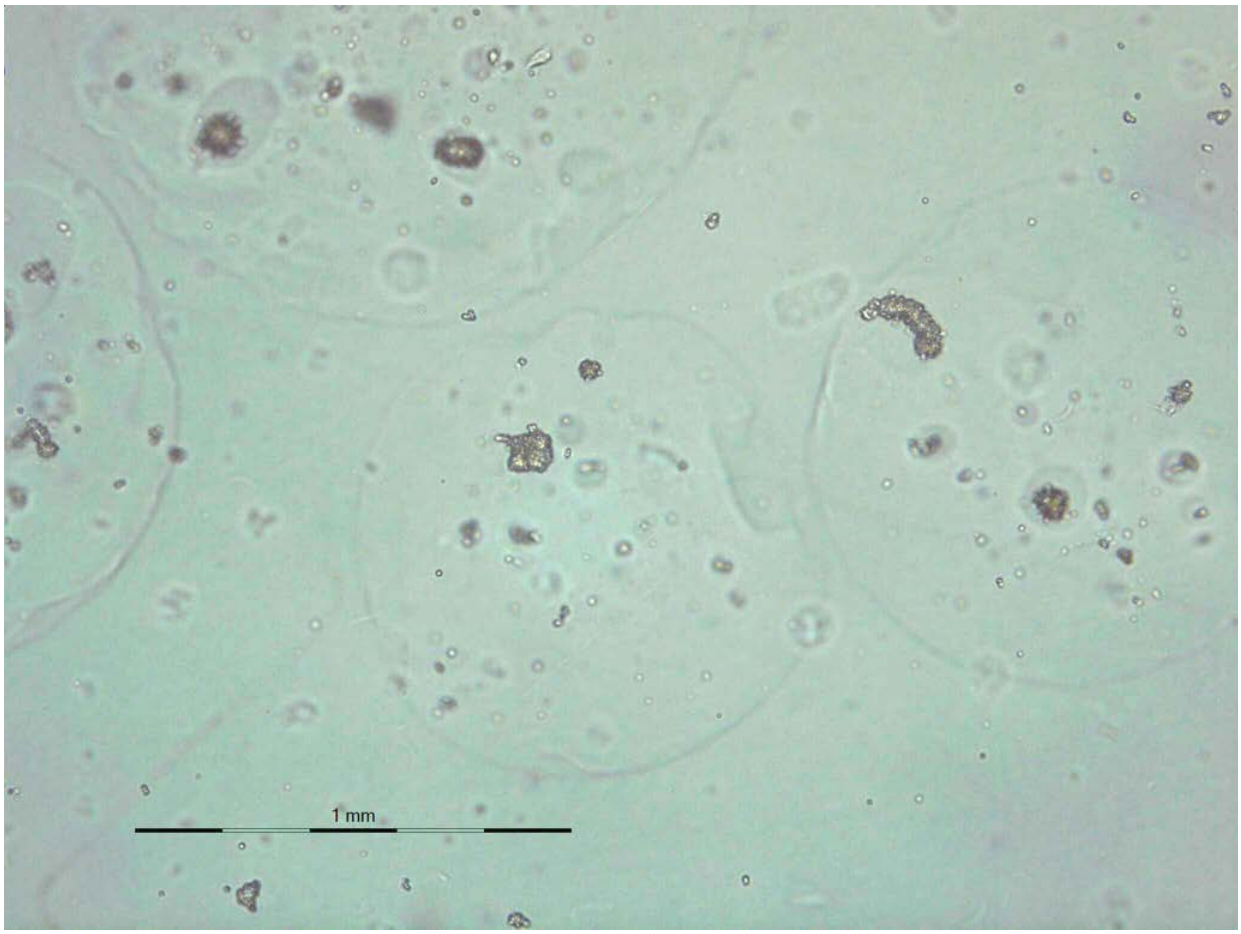

Figure B5.1. Results of insufficient cross-linking rate.
Islet microspheres seen above were fabricated with insufficient UV light intensity and were thus very weak and easily damaged. Empty void spaces can be seen where islets were too loosely entrapped, and fell out. Scale bar = 1 mm.

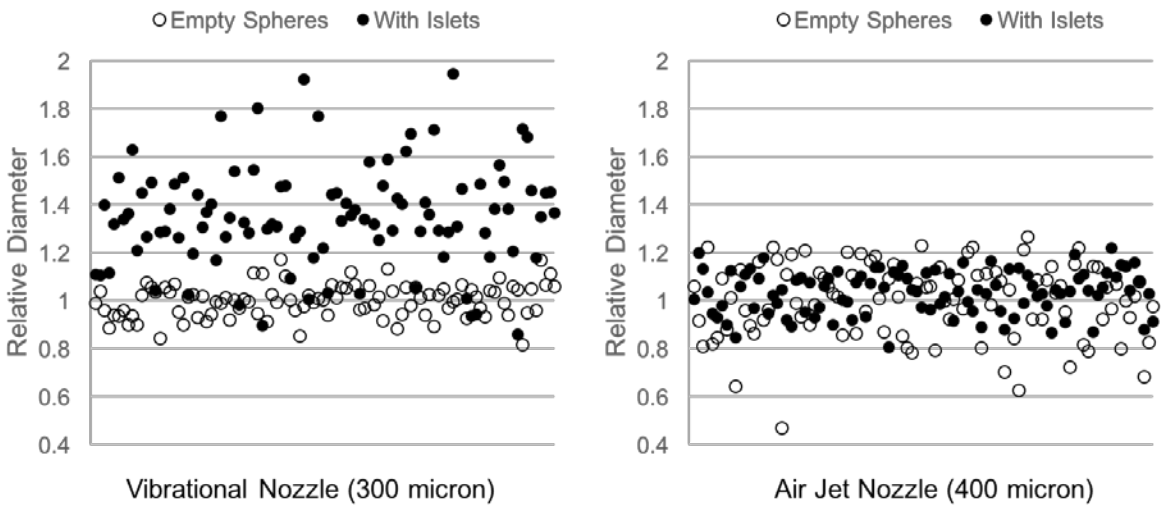

Figure B6.1. Comparison of droplet generation nozzle systems.
Empty and islet containing microspheres were fabricated using two different droplet generation systems. The diameters of 100 individual microspheres produced by either a vibrational nozzle (left) or air jet nozzle (*right*) were measured, and then normalized to the average diameter of the empty spheres for each nozzle type.

Precursor Formula	Average MW	Initial Mass (g)	Swollen Mass (g)	Fold Increase
30% 10 kDa	*10 kDa*	*0.2705*	*0.721*	*2.67*
20/10% Hybrid	*8.9 kDa*	*0.3016*	*0.5630*	*1.87*
18/12% Hybrid	*10 kDa*	*0.2735*	*0.5435*	*1.99*
15/15% Hybrid	*11.7 kDa*	*0.2906*	*0.6399*	*2.20*
12/18% Hybrid	*13.36 kDa*	*0.2933*	*0.7203*	*2.46*
10/20% Hybrid	*14.46 kDa*	*0.2770*	*0.7276*	*2.62*

Table B4.1. PEGDA swelling study results.
Hybrid gel precursor was made by combining PEGDA 3.4 kDa and 20 kDa at various ratios. Formulae for hybrid gels list the mass fraction of 3.4 kDa first, followed by 20 kDa.

REFERENCES

1 Shapiro AM, Lakey JR, Ryan EA, Korbutt GS, Toth E, Warnock GL, *et al.* Islet transplantation in seven patients with type 1 diabetes mellitus using a glucocorticoid-free immunosuppressive regimen. *N Engl J Med* 2000;**343**::230–8. https://doi.org/10.1056/NEJM200007273430401.

2 Eggerman T, Arreaza-Rubin G, Hering B. *Collaborative Islet Transplant Registry Eighth Annual Report*. The EMMES Corporation; 2016.

3 Wisel SA, Braun HJ, Stock PG. Current outcomes in islet versus solid organ pancreas transplant for β-cell replacement in type 1 diabetes. *Curr Opin Organ Transplant* 2016;**21**::399–404. https://doi.org/10.1097/MOT.0000000000000332.

4 Barton FB, Rickels MR, Alejandro R, Hering BJ, Wease S, Naziruddin B, *et al.* Improvement in outcomes of clinical islet transplantation: 1999-2010. *Diabetes Care* 2012;**35**::1436–45. https://doi.org/10.2337/dc12-0063.

5 Pepper AR, Gala-Lopez B, Ziff O, Shapiro AJ. Current status of clinical islet transplantation. *World J Transplant* 2013;**3**::48–53. https://doi.org/10.5500/wjt.v3.i4.48.

6 Cho NH, Whiting D. *IDF Diabetes Atlas Seventh Edition*. International Diabetes Federation; 2015.

7 Eggerman T, Hering B. *Collaborative Islet Transplant Registry Annual Report*. The EMMES Corporation; 2004.

8 Ricordi C, Lacy PE, Finke EH, Olack BJ, Scharp DW. Automated method for isolation of human pancreatic islets. *Diabetes* 1988;**37**::413–20.

9 Pisania A, Weir GC, O'Neil JJ, Omer A, Tchipashvili V, Lei J, *et al.* Quantitative analysis of cell composition and purity of human pancreatic islet preparations. *Lab Invest* 2010;**90**::1661–75. https://doi.org/10.1038/labinvest.2010.124.

10 Tanioka Y, Sutherland DE, Kuroda Y, Gilmore TR, Asaheim TC, Kronson JW, *et al.* Excellence of the two-layer method (University of Wisconsin solution/perfluorochemical) in pancreas preservation before islet isolation. *Surgery* 1997;**122**::435–41; discussion 441–2. https://doi.org/10.1016/S0039-6060(97)90037-4.

11 Eckhard M, Brandhorst D, Brandhorst H, Brendel MD, Bretzel RG. Optimization in osmolality and range of density of a continuous ficoll-sodium-diatrizoate gradient for isopycnic purification of isolated human islets. *Transplant Proc* 2004;**36**::2849–54. https://doi.org/10.1016/j.transproceed.2004.09.078.

12 Noguchi H, Naziruddin B, Shimoda M, Fujita Y, Chujo D, Takita M, *et al.* Evaluation of osmolality of density gradient for human islet purification. *Cell Transplant* 2012;**21**::493–500. https://doi.org/10.3727/096368911X605402.

13 Vincent R, Nadeau D. Adjustment of the osmolality of Percoll for the isopycnic separation of cells and cell organelles. *Anal Biochem* 1984;**141**::322–8. https://doi.org/10.1016/0003-2697(84)90049-6.

14 Noguchi H, Naziruddin B, Shimoda M, Chujo D, Takita M, Sugimoto K, *et al.* A Combined Continuous Density/Osmolality Gradient for Supplemental Purification of Human Islets. *Cell Medicine* 2012;**3**::3341. https://doi.org/10.3727/215517912X639388.

15 Taylor MJ, Baicu S, Greene E, Vazquez A, Brassil J. Islet isolation from juvenile porcine pancreas after 24-h hypothermic machine perfusion preservation. *Cell Transplant* 2010;**19**::613–28. https://doi.org/10.3727/096368910X486316.

16 Niclauss N, Wojtusciszyn A, Morel P, Demuylder-Mischler S, Brault C, Parnaud G, *et al.* Comparative impact on islet isolation and transplant outcome of the preservation solutions Institut Georges Lopez-1, University of Wisconsin, and Celsior. *Transplantation* 2012;**93**::703–8. https://doi.org/10.1097/TP.0b013e3182476cc8.
17 MacGregor RR, Williams SJ, Tong PY, Kover K, Moore WV, Stehno-Bittel L. Small rat islets are superior to large islets in in vitro function and in transplantation outcomes. *Am J Physiol Endocrinol Metab* 2006;**290**::E771–9. https://doi.org/10.1152/ajpendo.00097.2005.
18 Williams SJ, Huang H-HH, Kover K, Moore W, Berkland C, Singh M, *et al.* Reduction of diffusion barriers in isolated rat islets improves survival, but not insulin secretion or transplantation outcome. *Organogenesis* 2010;**6**::115–24.
19 Williams SJ, Schwasinger-Schmidt T, Zamierowski D, Stehno-Bittel L. Diffusion into human islets is limited to molecules below 10 kDa. *Tissue Cell* 2012;**44**::332–41. https://doi.org/10.1016/j.tice.2012.05.001.
20 Lehmann R, Zuellig RA, Kugelmeier P, Baenninger PB, Moritz W, Perren A, *et al.* Superiority of small islets in human islet transplantation. *Diabetes* 2007;**56**::594–603. https://doi.org/10.2337/db06-0779.
21 Steiner DJ, Kim A, Miller K, Hara M. Pancreatic islet plasticity: interspecies comparison of islet architecture and composition. *Islets* 2010;**2**::135–45.
22 Suszynski TM, Wilhelm JJ, Radosevich DM, Balamurugan AN, Sutherland DE, Beilman GJ, *et al.* Islet size index as a predictor of outcomes in clinical islet autotransplantation. *Transplantation* 2014;**97**::1286–91. https://doi.org/10.1097/01.TP.0000441873.35383.1e.
23 Ricordi C, Gray DW, Hering BJ, Kaufman DB, Warnock GL, Kneteman NM, *et al.* Islet isolation assessment in man and large animals. *Acta Diabetol Lat* 1990;**27**::185–95. https://doi.org/10.1007/BF02581331.
24 United States Department of Health and Human Services. *Organ Procurement and Transplantation Network: National Data*. 2017.
25 Kandaswamy R, Sutherland DE. Pancreas versus islet transplantation in diabetes mellitus: How to allocate deceased donor pancreata? *Transplant Proc* 2006;**38**::365–7. https://doi.org/10.1016/j.transproceed.2006.01.005.
26 Sutherland DE, Gruessner RW, Dunn DL, Matas AJ, Humar A, Kandaswamy R, *et al.* Lessons learned from more than 1,000 pancreas transplants at a single institution. *Ann Surg* 2001;**233**::463–501.
27 Zeng Y, Ricordi C, Lendoire J, Carroll PB, Alejandro R, Bereiter DR, *et al.* The effect of prednisone on pancreatic islet autografts in dogs. *Surgery* 1993;**113**::98–102.
28 Brendel M, Schulz A, Bretzel R. *International Islet Transplant Registry report*. Giessen, Germany: University of Giessen; 1999.
29 Ryan EA, Paty BW, Senior PA, Bigam D, Alfadhli E, Kneteman NM, *et al.* Five-year follow-up after clinical islet transplantation. *Diabetes* 2005;**54**::2060–9.
30 Al-Adra DP, Gill RS, Imes S, O'Gorman D, Kin T, Axford SJ, *et al.* Single-donor islet transplantation and long-term insulin independence in select patients with type 1 diabetes mellitus. *Transplantation* 2014;**98**::1007–12. https://doi.org/10.1097/TP.0000000000000217.
31 Bellin MD, Barton FB, Heitman A, Harmon JV, Kandaswamy R, Balamurugan

AN, *et al.* Potent induction immunotherapy promotes long-term insulin independence after islet transplantation in type 1 diabetes. *Am J Transplant* 2012;**12**::1576–83. https://doi.org/10.1111/j.1600-6143.2011.03977.x.
32 Lablanche S, Borot S, Wojtusciszyn A, Bayle F, Tétaz R, Badet L, *et al.* Five-Year Metabolic, Functional, and Safety Results of Patients With Type 1 Diabetes Transplanted With Allogenic Islets Within the Swiss-French GRAGIL Network. *Diabetes Care* 2015;**38**::1714–22. https://doi.org/10.2337/dc15-0094.
33 Vantyghem M-CC, Defrance F, Quintin D, Leroy C, Raverdi V, Prévost G, *et al.* Treating diabetes with islet transplantation: lessons from the past decade in Lille. *Diabetes Metab* 2014;**40**::108–19. https://doi.org/10.1016/j.diabet.2013.10.003.
34 Qi M, Kinzer K, Danielson KK, Martellotto J, Barbaro B, Wang Y, *et al.* Five-year follow-up of patients with type 1 diabetes transplanted with allogeneic islets: the UIC experience. *Acta Diabetol* 2014;**51**::833–43. https://doi.org/10.1007/s00592-014-0627-6.
35 Gruessner RW, Gruessner AC. The current state of pancreas transplantation. *Nat Rev Endocrinol* 2013;**9**::555–62. https://doi.org/10.1038/nrendo.2013.138.
36 Kandaswamy R, Skeans MA, Gustafson SK, Carrico RJ, Tyler KH, Israni AK, *et al.* OPTN/SRTR 2013 Annual Data Report: pancreas. *Am J Transplant* 2015;**15 Suppl 2**::1–20. https://doi.org/10.1111/ajt.13196.
37 Srinivasan P, Huang GC, Amiel SA, Heaton ND. Islet cell transplantation. *Postgrad Med J* 2007;**83**::224–9. https://doi.org/10.1136/pgmj.2006.053447.
38 Froud T, Ricordi C, Baidal DA, Hafiz MM, Ponte G, Cure P, *et al.* Islet transplantation in type 1 diabetes mellitus using cultured islets and steroid-free immunosuppression: Miami experience. *Am J Transplant* 2005;**5**::2037–46. https://doi.org/10.1111/j.1600-6143.2005.00957.x.
39 Yang HK, Yoon K-HH. Current status of encapsulated islet transplantation. *J Diabetes Complicat* 2015;**29**::737–43. https://doi.org/10.1016/j.jdiacomp.2015.03.017.
40 Shapiro AM, Pokrywczynska M, Ricordi C. Clinical pancreatic islet transplantation. *Nat Rev Endocrinol* 2016. https://doi.org/10.1038/nrendo.2016.178.
41 Li RH, Altreuter DH, Gentile FT. Transport characterization of hydrogel matrices for cell encapsulation. *Biotechnology and …* 1996. https://doi.org/10.1002/(SICI)1097-0290(19960520)50:4<365::AID-BIT3>3.0.CO;2-J.
42 Amsden B, Turner N. Diffusion characteristics of calcium alginate gels. *Biotechnol Bioeng* 1999;**65**::605–10. https://doi.org/10.1002/(SICI)1097-0290(19991205)65:5<605::AID-BIT14>3.0.CO;2-C.
43 Dembczynski, Jankowski. Characterisation of small molecules diffusion in hydrogel-membrane liquid-core capsules. *Biochem Eng J* 2000;**6**::41–4. https://doi.org/10.1016/S1369-703X(00)00070-X.
44 Shoichet MS, Li RH, White ML, Winn SR. Stability of hydrogels used in cell encapsulation: An in vitro comparison of alginate and agarose. *Biotechnol Bioeng* 1996;**50**::374–81. https://doi.org/10.1002/(SICI)1097-0290(19960520)50:4<374::AID-BIT4>3.0.CO;2-I.
45 Sakata N, Sumi S, Yoshimatsu G, Goto M, Egawa S, Unno M. Encapsulated islets transplantation: Past, present and future. *World J Gastrointest Pathophysiol* 2012;**3**::19–26. https://doi.org/10.4291/wjgp.v3.i1.19.
46 Armstrong JK, Wenby RB, Meiselman HJ, Fisher TC. The hydrodynamic radii of

macromolecules and their effect on red blood cell aggregation. *Biophys J* 2004;**87**::4259–70. https://doi.org/10.1529/biophysj.104.047746.
47 Lim F, Sun AM. Microencapsulated islets as bioartificial endocrine pancreas. *Science* 1980;**210**::908–10. https://doi.org/10.1126/science.6776628.
48 Dufrane D, Goebbels R-MM, Saliez A, Guiot Y, Gianello P. Six-month survival of microencapsulated pig islets and alginate biocompatibility in primates: proof of concept. *Transplantation* 2006;**81**::1345–53. https://doi.org/10.1097/01.tp.0000208610.75997.20.
49 Langlois G, Dusseault J, Bilodeau S, Tam SK, Magassouba D, Hallé J-PP. Direct effect of alginate purification on the survival of islets immobilized in alginate-based microcapsules. *Acta Biomater* 2009;**5**::3433–40. https://doi.org/10.1016/j.actbio.2009.05.029.
50 Hillberg AL, Kathirgamanathan K, Lam JBB, Law LY, Garkavenko O, Elliott RB. Improving alginate-poly-L-ornithine-alginate capsule biocompatibility through genipin crosslinking. *J Biomed Mater Res Part B Appl Biomater* 2013;**101**::258–68. https://doi.org/10.1002/jbm.b.32835.
51 Zhang WJ, Laue C, Hyder A, Schrezenmeir J. Purity of alginate affects the viability and fibrotic overgrowth of encapsulated porcine islet xenografts. *Transplant Proc* 2001;**33**::3517–9.
52 Park H-SS, Kim J-WW, Lee S-HH, Yang HK, Ham D-SS, Sun C-LL, *et al.* Antifibrotic effect of rapamycin containing polyethylene glycol-coated alginate microcapsule in islet xenotransplantation. *J Tissue Eng Regen Med* 2015. https://doi.org/10.1002/term.2029.
53 Veiseh O, Doloff JC, Ma M, Vegas AJ, Tam HH, Bader AR, *et al.* Size- and shape-dependent foreign body immune response to materials implanted in rodents and non-human primates. *Nat Mater* 2015;**14**::643–51. https://doi.org/10.1038/nmat4290.
54 Buder B, Alexander M, Krishnan R, Chapman DW, Lakey JR. Encapsulated islet transplantation: strategies and clinical trials. *Immune Netw* 2013;**13**::235–9. https://doi.org/10.4110/in.2013.13.6.235.
55 Tuch BE, Keogh GW, Williams LJ, Wu W, Foster JL, Vaithilingam V, *et al.* Safety and viability of microencapsulated human islets transplanted into diabetic humans. *Diabetes Care* 2009;**32**::1887–9. https://doi.org/10.2337/dc09-0744.
56 Gotfredsen CF, Stewart MG, O'Shea GM, Vose JR, Horn T, Moody AJ. The fate of transplanted encapsulated islets in spontaneously diabetic BB/Wor rats. *Diabetes Res* 1990;**15**::157–63.
57 Duvivier-Kali VF, Omer A, Lopez-Avalos MD, O'Neil JJ, Weir GC. Survival of microencapsulated adult pig islets in mice in spite of an antibody response. *Am J Transplant* 2004;**4**::1991–2000. https://doi.org/10.1111/j.1600-6143.2004.00628.x.
58 Suzuki K, Bonner-Weir S, Trivedi N, Yoon KH, Hollister-Lock J, Colton CK, *et al.* Function and survival of macroencapsulated syngeneic islets transplanted into streptozocin-diabetic mice. *Transplantation* 1998;**66**::21–8.
59 Juste S, Lessard M, Henley N, Ménard M, Hallé J. Effect of poly-L-lysine coating on macrophage activation by alginate-based microcapsules: Assessment using a new in vitro method. *J Biomed Mater Res A* 2005;**72A**::389–98. https://doi.org/10.1002/jbm.a.30254.
60 Ludwig B, Zimerman B, Steffen A, Yavriants K, Azarov D, Reichel A, *et al.* A

novel device for islet transplantation providing immune protection and oxygen supply. *Horm Metab Res* 2010;**42**::918–22. https://doi.org/10.1055/s-0030-1267916.
61 Sutherland D, Matas AJ, Najarian JS. Pancreas and islet transplantation. *World Journal of Surgery* 1977.
62 Rajotte RV, Warnock GL, Evans MG. Isolation of viable islets of Langerhans from collagenase-perfused canine and human pancreata. *Transplantation …* 1987.
63 Warnock GL, Rajotte RV. Critical mass of purified islets that induce normoglycemia after implantation into dogs. *Diabetes* 1988. https://doi.org/10.2337/diab.37.4.467.
64 Warnock GL, Cattral MS, Rajotte RV. Normoglycemia after implantation of purified islet cells in dogs. *Can J Surg* 1988;**31**::421–6.
65 Warnock GL, Cattral MS, Evans MG. Mass isolation of pure canine islets. *Transplantation …* 1989.
66 Warnock GL, Kneteman NM, Evans MG. Comparison of automated and manual methods for islet isolation. *Canadian Journal of …* 1990.
67 Warnock GL, Dabbs KD, Evans MG, Cattral MS, Kneteman NM, Rajotte RV. Critical mass of islets that function after implantation in a large mammalian. *Horm Metab Res Suppl* 1990;**25**::156–61.
68 Vrabelova D, Adin C, Gilor C, Rajab A. Pancreatic islet transplantation: from dogs to humans and back again. *Vet Surg* 2014;**43**::631–41. https://doi.org/10.1111/j.1532-950X.2014.12224.x.
69 Alejandro R, Cutfield RG, Shienvold FL, Polonsky KS, Noel J, Olson L, *et al.* Natural history of intrahepatic canine islet cell autografts. *J Clin Invest* 1986;**78**::1339–48. https://doi.org/10.1172/JCI112720.
70 Kneteman NM, Warnock GL, Evans MG, Nason RW, Rajotte RV. Prolonged function of canine pancreatic fragments autotransplanted to the spleen by venous reflux. *Transplantation* 1990;**49**::679–81.
71 Kin T, O'Neil JJ, Pawlick R, Korbutt GS, Shapiro AM, Lakey JR. The use of an approved biodegradable polymer scaffold as a solid support system for improvement of islet engraftment. *Artif Organs* 2008;**32**::990–3. https://doi.org/10.1111/j.1525-1594.2008.00688.x.
72 Alejandro R, Latif Z, Polonsky KS, Shienvold FL, Civantos F, Mint DH. Natural history of multiple intrahepatic canine islet allografts during and following administration of cyclosporine. *Transplantation* 1988;**45**::1036–44.
73 Klausner J. *State of Pet Health 2011 Report vol. 1*. Banfield Pet Hospital; 2011.
74 Aja D. *State of Pet Health 2016 Report*. Banfield Pet Hospital; 2016.
75 Fleeman LM, Rand JS. Management of canine diabetes. *Vet Clin North Am Small Anim Pract* 2001;**31**::855–80, vi.
76 Scharp DW, Marchetti P. Encapsulated islets for diabetes therapy: history, current progress, and critical issues requiring solution. *Adv Drug Deliv Rev* 2014;**67-68**::35–73. https://doi.org/10.1016/j.addr.2013.07.018.
77 Burghen GA, Murrell LR. Factors influencing isolation of islets of Langerhans. *Diabetes* 1989;**38 Suppl 1**::129–32. https://doi.org/10.2337/diab.38.1.S129.
78 Hubert T, Gmyr V, Arnalsteen L, Jany T, Triponez F, Caiazzo R, *et al.* Influence of preservation solution on human islet isolation outcome. *Transplantation*

2007;**83**::270–6. https://doi.org/10.1097/01.tp.0000251723.97483.16.
79 Jung HS, Choi S-HH, Kim S-JJ, Lee KT, Lee JK, Jang K-TT, *et al.* A better yield of islet cell mass from living pancreatic donors compared with cadaveric donors. *Clin Transplant* 2007;**21**::738–43. https://doi.org/10.1111/j.1399-0012.2007.00731.x.
80 Contreras JL, Eckstein C, Smyth CA, Sellers MT, Vilatoba M, Bilbao G, *et al.* Brain death significantly reduces isolated pancreatic islet yields and functionality in vitro and in vivo after transplantation in rats. *Diabetes* 2003;**52**::2935–42.
81 London NJ, Swift SM, Clayton HA. Isolation, culture and functional evaluation of islets of Langerhans. *Diabetes Metab* 1998;**24**::200–7.
82 Brandhorst D, Brandhorst H, Hering BJ, Federlin K, Bretzel RG. Islet isolation from the pancreas of large mammals and humans: 10 years of experience. *Exp Clin Endocrinol Diabetes* 1995;**103 Suppl 2**::3–14. https://doi.org/10.1055/s-0029-1211386.
83 Shimoda M, Noguchi H, Fujita Y, Takita M, Ikemoto T, Chujo D, *et al.* Islet purification method using large bottles effectively achieves high islet yield from pig pancreas. *Cell Transplantation* 2012;**21**::501–8. https://doi.org/10.3727/096368911x605411.
84 Shimoda M, Itoh T, Iwahashi S, Takita M, Sugimoto K, Kanak MA, *et al.* An effective purification method using large bottles for human pancreatic islet isolation. *Islets* 2012;**4**::398–404. https://doi.org/10.4161/isl.23008.
85 Alejandro R, Strasser S, Zucker PF, Mintz DH. Isolation of pancreatic islets from dogs. Semiautomated purification on albumin gradients. *Transplantation* 1990;**50**::207–10.
86 Barbaro B, Salehi P, Wang Y, Qi M, Gangemi A, Kuechle J, *et al.* Improved human pancreatic islet purification with the refined UIC-UB density gradient. *Transplantation* 2007;**84**::1200–3. https://doi.org/10.1097/01.tp.0000287127.00377.6f.
87 Kim S, Cui Z-KK, Fan J, Fartash A, Aghaloo TL, Lee M. Photocrosslinkable chitosan hydrogels functionalized with the RGD peptide and phosphoserine to enhance osteogenesis. *J Mater Chem B Mater Biol Med* 2016;**4**::5289–98. https://doi.org/10.1039/C6TB01154C.
88 Phelps EA, Headen DM, Taylor WR, Thulé PM, García AJJ. Vasculogenic bio-synthetic hydrogel for enhancement of pancreatic islet engraftment and function in type 1 diabetes. *Biomaterials* 2013;**34**::4602–11. https://doi.org/10.1016/j.biomaterials.2013.03.012.
89 Lim D-JJ, Antipenko SV, Anderson JM, Jaimes KF, Viera L, Stephen BR, *et al.* Enhanced rat islet function and survival in vitro using a biomimetic self-assembled nanomatrix gel. *Tissue Eng Part A* 2011;**17**::399–406. https://doi.org/10.1089/ten.TEA.2010.0151.
90 Prestwich GD. Engineering a clinically-useful matrix for cell therapy. *Organogenesis* 2008. https://doi.org/10.4161/org.6152.
91 Prestwich GD. Hyaluronic acid-based clinical biomaterials derived for cell and molecule delivery in regenerative medicine. *J Control Release* 2011;**155**::193–9. https://doi.org/10.1016/j.jconrel.2011.04.007.
92 Burdick JA, Prestwich GD. Hyaluronic acid hydrogels for biomedical applications. *Adv Mater Weinheim* 2011;**23**::H41–56. https://doi.org/10.1002/adma.201003963.
93 Vanderhooft JL, Alcoutlabi M, Magda JJ, Prestwich GD. Rheological properties of

cross-linked hyaluronan-gelatin hydrogels for tissue engineering. *Macromol Biosci* 2009;**9**::20–8. https://doi.org/10.1002/mabi.200800141.
94 Liu Y, Shu XZ, Prestwich GD. Osteochondral defect repair with autologous bone marrow-derived mesenchymal stem cells in an injectable, in situ, cross-linked synthetic extracellular matrix. *Tissue Eng* 2006;**12**::3405–16. https://doi.org/10.1089/ten.2006.12.3405.
95 Cheng K, Blusztajn A, Shen D, Li T-SS, Sun B, Galang G, *et al.* Functional performance of human cardiosphere-derived cells delivered in an in situ polymerizable hyaluronan-gelatin hydrogel. *Biomaterials* 2012;**33**::5317–24. https://doi.org/10.1016/j.biomaterials.2012.04.006.
96 Constantin M, Bucatariu S-MM, Doroftei F, Fundueanu G. Smart composite materials based on chitosan microspheres embedded in thermosensitive hydrogel for controlled delivery of drugs. *Carbohydr Polym* 2017;**157**::493–502. https://doi.org/10.1016/j.carbpol.2016.10.022.
97 Tang D-WW, Yu S-HH, Wu W-SS, Hsieh H-YY, Tsai Y-CC, Mi F-LL. Hydrogel microspheres for stabilization of an antioxidant enzyme: Effect of emulsion cross-linking of a dual polysaccharide system on the protection of enzyme activity. *Colloids Surf B Biointerfaces* 2014;**113**::59–68. https://doi.org/10.1016/j.colsurfb.2013.09.002.
98 Klausner J. *State of Pet Health 2014 Report*. Banfield Pet Hospital; 2014.
99 Ao Z, Matayoshi K, Lakey JR, Rajotte RV, Warnock GL. Survival and function of purified islets in the omental pouch site of outbred dogs. *Transplantation* 1993;**56**::524–9.
100 Abalovich AG, Bacqué MC, Grana D, Milei J. Pig pancreatic islet transplantation into spontaneously diabetic dogs. *Transplant Proc* 2009;**41**::328–30. https://doi.org/10.1016/j.transproceed.2008.08.159.
101 Wang T, Adcock J, Kühtreiber W, Qiang D, Salleng KJ, Trenary I, *et al.* Successful allotransplantation of encapsulated islets in pancreatectomized canines for diabetic management without the use of immunosuppression. *Transplantation* 2008;**85**::331–7. https://doi.org/10.1097/TP.0b013e3181629c25.
102 Soon-Shiong P, Feldman E, Nelson R, Heintz R, Yao Q, Yao Z, *et al.* Long-term reversal of diabetes by the injection of immunoprotected islets. *Proc Natl Acad Sci USA* 1993;**90**::5843–7. https://doi.org/10.1073/pnas.90.12.5843.
103 Vrabelova D, Adin CA, Kenzig A, Gilor C, Xu F, Buss JL, *et al.* Evaluation of a high-yield technique for pancreatic islet isolation from deceased canine donors. *Domest Anim Endocrinol* 2014;**47**::119–26. https://doi.org/10.1016/j.domaniend.2013.01.006.
104 Wieczorek G, Pospischil A, Perentes E. A comparative immunohistochemical study of pancreatic islets in laboratory animals (rats, dogs, minipigs, nonhuman primates). *Exp Toxicol Pathol* 1998;**50**::151–72. https://doi.org/10.1016/S0940-2993(98)80078-X.
105 Iwanaga Y, Sutherland D, Harmon J, Papas K. Pancreas preservation for pancreas and islet transplantation. *Curr Opin Organ Tran* 2008;**13**::445. https://doi.org/10.1097/MOT.0b013e328303df04.
106 Giraud S, Hauet T, Eugene M, Mauco G, Barrou B. A new preservation solution (SCOT 15) Improves the islet isolation process from pancreata of non-heart-beating donors: a Murine model. *Transplant Proc* 2009;**41**::3293–5.

https://doi.org/10.1016/j.transproceed.2009.08.042.
107 Guibert EE, Petrenko AY, Balaban CL, Somov AY, Rodriguez JVV, Fuller BJ. Organ Preservation: Current Concepts and New Strategies for the Next Decade. *Transfus Med Hemother* 2011;**38**::125–42. https://doi.org/10.1159/000327033.
108 Paushter DH, Qi M, Danielson KK, Harvat TA, Kinzer K, Barbaro B, *et al.* Histidine-tryptophan-ketoglutarate and University of Wisconsin solution demonstrate equal effectiveness in the preservation of human pancreata intended for islet isolation: a large-scale, single-center experience. *Cell Transplant* 2013;**22**::1113–21. https://doi.org/10.3727/096368912X657332.
109 Kühtreiber WM, Ho LT, Kamireddy A, Yacoub JA, Scharp DW. Islet isolation from human pancreas with extended cold ischemia time. *Transplant Proc* 2010;**42**::2027–31. https://doi.org/10.1016/j.transproceed.2010.05.099.
110 Amoli MM, Moosavizadeh R, Larijani B. Optimizing conditions for rat pancreatic islets isolation. *Cytotechnology* 2005;**48**::75–8. https://doi.org/10.1007/s10616-005-3586-5.
111 Jin S-MM, Lee H-SS, Oh S-HH, Park HJ, Park JB, Kim JH, *et al.* Adult porcine islet isolation using a ductal preservation method and purification with a density gradient composed of histidine-tryptophan-ketoglutarate solution and iodixanol. *Transplant Proc* 2014;**46**::1628–32. https://doi.org/10.1016/j.transproceed.2014.03.004.
112 Chadwick DR, Robertson GS, Toomey P, Contractor H, Rose S, James RF, *et al.* Pancreatic islet purification using bovine serum albumin: the importance of density gradient temperature and osmolality. *Cell Transplant* 1993;**2**::355–61.
113 Novikova L, Smirnova IV, Rawal S, Dotson AL, Benedict SH, Stehno-Bittel L. Variations in rodent models of type 1 diabetes: islet morphology. *J Diabetes Res* 2013;**2013**::965832. https://doi.org/10.1155/2013/965832.
114 Behboo R, Carroll PB, Ukah F, Gao W, Kirsch D, Dedousis N, *et al.* One-hour of hypothermic incubation in Euro-Collins improves islet purification. *Transplant Proc* 1994;**26**::645.
115 Ståhle M, Honkanen-Scott M, Ingvast S, Korsgren O, Friberg AS. Human islet isolation processing times shortened by one hour: minimized incubation time between tissue harvest and islet purification. *Transplantation* 2013;**96**::e91–3. https://doi.org/10.1097/01.TP.0000437562.31212.d5.
116 Latif ZA, Noel J, Alejandro R. A simple method of staining fresh and cultured islets. *Transplantation* 1988;**45**::827–30.
117 Ramachandran K, Peng X, Bokvist K, Stehno-Bittel L. Assessment of re-aggregated human pancreatic islets for secondary drug screening. *Br J Pharmacol* 2014;**171**::3010–22. https://doi.org/10.1111/bph.12622.
118 Ramachandran K, Williams SJ, Huang H-HH, Novikova L, Stehno-Bittel L. Engineering islets for improved performance by optimized reaggregation in a micromold. *Tissue Eng Part A* 2013;**19**::604–12. https://doi.org/10.1089/ten.TEA.2012.0553.
119 Yang S-YY, Lee J-JJ, Lee J-HH, Lee K, Oh SH, Lim Y-MM, *et al.* Secretagogin affects insulin secretion in pancreatic β-cells by regulating actin dynamics and focal adhesion. *Biochem J* 2016;**473**::1791–803. https://doi.org/10.1042/BCJ20160137.
120 Huang J-CC, Lu W-TT, Hsu BR, Kuo C-HH, Fu S-HH, Chen H-MM, *et al.* Canine

islet isolation, cryopreservation, and transplantation to nude mice. *Chang Gung Med J* 2003;**26**::722–8.
121 Woolcott OO, Bergman RN, Richey JM, Kirkman EL, Harrison LN, Ionut V, *et al.* Simplified method to isolate highly pure canine pancreatic islets. *Pancreas* 2012;**41**::31–8. https://doi.org/10.1097/MPA.0b013e318221fd0e.
122 Tsuchitani M, Sato J, Kokoshima H. A comparison of the anatomical structure of the pancreas in experimental animals. *J Toxicol Pathol* 2016;**29**::147–54. https://doi.org/10.1293/tox.2016-0016.
123 Gersell DJ, Gingerich RL, Greider MH. Regional distribution and concentration of pancreatic polypeptide in the human and canine pancreas. *Diabetes* 1979;**28**::11–5.
124 Van der Burg MP, Guicherit OR, Frölich M, Prins FA, Bruijn JA, Gooszen HG. Cell preservation in University of Wisconsin solution during isolation of canine islets of Langerhans. *Cell Transplant* 1994;**3**::315–24.
125 Kenmochi T, Asano T, Jingu K, Matsui Y, Maruyama M, Akutsu N, *et al.* Effectiveness of hydroxyethyl starch (HES) on purification of pancreatic islets. *J Surg Res* 2003;**111**::16–22. https://doi.org/10.1016/S0022-4804(03)00055-6.
126 Chadwick DR, Robertson GS, Contractor HH, Rose S, Johnson PR, James RF, *et al.* Storage of pancreatic digest before islet purification. The influence of colloids and the sodium to potassium ratio in University of Wisconsin-based preservation solutions. *Transplantation* 1994;**58**::99–104.
127 Southard JH, van Gulik TM, Ametani MS, Vreugdenhil PK, Lindell SL, Pienaar BL, *et al.* Important components of the UW solution. *Transplantation* 1990;**49**::251–7.
128 Woods EJ, Zieger MA, Lakey JR, Liu J, Critser JK. Osmotic characteristics of isolated human and canine pancreatic islets. *Cryobiology* 1997;**35**::106–13. https://doi.org/10.1006/cryo.1997.2029.
129 Hauet T, Goujon JM, Baumert H, Petit I, Carretier M, Eugene M, *et al.* Polyethylene glycol reduces the inflammatory injury due to cold ischemia/reperfusion in autotransplanted pig kidneys. *Kidney Int* 2002;**62**::654–67. https://doi.org/10.1046/j.1523-1755.2002.00473.x.
130 Hauet T, Mothes D, Goujon JM, Carretier M, Eugene M. Protective effect of polyethylene glycol against prolonged cold ischemia and reperfusion injury: study in the isolated perfused rat kidney. *J Pharmacol Exp Ther* 2001;**297**::946–52.
131 Ganote CE, Worstell J, Iannotti JP, Kaltenbach JP. Cellular swelling and irreversible myocardial injury. Effects of polyethylene glycol and mannitol in perfused rat hearts. *The American Journal of Pathology* 1977;**88**::95.
132 Neuzillet Y, Giraud S, Lagorce L, Eugene M, Debre P, Richard F, *et al.* Effects of the molecular weight of peg molecules (8, 20 and 35 KDA) on cell function and allograft survival prolongation in pancreatic islets transplantation. *Transplant Proc* 2006;**38**::2354–5. https://doi.org/10.1016/j.transproceed.2006.06.117.
133 Noguchi H, Ikemoto T, Naziruddin B, Jackson A, Shimoda M, Fujita Y, *et al.* Iodixanol-Controlled Density Gradient During Islet Purification Improves Recovery Rate in Human Islet Isolation. *Transplantation* 2009;**87**::1629. https://doi.org/10.1097/TP.0b013e3181a5515c.
134 Wang Y, Danielson KK, Ropski A, Harvat T, Barbaro B, Paushter D, *et al.* Systematic analysis of donor and isolation factor's impact on human islet yield and size

distribution. *Cell Transplant* 2013;**22**::2323–33. https://doi.org/10.3727/096368912X662417.
135 Lakey JR, Cavanagh TJ, Zieger MA, Wright M. Evaluation of a purified enzyme blend for the recovery and function of canine pancreatic islets. *Cell Transplant* 1998;**7**::365–72.
136 Kaufman DB, Morel P, Field MJ, Munn SR, Sutherland DE. Purified canine islet autografts. Functional outcome as influenced by islet number and implantation site. *Transplantation* 1990;**50**::385–91.
137 Evans MG, Warnock GL, Kneteman NM, Rajotte RV. Reversal of diabetes in dogs by transplantation of pure cryopreserved islets. *Transplantation* 1990;**50**::202–6.
138 Alejandro R, Barton FB, Hering BJ, Wease S. 2008 Update from the Collaborative Islet Transplant Registry. *Transplantation* 2008;**86**::1783–8. https://doi.org/10.1097/TP.0b013e3181913f6a.
139 Division of Diabetes Translation. *National Diabetes Statistics Report, 2014*. National Center for Chronic Disease Prevention and Health Promotion: Centers for Disease Control and Prevention; 2014.
140 Graham JG, Zhang X, Goodman A, Pothoven K, Houlihan J, Wang S, *et al.* PLG scaffold delivered antigen-specific regulatory T cells induce systemic tolerance in autoimmune diabetes. *Tissue Eng Part A* 2013;**19**::1465–75. https://doi.org/10.1089/ten.tea.2012.0643.
141 Maehr R, Chen S, Snitow M, Ludwig T, Yagasaki L, Goland R, *et al.* Generation of pluripotent stem cells from patients with type 1 diabetes. *Proc Natl Acad Sci USA* 2009;**106**::15768–73. https://doi.org/10.1073/pnas.0906894106.
142 Calafiore R, Basta G. Clinical application of microencapsulated islets: actual prospectives on progress and challenges. *Adv Drug Deliv Rev* 2014;**67-68**::84–92. https://doi.org/10.1016/j.addr.2013.09.020.
143 Dufrane D, Gianello P. Macro- or microencapsulation of pig islets to cure type 1 diabetes. *World J Gastroenterol* 2012;**18**::6885–93. https://doi.org/10.3748/wjg.v18.i47.6885.
144 Elliott RB, Escobar L, Tan PL, Muzina M, Zwain S, Buchanan C. Live encapsulated porcine islets from a type 1 diabetic patient 9.5 yr after xenotransplantation. *Xenotransplantation* 2007;**14**::157–61. https://doi.org/10.1111/j.1399-3089.2007.00384.x.
145 Kirk K, Hao E, Lahmy R, Itkin-Ansari P. Human embryonic stem cell derived islet progenitors mature inside an encapsulation device without evidence of increased biomass or cell escape. *Stem Cell Res* 2014;**12**::807–14. https://doi.org/10.1016/j.scr.2014.03.003.
146 Campanha-Rodrigues AL, Grazioli G, Oliveira TC, Campos-Lisbôa AC, Mares-Guia TR, Sogayar MC. Therapeutic potential of laminin-biodritin microcapsules for type 1 diabetes mellitus. *Cell Transplant* 2015;**24**::247–61. https://doi.org/10.3727/096368913X675160.
147 Mohan N, Gupta V, Sridharan B, Sutherland A, Detamore MS. The potential of encapsulating ‘raw materials’ in 3D osteochondral gradient scaffolds. *Biotechnol Bioeng* 2014;**111**::829–41. https://doi.org/10.1002/bit.25145.
148 Murali R, Ponrasu T, Cheirmadurai K, Thanikaivelan P. Biomimetic hybrid porous

scaffolds immobilized with platelet derived growth factor-BB promote cellularization and vascularization in tissue engineering. *J Biomed Mater Res A* 2015. https://doi.org/10.1002/jbm.a.35574.
149 Liao SW, Rawson J, Omori K, Ishiyama K, Mozhdehi D, Oancea AR, *et al.* Maintaining functional islets through encapsulation in an injectable saccharide-peptide hydrogel. *Biomaterials* 2013;**34**::3984–91. https://doi.org/10.1016/j.biomaterials.2013.02.007.
150 Williams SJ, Wang Q, Macgregor RR, Siahaan TJ, Stehno-Bittel L, Berkland C. Adhesion of pancreatic beta cells to biopolymer films. *Biopolymers* 2009;**91**::676–85. https://doi.org/10.1002/bip.21196.
151 Integrated Islet Distribution Program. Standard Operating Procedure for Potency Test: Glucose Stimulated Insulin Release Assay 2012.
152 Graham ML, Bellin MD, Papas KK, Hering BJ, Schuurman H-JJ. Species incompatibilities in the pig-to-macaque islet xenotransplant model affect transplant outcome: a comparison with allotransplantation. *Xenotransplantation* 2011;**18**::328–42. https://doi.org/10.1111/j.1399-3089.2011.00676.x.
153 Kobayashi T, Harb G, Rajotte RV, Korbutt GS, Mallett AG, Arefanian H, *et al.* Immune mechanisms associated with the rejection of encapsulated neonatal porcine islet xenografts. *Xenotransplantation* 2006;**13**::547–59. https://doi.org/10.1111/j.1399-3089.2006.00349.x.
154 Safley SA, Cui H, Cauffiel SM, Xu B-YY, Wright JR, Weber CJ. Encapsulated piscine (tilapia) islets for diabetes therapy: studies in diabetic NOD and NOD-SCID mice. *Xenotransplantation* 2014;**21**::127–39. https://doi.org/10.1111/xen.12086.
155 Nakazawa M, Tawaratani T, Uchimoto H, Kawaminami A, Ueda M, Ueda A, *et al.* Spontaneous neoplastic lesions in aged Sprague-Dawley rats. *Exp Anim* 2001;**50**::99–103.
156 Gehrke SH, Fisher JP, Palasis M, Lund ME. Factors determining hydrogel permeability. *Ann N Y Acad Sci* 1997;**831**::179–207.
157 Pluen A, Netti PA, Jain RK, Berk DA. Diffusion of macromolecules in agarose gels: comparison of linear and globular configurations. *Biophys J* 1999;**77**::542–52. https://doi.org/10.1016/S0006-3495(99)76911-0.
158 Durst CA, Cuchiara MP, Mansfield EG, West JL. Flexural characterization of cell encapsulated PEGDA hydrogels with applications for tissue engineered heart valves. *Acta Biomaterialia* 2011. https://doi.org/10.1016/j.actbio.2011.02.018.
159 Pinkse GG, Bouwman WP, Jiawan-Lalai R, Terpstra OT, Bruijn JA, de Heer E. Integrin signaling via RGD peptides and anti-beta1 antibodies confers resistance to apoptosis in islets of Langerhans. *Diabetes* 2006;**55**::312–7.
160 Weber LM, Hayda KN, Haskins K, Anseth KS. The effects of cell-matrix interactions on encapsulated beta-cell function within hydrogels functionalized with matrix-derived adhesive peptides. *Biomaterials* 2007;**28**::3004–11. https://doi.org/10.1016/j.biomaterials.2007.03.005.
161 Bertelli E, Bendayan M. Association between endocrine pancreas and ductal system. More than an epiphenomenon of endocrine differentiation and development? *J Histochem Cytochem* 2005;**53**::1071–86. https://doi.org/10.1369/jhc.5R6640.2005.
162 Murray HE, Paget MB, Bailey CJ, Downing R. Sustained insulin secretory

response in human islets co-cultured with pancreatic duct-derived epithelial cells within a rotational cell culture system. *Diabetologia* 2009;**52**::477–85. https://doi.org/10.1007/s00125-008-1247-x.
163 Sujatha SR, Pulimood A, Gunasekaran S. Comparative immunocytochemistry of isolated rat & monkey pancreatic islet cell types. *Indian J Med Res* 2004;**119**::38–44.
164 Silva CM, Ribeiro AJJ, Ferreira D, Veiga F. Insulin encapsulation in reinforced alginate microspheres prepared by internal gelation. *Eur J Pharm Sci* 2006;**29**::148–59. https://doi.org/10.1016/j.ejps.2006.06.008.
165 Darrabie MD, Kendall WF, Opara EC. Characteristics of Poly-L-Ornithine-coated alginate microcapsules. *Biomaterials* 2005;**26**::6846–52. https://doi.org/10.1016/j.biomaterials.2005.05.009.
166 Mazzitelli S, Tosi A, Balestra C, Nastruzzi C, Luca G, Mancuso F, *et al.* Production and characterization of alginate microcapsules produced by a vibrational encapsulation device. *J Biomater Appl* 2008;**23**::123–45. https://doi.org/10.1177/0885328207084958.
167 Hals IK, Rokstad AM, Strand BL, Oberholzer J, Grill V. Alginate microencapsulation of human islets does not increase susceptibility to acute hypoxia. *J Diabetes Res* 2013;**2013**::374925. https://doi.org/10.1155/2013/374925.
168 Vaithilingam V, Quayum N, Joglekar MV, Jensen J, Hardikar AA, Oberholzer J, *et al.* Effect of alginate encapsulation on the cellular transcriptome of human islets. *Biomaterials* 2011;**32**::8416–25. https://doi.org/10.1016/j.biomaterials.2011.06.044.
169 Smidsrød O, Skja G. Alginate as immobilization matrix for cells. *Trends in Biotechnology* 1990.
170 Sun Y, Ma X, Zhou D, Vacek I, Sun AM. Normalization of diabetes in spontaneously diabetic cynomologus monkeys by xenografts of microencapsulated porcine islets without immunosuppression. *J Clin Invest* 1996;**98**::1417–22. https://doi.org/10.1172/JCI118929.
171 Penko D, Rojas Canales D, Mohanasundaram D, Peiris HS, Sun WY, Drogemuller CJ, *et al.* Endothelial progenitor cells enhance islet engraftment, influence beta cell function and modulate islet connexin 36 expression. *Cell Transplant* 2013. https://doi.org/10.3727/096368913X673423.
172 De Vos P, Faas MM, Strand B, Calafiore R. Alginate-based microcapsules for immunoisolation of pancreatic islets. *Biomaterials* 2006.
173 Zimmermann H, Zimmermann D, Reuss R, Feilen PJ, Manz B, Katsen A, *et al.* Towards a medically approved technology for alginate-based microcapsules allowing long-term immunoisolated transplantation. *J Mater Sci Mater Med* 2005;**16**::491–501. https://doi.org/10.1007/s10856-005-0523-2.
174 Zimmermann H, Shirley SG, Zimmermann U. Alginate-based encapsulation of cells: past, present, and future. *Current Diabetes Reports* 2007.
175 Hoesli CA, Raghuram K, Kiang RL, Mocinecová D, Hu X, Johnson JD, *et al.* Pancreatic cell immobilization in alginate beads produced by emulsion and internal gelation. *Biotechnol Bioeng* 2011;**108**::424–34. https://doi.org/10.1002/bit.22959.
176 Jacobs-Tulleneers-Thevissen D, Chintinne M, Ling Z, Gillard P, Schoonjans L, Delvaux G, *et al.* Sustained function of alginate-encapsulated human islet cell implants in the peritoneal cavity of mice leading to a pilot study in a type 1 diabetic patient.

Diabetologia 2013;**56**::1605–14. https://doi.org/10.1007/s00125-013-2906-0.
177 Ooi HW, Ketterer B, Trouillet V, Franzreb M, Barner-Kowollik C. Thermoresponsive Agarose Based Microparticles for Antibody Separation. *Biomacromolecules* 2016;**17**::280–90. https://doi.org/10.1021/acs.biomac.5b01391.
178 Yun Y, Goetz D, Yellen P, Chen W. Hyaluronan microspheres for sustained gene delivery and site-specific targeting. *Biomaterials* 2004;**25**: https://doi.org/10.1016/S0142-9612(03)00467-8.
179 Landázuri N, Levit RD, Joseph G, Ortega-Legaspi JM, Flores CA, Weiss D, *et al.* Alginate microencapsulation of human mesenchymal stem cells as a strategy to enhance paracrine-mediated vascular recovery after hindlimb ischaemia. *J Tissue Eng Regen Med* 2016;**10**::222–32. https://doi.org/10.1002/term.1680.
180 Ravi M, Paramesh V, Kaviya SR, Anuradha E, Solomon FD. 3D cell culture systems: advantages and applications. *J Cell Physiol* 2015;**230**::16–26. https://doi.org/10.1002/jcp.24683.
181 Rockwood DN, Gil ES, Park S-HH, Kluge JA, Grayson W, Bhumiratana S, *et al.* Ingrowth of human mesenchymal stem cells into porous silk particle reinforced silk composite scaffolds: An in vitro study. *Acta Biomater* 2011;**7**::144–51. https://doi.org/10.1016/j.actbio.2010.07.020.
182 Xu T, Molnar P, Gregory C, Das M, Boland T, Hickman JJ. Electrophysiological characterization of embryonic hippocampal neurons cultured in a 3D collagen hydrogel. *Biomaterials* 2009;**30**::4377–83. https://doi.org/10.1016/j.biomaterials.2009.04.047.
183 Ligon SC, Husár B, Wutzel H, Holman R. Strategies to reduce oxygen inhibition in photoinduced polymerization. *Chemical …* 2013. https://doi.org/10.1021/cr3005197.
184 Biswal D, Hilt JZ. Analysis of oxygen inhibition in photopolymerizations of hydrogel micropatterns using FTIR imaging. *Macromolecules* 2009. https://doi.org/10.1021/ma801600c.
185 Oytun F, Kahveci MU, Yagci Y. Sugar overcomes oxygen inhibition in photoinitiated free radical polymerization. *Journal of Polymer Science …* 2013. https://doi.org/10.1002/pola.26554.
186 Shenoy R, Bowman CN. Mechanism and Implementation of Oxygen Inhibition Suppression in Photopolymerizations by Competitive Photoactivation of a Singlet Oxygen Sensitizer. *Macromolecules* 2010;**43**::7964–70. https://doi.org/10.1021/ma1012682.
187 Qi M, Mørch Y, Lacík I, Formo K, Marchese E, Wang Y, *et al.* Survival of human islets in microbeads containing high guluronic acid alginate crosslinked with Ca2+ and Ba2+. *Xenotransplantation* 2012;**19**::355–64. https://doi.org/10.1111/xen.12009.
188 Calafiore R, Basta G. Artificial pancreas to treat type 1 diabetes mellitus. *Methods Mol Med* 2007;**140**::197–236. https://doi.org/10.1007/978-1-59745-443-8_12.
189 Soon-Shiong P, Feldman E, Nelson R, Komtebedde J, Smidsrod O, Skjak-Braek G, *et al.* Successful reversal of spontaneous diabetes in dogs by intraperitoneal microencapsulated islets. *Transplantation* 1992;**54**::769–74.
190 Kerby A, Bohman S, Westberg H, Jones P, King A. Immunoisolation of islets in high guluronic acid barium-alginate microcapsules does not improve graft outcome at the subcutaneous site. *Artif Organs* 2012;**36**::564–70. https://doi.org/10.1111/j.1525-

1594.2011.01411.x.
191 Falkowski R, Medini M, Olabisi R. The effects of molecular weight on viability within PEGDA hydrogel microspheres. *… Conference (NEBEC)* 2014.
192 Pradhan S, Clary JM, Seliktar D, Lipke EA. A three-dimensional spheroidal cancer model based on PEG-fibrinogen hydrogel microspheres. *Biomaterials* 2017;**115**::141–54. https://doi.org/10.1016/j.biomaterials.2016.10.052.
193 Swioklo S, Connon CJ. Keeping cells in their place: the future of stem cell encapsulation. *Expert Opin Biol Ther* 2016;**16**::1181–3. https://doi.org/10.1080/14712598.2016.1213811.
194 Wilson JL, McDevitt TC. Stem cell microencapsulation for phenotypic control, bioprocessing, and transplantation. *Biotechnol Bioeng* 2013;**110**::667–82. https://doi.org/10.1002/bit.24802.
195 Williams CG, Malik AN, Kim TK, Manson PN, Elisseeff JH. Variable cytocompatibility of six cell lines with photoinitiators used for polymerizing hydrogels and cell encapsulation. *Biomaterials* 2005;**26**::1211–8. https://doi.org/10.1016/j.biomaterials.2004.04.024.
196 Sabnis A, Rahimi M, Chapman C, Nguyen KT. Cytocompatibility studies of an in situ photopolymerized thermoresponsive hydrogel nanoparticle system using human aortic smooth muscle cells. *J Biomed Mater Res A* 2009;**91**::52–9. https://doi.org/10.1002/jbm.a.32194.
197 Mironi-Harpaz I, Wang D, Venkatraman S, Seliktar D. Photopolymerization of cell-encapsulating hydrogels: crosslinking efficiency versus cytotoxicity. *Acta Biomater* 2012;**8**::1838–48. https://doi.org/10.1016/j.actbio.2011.12.034.
198 Fairbanks BD, Schwartz MP, Bowman CN, Anseth KS. Photoinitiated polymerization of PEG-diacrylate with lithium phenyl-2,4,6-trimethylbenzoylphosphinate: polymerization rate and cytocompatibility. *Biomaterials* 2009;**30**::6702–7. https://doi.org/10.1016/j.biomaterials.2009.08.055.
199 Weber LM, Lopez CG, Anseth KS. Effects of PEG hydrogel crosslinking density on protein diffusion and encapsulated islet survival and function. *J Biomed Mater Res A* 2009;**90**::720–9. https://doi.org/10.1002/jbm.a.32134.
200 Hagel V, Haraszti T, Boehm H. Diffusion and interaction in PEG-DA hydrogels. *Biointerphases* 2013;**8**::36. https://doi.org/10.1186/1559-4106-8-36.
201 Gebhart GF. *Recognition and Alleviation of Pain in Laboratory Animals* . The National Academic Press; 2009.
202 Klopfleisch R, Jung F. The pathology of the foreign body reaction against biomaterials. *J Biomed Mater Res A* 2016. https://doi.org/10.1002/jbm.a.35958.
203 Koh TJ, DiPietro LA. Inflammation and wound healing: the role of the macrophage. *Expert Rev Mol Med* 2011;**13**::e23. https://doi.org/10.1017/S1462399411001943.
204 DiEgidio P, Friedman HI, Gourdie RG, Riley AE, Yost MJ, Goodwin RL. Biomedical implant capsule formation: lessons learned and the road ahead. *Ann Plast Surg* 2014;**73**::451–60. https://doi.org/10.1097/SAP.0000000000000287.
205 Matlaga BF, Yasenchak LP, Salthouse TN. Tissue response to implanted polymers: the significance of sample shape. *J Biomed Mater Res* 1976;**10**::391–7. https://doi.org/10.1002/jbm.820100308.

206 Kamath S, Bhattacharyya D, Padukudru C, Timmons RB, Tang L. Surface chemistry influences implant-mediated host tissue responses. *J Biomed Mater Res A* 2008;**86**::617–26. https://doi.org/10.1002/jbm.a.31649.
207 Allison DD, Grande-Allen KJ. Review. Hyaluronan: a powerful tissue engineering tool. *Tissue Eng* 2006;**12**::2131–40. https://doi.org/10.1089/ten.2006.12.2131.
208 Nussinovitch, Gershon, Nussinovitch. Liquid-core hydrocolloid capsules. *Food Hydrocolloids* 1996;**10**::21–6. https://doi.org/10.1016/S0268-005X(96)80049-X.
209 Zhang L, Salsac A-VV. Can sonication enhance release from liquid-core capsules with a hydrogel membrane? *J Colloid Interface Sci* 2012;**368**::648–54. https://doi.org/10.1016/j.jcis.2011.11.038.
210 Yoo I-K, Seong G, Chang H, Park J. Encapsulation of Lactobacillus casei cells in liquid-core alginate capsules for lactic acid production. *Enzyme and Microbial Technology* 1996;**19**: https://doi.org/10.1016/S0141-0229(96)00016-6.
211 Wyss A, von Stockar U, Marison IW. Production and characterization of liquid-core capsules made from cross-linked acrylamide copolymers for biotechnological applications. *Biotechnol Bioeng* 2004;**86**::563–72. https://doi.org/10.1002/bit.20050.
212 Chang HN, Seong GH, Yoo IK, Park JK, Seo JH. Microencapsulation of recombinant Saccharomyces cerevisiae cells with invertase activity in liquid-core alginate capsules. *Biotechnol Bioeng* 1996;**51**::157–62. https://doi.org/10.1002/(SICI)1097-0290(19960720)51:2<157::AID-BIT4>3.0.CO;2-I.
213 Sharma B, Fermanian S, Gibson M, Unterman S, Herzka DA, Cascio B, *et al.* Human cartilage repair with a photoreactive adhesive-hydrogel composite. *Sci Transl Med* 2013;**5**::167ra6. https://doi.org/10.1126/scitranslmed.3004838.
214 Wang D-AA, Varghese S, Sharma B, Strehin I, Fermanian S, Gorham J, *et al.* Multifunctional chondroitin sulphate for cartilage tissue-biomaterial integration. *Nat Mater* 2007;**6**::385–92. https://doi.org/10.1038/nmat1890.
215 Browning MB, Cereceres SN, Luong PT, Cosgriff-Hernandez EM. Determination of the in vivo degradation mechanism of PEGDA hydrogels. *J Biomed Mater Res A* 2014;**102**::4244–51. https://doi.org/10.1002/jbm.a.35096.
216 Chiu YC, Cheng MH, Engel H, Kao SW, Larson JC. The role of pore size on vascularization and tissue remodeling in PEG hydrogels. *Biomaterials* 2011.
217 Nakayama Y, Matsuda T. Photocurable surgical tissue adhesive glues composed of photoreactive gelatin and poly (ethylene glycol) diacrylate. *Journal of Biomedical Materials …* 1999.